

**GAMMA PHOTON INDUCED
MODIFICATION OF SOME POLYMERS**

BY

TOKASWU

DEPARTMENT OF CHEMISTRY
SCHOOL OF CHEMICAL SCIENCES

SUBMITTED

In fulfillment of the requirement of the degree of

DOCTOR OF PHILOSOPHY

in

CHEMISTRY

of

NAGALAND UNIVERSITY

LUMAMI – 798602

INDIA

Dedicated
to
my parents

Declaration

The Nagaland University

Month : August, Year : 2007

I Mr. Toka Swu, hereby declare that the subject matter of this thesis is the record of work done by me, that contents of this thesis did not form the basis of the award of any previous degree to me or to the best of my knowledge to anybody else, and that the thesis has not been submitted by me for any other research degree in any other University/Institute.

This is being submitted to the Nagaland University for the degree of **DOCTOR OF PHILOSOPHY** in Chemistry.

Mr. Toka Swu

(Head)
Department of Chemistry
Nagaland University.

Dipak Sinha
Supervisor

Acknowledgements

At the outset, I would like to express my heartfelt gratitude to my supervisor Dr. Dipak Sinha for his indispensable guidance, encouragement and his ever willingness to help me in all manner of ways, whereby this work has been placed in an enviable position to be submitted. I am deeply indebted to him for his keen personal interest in my research works and also for painstakingly reviewing the whole of my thesis with such diligence.

My deep sense of gratitude to Prof. K.K. Dwivedi, Counselor, Indian Embassy, Washington, USA, for providing the polymeric materials.

I wish to thank Dr. V.G. Dedgaonkar, Pune University, for his help in gamma irradiation and also to Dr. Alok Srivastava, Punjab University, Chandigarh, for initial help of preparing the samples.

The immense help received from Dr.(Mrs) Upasana Bora Sinha, Lecturer, Department of Chemistry, Nagaland University is highly acknowledged.

I express my sincere thanks to Dr. Dietmar Fink, HMI, Germany for helping me out in analytical computations.

Special thanks to Dr(Mrs) M. Indira Devi, HOD and all the faculty members of Chemistry Department, N.U. for their valuable suggestions and advices through out my research works.

I also extend my gratitude to Prof. N. Kumar, visiting Professor, who was a great source of inspiration to me.

I am thankful to IIT (Indian Institute of Technology) Guwahati and NEHU (North Eastern Hill University) Shillong, for allowing me to use all the instruments.

The help and cooperation received from the non-teaching staffs, Department of Chemistry are gratefully acknowledged.

A deep note of appreciation is due to my research colleagues and friends Alimenla, Latonglila, Anil and Manob Bora who stood by my side through all odds. The sharing of their research works, experiences and dreams renewed my zeal to work even harder.

I feel my acknowledgement will be incomplete until I appreciate the constant prayer supports and encouragements received from my parents and family members.

Above all, I thank the Almighty God who abides with me throughout my life.



Toka Swu

CONTENTS

| | Page No. |
|---|----------|
| CHAPTER 1 INTRODUCTION | 2 |
| 1.1 Radiation induced changes or modifications of polymers | 5 |
| CHAPTER 2 TYPES OF RADIATION AND THEIR INTERACTION WITH MATTER | |
| 2.1 Types of Radiation | 24 |
| 2.2 Interaction of Radiation with matter | 25 |
| 2.3 Interaction of Radiation with polymers | 29 |
| 2.4 Mechanism of ion-matter interaction | 31 |
| 2.5 Formation of Nuclear Tracks | 32 |
| 2.5.1 Track Registration Criteria | 36 |
| 2.5.2 Theories used for track formation | 37 |
| References | 41 |
| CHAPTER 3 TECHNIQUES OF CHARACTERIZATION OF IRRADIATED POLYMERS | |
| 3.1 IR Technique | 48 |
| 3.2 UV-VIS Spectroscopy | 50 |
| 3.3 Thermo Gravimetric Analysis (TGA) | 52 |
| 3.4 Differential Scanning Calorimetry | 52 |
| 3.5 X-Ray Diffraction (XRD) | 53 |
| 3.6 Track Technique | 54 |
| 3.6.1 Heavy ion sources | 55 |
| 3.6.2 Methods and formulation associated with Track studies | 56 |
| References | 59 |

CHAPTER-4 EXPERIMENTAL TECHNIQUES

| | | |
|------|--|----|
| 4.1 | Preparation of Detectors | 63 |
| 4.2 | Irradiation of Detectors | 68 |
| 4.3 | Chemical etching for track development | 69 |
| 4.4 | Measurement of track parameters | 69 |
| 4.5 | Determination of Bulk-etch rate and Track-etch rate | 71 |
| 4.6 | IR spectra | 72 |
| 4.7 | UV-VIS Spectra | 72 |
| 4.8 | Thermogravimetric Study | 73 |
| 4.9 | DSC Study | 73 |
| 4.10 | XRD Study | 73 |
| | References | 74 |

CHAPTER-5 RESULTS AND DISCUSSIONS 75

| | | |
|---------|---|-----|
| PART-1: | Gamma radiation effect on Polyvinylchloride | 77 |
| 5.1.1 | Introduction | 78 |
| 5.1.2 | Investigation Procedure | 79 |
| 5.1.3 | Results and Discussions | 80 |
| | Conclusions | 90 |
| | References | 91 |
| PART-2: | Gamma radiation effect on Polypropylene | 93 |
| 5.2.1 | Introduction | 94 |
| 5.2.2 | Investigation Procedure | 98 |
| 5.2.3 | Results and Discussions | 99 |
| | Conclusions | 108 |
| | References | 109 |
| PART-3: | Gamma radiation effect on Polycarbonate | 111 |
| 5.3.1 | Introduction | 112 |
| 5.3.2 | Investigation Procedure | 114 |
| 5.3.3 | Results and Discussions | 116 |
| | Conclusions | 125 |
| | References | 126 |

| | | |
|---------------------------------|--|-----|
| PART-4: | Gamma radiation effect on Polyallyldiglycolcarbonate | 127 |
| 5.4.1 | Introduction | 128 |
| 5.4.2 | Investigation Procedure | 131 |
| 5.4.3 | Results and Discussions. | 133 |
| | Conclusions | 142 |
| | References | 143 |
| CHAPTER- 6: FUTURE PERSPECTIVES | | 145 |
| 6.1 | Background | 146 |
| 6.2 | Future Work Plan | 148 |
| 6.2.1 | Review of Literature in the Proposed Area | 149 |
| 6.2.2 | Objectives of the Future Course of Work | 151 |
| | References | 153 |

Chapter - 1

CHAPTER-1**INTRODUCTION**

The study of radiation induced modifications in polymers is a recent yet an expanding field of research. Owing to its technological applications, it has received an immense deal of attention and is being extensively investigated. Modifications induced by irradiation may sometimes enable in achieving the desired and improved physical and chemical properties of the polymers for specific use. Thus the study of polymer modifications which comprises a study of physico-chemical variations in polymer due to irradiation is of great importance.

Radiations are produced both naturally and artificially and are thus omnipresent. They comprise of charged particles like electrons, protons, alpha particles, fission-fragments, accelerated heavy ions and electromagnetic radiations such as x-rays and gamma-rays. All these types of radiations interact with any type of substances coming in their path, irrespective of their molecular structure generating variety of species [1] through dissipation of radiation's energy. Thus, polymers on irradiation get electronically ionized or excited resulting in structural alternations, which in turn affects their properties [2]. These changes in the polymer depend on the radiation doses, internal structure of polymer such as types of functional group present, chain length, etc. When the energy of the radiation exceeds the bond energy, the polymer having absorbed energy may suffer bond cleavage giving rise to a non-saturated fragment called 'free radical'. These free radicals are very reactive and may cause different chemical transformation within the polymer molecule by reacting with other parts of the same molecule. As a result, chain scissions, cross-linking,

etc. takes place. Various gaseous molecular species are released during irradiation. The most prominent emission is hydrogen, followed by less abundant heavier molecular species which are scission products from the pendant side groups and chain-end segments, and their reaction products. Figure-1.1 illustrates various functional chemical entities created by irradiation. Cross-linking occurs when two free dangling ion or radical pairs on neighboring chains unite, whereas double or triple bonds are formed if two neighboring radicals in the same chain unite.

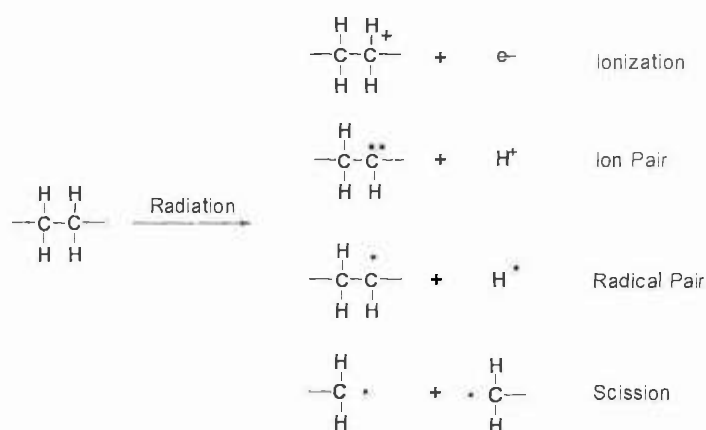


Fig. 1.1. Typical consequences induced by ion irradiation which include electronic excitation, phonons, ionization, ion pair formation, radical formation, and chain scission.

Irradiation of polymers sometimes also results in gas evolution, formation of double bonds and molecular emissions. The anisotropy of the interaction of energetic ions with polymer leads to chain scission, chain aggregation, formation of double bonds and molecular emissions. Molecular emissions from polymers always occur with a release of neutral hydrogen and carbon-hydrogen groups and thus make a significant change in the polymer stoichiometry. If present in

the polymer chains, other atomic species (O, F, Cl, N etc.) are also ejected. It is an established fact that upon irradiation, polymers get depleted of hydrogen, and as a consequence of this the polymer chains are modified. Smaller units are formed by chain scission, double bonds become abundant and radicals emerge. Due to their electrostatic attraction, these small carbon enriched units may agglomerate to electrically conductive clusters. Such structural and bonding may result in modifications of the polymer properties such as thermal stability [3], optical [4], morphology [5], molecular weight [6], etching characteristics [7-10], glass transition temperature [11], electrical properties [12] and many other properties[13], etc.

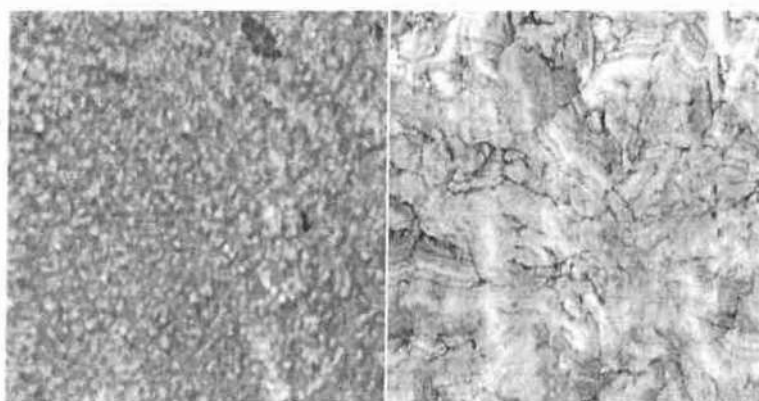


Fig.1. 2. A representative diagram showing the morphological change: LFM micrographs (i.e. friction images) of (a) pristine PP, and (b) polypropylene foils irradiated with 3 GeV ^{238}U ions at a fluence of 10^{11} cm^{-2} . The transition from small structure less grains towards large laminar units can clearly be recognized. Image size: $1.5 \mu\text{m} \times 1.5 \mu\text{m}$ each (this figure is taken from the book "Fundamentals of Ion-Irradiated Polymers" by D. Fink, Springer, 2004 [1]).

A representative diagram showing the morphological change of pristine Polypropylene and irradiated foils with 3 GeV ^{238}U ions at a fluence of 10^{11} cm^{-2} is shown in Figure 1.2. The figure clearly shows the transition from small structure less grains towards large laminar units [1].

1.1 RADIATION INDUCED CHANGES OR MODIFICATIONS OF POLYMERS

Irradiation of polymeric material induces irreversible changes in their macromolecular structure [1]. It can be used to change in a controlled way the physical properties of thin films or to modify the near surface characteristics of a bulk polymer. Sun *et.al.* have observed that gradual amorphisation in polycarbonate polymer takes place due to increase in ion fluence [14, 15]. XRD measurements show the decrease of the main XRD peak intensity. Progressive amorphisation process of Makrofol polymer with increasing fluence is traced [14] by XRD measurements Figure 1.3.

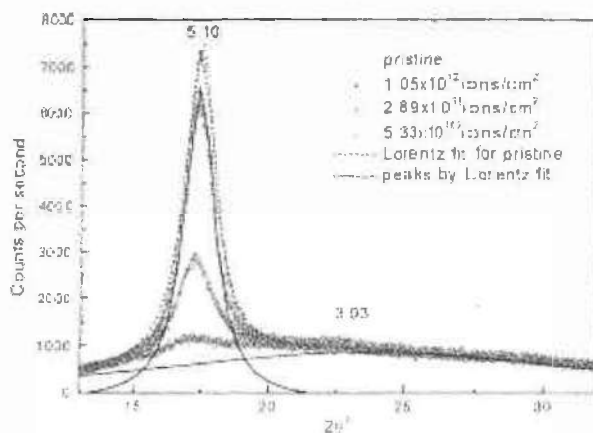


Fig. 1. 3. XRD spectra of Makrofol polymer irradiated with Xe ions at 7.62 keV/nm at different fluence

Significant effects of ion irradiation are observed even at fluence as low as 10^{11} ions/cm² [14, 15] where chemical modifications take place. Primary phenomena associated with radiation interaction are chain scission, chain aggregation, formation of double bonds and molecular emission. All these effects depend on target parameters (composition, molecular weight, temperature, etc.) and on ion beam parameters (energy, mass, charge and fluence). Molecular emission from polymers always occurs with the release of neutral hydrogen and carbon-hydrogen groups and with a significant change of the polymer

stoichiometry [16]. If present in the polymer chain, other atomic species (O, F, Cl, and N) are also ejected [17]. After irradiation, most of the properties of polymers (optical, electrical, mechanical, surface etc.) are modified together with its chemical behaviors as reported by analytical measurements [16, 17, 18, 19]. At high fluence (10^{14} - 10^{17} ions/cm²) an enrichment of carbon generally occurs, leading to more or less complete carbonisation (Figure 1.4) such that the final sample composition may have little memory of the original chain structure [20]. Properties of such materials are similar to amorphous carbon in terms of optical absorbance, electrical properties, hardness and chemical inertness, but they may eventually contain heteroatom like N, O, S, if these are present in the original polymer structure [21]. Application of radiation on polymers leads to a change in the electrical conductivity, which has been studied by Mishra *et. al.* [22] and Fink *et. al.* [23], have recently reported ion irradiation effect on polymers for electronic applications. Surface modification and nanoparticle formation by negative ion implantation of polymers have been reported by Boldyryeva *et.al.* [24]. Modifications of nanostructured materials by energetic ion beams is one of the recent applications of energetic ions [25]. Scissioning of chains and radicals formation in PP film due to gamma irradiation have been observed by Pedro *et. al.* [26]. Davenas *et. al.* [27] and Fink *et. al.* [28] have correlated the changes in the optical properties with the mechanism of energy deposition. Ion beam effects on PMMA have been studied by Mladenov and Emmoth [29] and its applications on fabricating light guides by Kulish *et al.* [30]. Phase transition during irradiation of ferroelectric polymers has been reported by Legrad *et al.* [31]. Improvements in surface smoothness, hardness and wear resistance of

polymers by multiple ion implantations have been studied by Lee et al. [32].

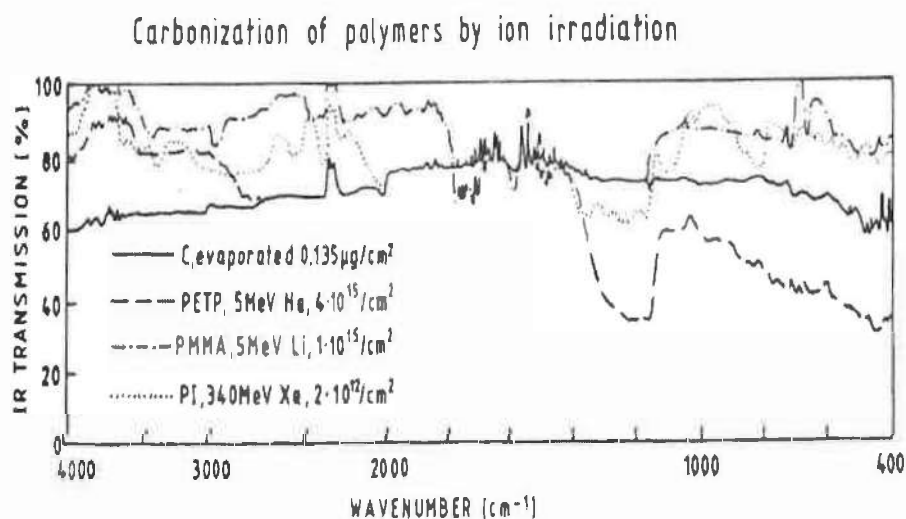


Fig. 1.4. Illustration of the effect of carbonization of different polymers by ion beam irradiation, after deposition of elevated energy densities, as visualized by IR spectrometry [20]

When radiation is absorbed by matter, ions and free radicals are formed, which are the precursors of all subsequent chemical transformations. Free radicals arise as a result of bond scissions. In liquids the lifetime of these species is extremely short. They combine, as a result of very rapid radical-radical coupling and positive ion interactions, with either electrons or negative ions. The same situation is met in a polymer above its glass transition temperature, where the high mobility of the polymer favours encounters of the various reactive species. In contrast, if the polymer is irradiated in a vitreous state, mobility is considerably reduced and trapped radicals and ions are always present. The life times of these species may become extremely long (weeks or months) and are essentially determined by

the temperature : the farther away the system from its glass transition temperature, the longer the life time of trapped species. Free radicals are detected by ESR signals [33, 34] which can be used to determine their concentration, their nature and the kinetics of their decay. Ionic species also often give ESR signals. They can be characterised by radiation induced conductivity or by post irradiation thermoluminescence which is caused by positive- negative charge combination. Trapped ions or radicals absorb light and may be responsible for more or less transient discolouration. Crystallinity of polymer is also responsible for the trapping of transient species, particularly radicals [1]. If, however, the system is above T_g (glass transition temperature) the mobility of the polymeric segments is large enough for the valences to "move out" of the crystalline zones, usually by inter and intramolecular atom (hydrogen) transfer. The most obvious changes in the bulk properties of irradiated polymers are brought about by modification of their molecular weight due to cross-linking or degradation. Cross-linking increases the modulus and hardness of the polymer, but this effect become apparent only for very high cross-link densities. If, however, the polymer is partially crystalline, such as polyethylene, moderate cross linking imparts to the material a nonmelting behaviour [1]. Above its crystalline melting point a cross linked polymer does not flow, but exhibits rubber elasticity. This modification is of great commercial importance for numerous products such as insulators, hot-water pipes and others, and this accounts for the fairly large scale manufacture of radiation cross-linked polymers in industry. Radiation degradation is a random chain scission process which gradually reduces the molecular weight of the polymer. Low molecular weight products are produced statistically and they may plasticize the material. As a result of this

the polymer weakens and loses most of its valuable properties after high radiation doses. The release of gaseous products under ion irradiation are investigated in situ by using infrared and mass spectroscopy. Using the spectra of several pure reference gases, the volatile products are generally identified [1]. Different types of gases like, acetylene, carbon monoxide, carbon dioxide, methane, etc are released during irradiation. The types of evolved gases depends on the polymer structure and also types of irradiation used. Complementing information is obtained from the analysis of the residual gas by mass spectroscopy during the ion irradiation. A typical mass spectrum is shown in Figure 1.5. The mass spectrum of the irradiated PI(Polyimide) with 760 MeV Kr ions [35] signifies main chain scission processes and the formation of volatile molecules with triple bonds. Mass fragments corresponding to masses between 24 and 26 amu is due to acetylene C_2H_2 and its hydro-deficient fragments $C_2H_2^+$, and C_2^+ . In addition, molecules of the olefin group $C_2H_3^+$ (27 amu), $C_2H_4^+$ (28 amu, probably intermixed with CO^+), and $C_2H_5^+$ (29 amu), and $C_2H_6^+$ (30 amu) are identified [35]. Besides the formation of unsaturated bonds, clear indication for the decomposition of the benzene rings is given by mass 65 from alkyl benzene derivatives and by mass 77 and 78 from benzene derivatives. Some of the degradation products may be useful. Thus, wastes of per fluorinated polymer (Teflon) are reclaimed by irradiation in air which converts a useless material into lower molecular weight polymers which find specific uses in sprays. Polyisobutylene(butyl rubber) is degraded by irradiation to yield lubricating oils, cellulose degrades to glucose. It has been observed by Biersack *et. al.*[36] that refractive index of a polymer can be altered by ion irradiation, which is again commercially important for optical

device fabrication. Differential scanning calorimetry (DSC) performed on an ion irradiated polycarbonate film [37] shows a

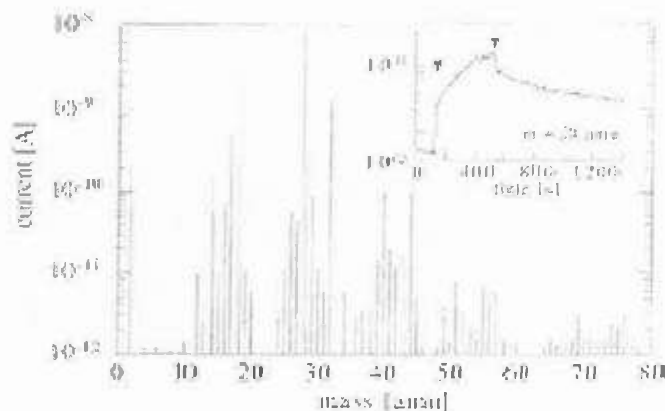


Fig. 1. 5. Mass distribution of ejected molecules recorded after the irradiation of PI with Kr ions (760 MeV) of a total fluence of 1.5×10^{10} ions/cm². The inset illustrates the gas evolution of a fragment with a mass of 24 amu. The arrows indicate the switch on and of the ion beam [35].

decrease in the glass transition temperature due to increase in ion fluence [Figure 1.6]. This decrease in the glass transition temperature is generally due to the increase in molecular mobility as a result of the scissoring of the polymer chains.

It is a well established fact that mechanical, physical, and chemical property changes in polymers are determined by the magnitude of cross-linking and scission. Cross-linking enhances mechanical stability while scission degrades mechanical strength [38]. Change in properties due to ion-beam irradiation and its potential application areas are described in details in references [39] and [40]. The main features are summarized below. Cross-linking generally increases hardness and slows diffusion, improves wear and scratch resistance, and decreases solubility in chemical solvents.

Electrical conductivity and optical density increases due to the formation of cross-links and conjugated double and triple bonds by irradiation. The delocalized p-electrons in the conjugated bonds are

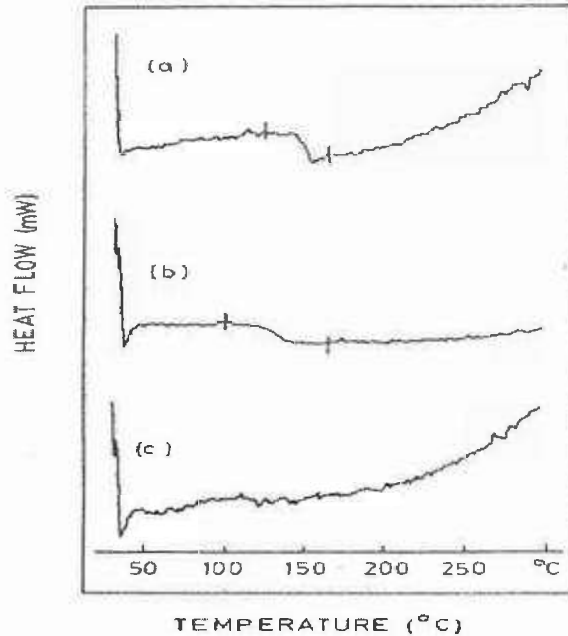
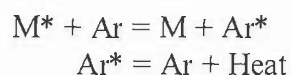


Fig.1.6. DSC curves of virgin and irradiated polycarbonate films: (a) virgin, (b) irradiated with the total ion fluence of 3.5×10^{12} ions, (c) irradiated with the total ion fluence of 7.0×10^{12} ions [37]

loosely bound and thus more mobile than the covalent π -bond electrons. Furthermore, charge carrier mobility increases by cross-links which facilitate the transport of charge carriers across the chains. Otherwise, charge carriers must hop across the chains for conduction. The loosely bound π -electrons can be excited by the energies of visible light, and thus colour changes occur because light is absorbed when these electrons are excited. Radiation induced defects such as anions and radicals (donors) and cations (acceptors) form a broadened band in the band gap and result in the absorption of light as well. Energetic blue light is absorbed first and the colour changes from pale yellow to reddish brown and eventually to a dark

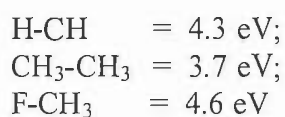
colour with increasing irradiation dose. At very high doses, a metallic luster appears because light is scattered by the abundant π -electrons similar to the effect of free electrons in metals. On the other hand, scission causes bond breakage and increases dissolution of polymers in solvents. This feature has been used for lithography [41].

Polymers can be stabilized against radiation damage by the addition of substances which either divert the absorbed energy towards other chemical processes or stabilize the free radicals produced, thereby preventing them from causing further damage. The first group of substances includes aromatic compounds which are known to act as "energy sinks". Thus, benzene protects cyclohexane and other saturated hydrocarbons from radiolysis by taking up their energy. An excited or ionized cyclohexane molecule transfers its excess energy to the aromatic compound. The latter being much more stable against radiation damage, (owing to the delocalization of the excited energy) most of the energies are converted in to heat and are dissipated in to the surroundings. This sequence of reactions can be represented as:



The presence of aromatic groups in repeating units in a polymer also accounts for the radiation stability of such polymers as Polystyrene, Polyaryletherketones, Polyarylimides etc. The second group of substances comprises of the so called "free radical scavengers" which readily react with free radicals and prevent them from initiating degradation processes. This group includes well-known "stabilisers", "anti-oxidant" and other additions which are present in most commercial polymers.

So far we have discussed the changes or modifications caused by the radiation. Basically all types of physical and chemical changes take place in the polymer because of the bond cleavages, giving rise to nonsaturated fragments called "free radicals". The most interesting phenomenon about this type of bond cleavage is that, in this radiation interaction, which particular bond will be broken can not be predicted, on the basis of energy consideration alone. This is because the energy spent in ionisation (20 eV or more) is much larger than the bond energies of simple organic molecules which are



These values are merely presented here to illustrate the differences in orders of magnitude between the energy deposited and the strengths of the chemical bonds present in the system. It follows that the energy available largely exceeds the amount required to cleave any bond. In spite of this, all the bonds are not broken in random. Experimental evidence shows that selectivity rules apply, which do not follow bond energy considerations alone.

It has already been an established fact that irradiation by swift heavy ions modifies the polymer properties to a significant extent. It is also well known that unlike charged particles gamma rays are a highly penetrating form of electromagnetic radiation. They do not lose energy at every interaction with the orbital electrons of the atoms constituting the material they pass through. The energy loss of gamma rays occurs either through collisions with atomic electrons or through scattering as a photon of a longer wave length or through producing electron-positron pairs. Thus gamma ray does not have a specific range in

matter as charged particles do. The principal methods of gamma interactions with matter are (a) *Photoelectric effect* (b) *Compton scattering* and (c) *Pair-Production*.

So it is expected that materials' response to high energy ion-beams is considerably different from those induced by γ -rays. However, unfortunately works on polymer modifications by gamma radiation have not been fully explored. Moreover the works reported so far on gamma effect on polymers are restricted to low doses. Only few works on gamma effect on polymer or polymeric track detectors have been reported in recent years. [7, 8,9,10, 42, 43, 44,]. It has been observed by Sinha & Dwivedi [42] that due to gamma exposure, polyallyl diglycol carbonate (PADC) detector changes drastically. The studies are performed in the very dose range of 10^1 - 10^6 Gy. It is observed that at the gamma dose of 10^6 Gy, thermal stability of the polymer decreases drastically [42]. The complete decomposition of the PADC detector takes place at much lower temperature (Figure 1.7). It has also been reported that polyallyl chain joined by diethyleneglycol links gets cleaved at the dose of 10^6 Gy leading to radical formation [7].

In the past, radiation effects have been the subject of intense investigation in radiation chemistry, mainly to understand the radiolysis and polymerization mechanisms induced by ionizing radiation such as electron beam and also by gamma-rays. However, studies have shown that materials' response to high energy ion-beams are considerably different from those induced by electron-beam and γ -rays. It has been well established that cross-linking or scission efficiency depends not only upon polymer structure but also upon the characteristics of the radiation sources, namely ion energy and ion species [45]. For example, poly methyl methacrylate (PMMA) degrades

and become more soluble in solvents when subjected to e-beam or γ -rays. For this reason, PMMA has been used as a positive photo-resist material in lithography for electronic applications [46, 47]. The

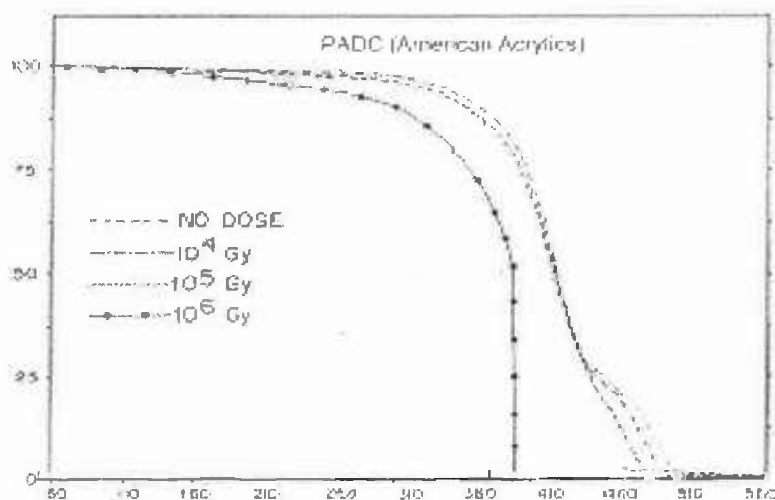


Fig.1. 7. TGA thermogram of gamma irradiated polyallyl diglycol carbonate (PADC- American Acrylics) polymeric detector [42].

propensity of degradation is attributable to a steric hindrance due to the methylester (CH_3OOC) groups attached to the PMMA backbone structure [48]. Large pendant groups restrict chain mobility and thus impede cross-linking. On the other hand, when PMMA is subjected to high energy ions such as 2 MeV Ar-ions, the surface hardness of PMMA increases dramatically, as a result of massive cross-linking, from the pristine value of 0.5 GPa to over 10 GPa after irradiation to a fluence of $1 \times 10^9 \text{ m}^{-2}$ [45].

So the study of polymer modification by gamma radiation can not be completed unless the effect of high gamma dose on different polymers are studied. Keeping this in mind, a study on different polymers like Polypropylene (PP), Polyvinyl Chloride (PVC),

Polycarbonate (PC), Polyallyl Diglycol Carbonate (three different types) is proposed in this thesis. The studies are done in the dose range of 10^1 - 10^6 Gy. Polyallyl Diglycol Carbonate is generally known as PADC track detector. These studies are expected to expand the knowledge of polymer modifications induced by gamma radiation.

Three different types of PADC polymeric track detectors are chosen here to study the effect of gamma irradiation on these detectors. These track detectors have been chosen keeping in mind their applications as nuclear track detectors. Since its inception about 40 years ago, the field of track detection using solid state nuclear track detectors (SSNTDs) has been constantly developed. Track detectors are being increasingly used in various fields like Biomedical [49], Environmental [50], Anthropology [51], Space research [52, 53] and nuclear sciences [54, 55]. For newer and more innovative applications of these detectors a systematic study on the effects of external factors like exposure to radiation, on their physical and chemical properties is essential. Experimental evidence shows that the track registration characteristics of plastic Solid State Nuclear Track Detectors (SSNTDs) are greatly affected when exposed to high doses of gamma rays [56-66]. The modifications in characteristics originate from the structural alterations produced by irradiation of polymers. The changes are strongly dependent on the internal structure of the absorbing substances and the radiation gamma doses. It may be expected that the interaction of gamma-rays with solid causes electronic ionisation (or excitation) of the orbital electrons and possibly atomic displacements. Since polymeric solid state nuclear track detectors consist of long chain organic molecules, the net effect on the material is the formation of many broken molecular chains, leading to a

reduction in the average molecular weight of the substance. Such radiation induced modifications of polymeric materials may influence their etching characteristics which in turn change the track registration properties of these track detectors.

Since the track detectors are being used increasingly in diverse fields such as radiation dosimetry, cosmic-ray study, heavy ion physics, microanalysis, uranium prospecting etc., so a proper characterisation of these detectors is necessary. Though the passage of lighter particles and gamma rays through these detectors can not be directly recorded, but the modifications that they produce on these detectors can be quantified. Keeping these factors in mind we have attempted to characterise the modifications that take place in track properties in three different types of PADC polymeric solids viz. PADC, (Persshore), PADC (Trastrak) and PADC (Homalite). Track properties of these detectors are studied in dose range of 10^1 Gy to 10^6 Gy.

In this dissertation we present a detailed account of the response of six polymeric materials exposed to different doses of gamma rays in terms of –

- registration and development of tracks in PADC detectors
- determination of bulk-etch rate, track-etch rate. etching-efficiency, critical angle and sensitivity under different etching conditions
- change in absorbance of transmittance caused by different doses of gamma radiation in the UV and VIS region for films like PVC, PC and PP
- changes in optical band gap due to gamma radiation
- modifications in chemical structure of polymer films
- changes in thermal properties due to gamma irradiation
- modifications in morphology.

REFERENCES

1. "Fundamentals of Ion-irradiated Polymers" by D. Fink, *Springer*, 2004.
2. Crystallinity changes and melting behaviour of the uniaxially oriented iPP exposed to high gamma doses of radiation. Z. Stojanovic, Z. Kacarevic-Popovic, S. Golavic, D. Milicevic and E. Suljovrujic. *Polymer Degradation and Stability*. 87, 2, 279-286, 2004.
3. Mechanical, thermal and morphological behaviour of the polystyrene/polypropylene (80/20) blend, irradiated with gamma-rays at low doses (0–70 kGy). C. Albano, J. Reyes, M. Ichazo, J. Gonza' lez, M. Herna' ndez, M. Rodr' y' guez. *Polymer Degradation and Stability*. 80, 251–261, 2003.
4. Spectroscopic and Thermal studies of Gamma-irradiated Polypropylene films. D. Sinha, T. Swu, S.P. Tripathy, R. Mishra, K.K. Dwivedi. *Radiation Effects and Defects in Solids*. 158 (No. 7), 531-537, 2003.
5. Effect of γ -radiation on the structure and morphology of polyvinyl alcohol films. N.V. Bhat, M.M. Nate, M.B. Kurup, V.A. Bambole and S. Sabharwal, *Nuclear Instruments and Methods in Physics Research B*. 237, 585-592, 2005.
6. Study of the effect of γ – dose rate on the oxidation of polypropylene. Adams Tidjani and Yasushi Watanabe. *Journal of Applied Polymer Science*. 60, 11, 1839 – 1845, 1996.
7. Modifications of radiation detection response of PADC track detectors by Photons. D. Sinha and K.K. Dwivedi. *Radiation Physics and Chemistry*. 53, 99-105, 1998.
8. Effects of gamma irradiation on the bulk and track etching properties of Cellulose Nitrate (Daicel 6000) and CR-39 plastics. R. Shweikani, S.A. Durrani and T. Tsuruta. *Nuclear Tracks Radiation Measurements*. 22, 153-156, 1993.
9. The etching and structural studies of gamma irradiated induced effects in CR-39 plastic track recorder S. Singh and S. Prasher. *Nuclear Instruments and Methods in Physics Research B*. 222, 4, 518-524, 2004.
10. Proceedings of the 22nd International Conference on Nuclear Tracks in Solids. *Radiation Measurements*. 40(Issues 2-6), 125-794, 2005.
11. Surface cross-linking of polycarbonate under irradiation at long wavelengths.. B. Claude, L. Gonon, J. Duchet, V. Verney, J.L. Gardette. *Polymer Degradation and Stability*. 83, 237 – 240, 2004.
12. Electrical conductivity studies of swift heavy ion modified PVC and PVC–PANI composite. A. Srivastava, V. Singh, A. Chandra, K. Witte, U.W. Scherer and T.V. Singh. *Nuclear Instruments and Methods in Physics Research B*. 244, 277-280, 2006.

13. Proceedings of the Sixth International Symposium on Swift Heavy Ions in Matter. *Nuclear Instruments and Methods in Physics Research B. 245(Issue1), 2006.*
14. Swift heavy ion induced amorphisation and chemical modification in polycarbonate Y. Sun, Z. Zhu, Z. Wang, Y. Jin, J. Liu, M. Hou, Q. Zhang. *Nuclear Instruments and Methods in Physics Research B. 209, 188–193, 2003.*
15. Damage process induced by swift heavy ion in polycarbonate. Y. Sun, Z. Zhu, Z. Wang, J. Liu, Y. Jin, M. Hou, Y. Wang, J. Duan. *Nuclear Instruments and Methods in Physics Research B. 212, 211–215, 2003.*
16. Change of hydrogen concentration after ion beam irradiation on polyimide films with 100–400 °C annealing. M. Watamori. *Nuclear Instruments and Methods in Physics Research B. 249, 159–161, 2006.*
17. Yields of CO₂ formation and scissions at ether bonds along nuclear tracks in CR-39. T. Yamauchi, R. Barillon, E. Balanzat, T. Asuka, K. Izumi, T. Masutani and K. Oda. *Radiation Measurements 40, 224–228, 2005.*
18. Surface modification and nanoparticle formation by negative ion implantation of polymers. H. Boldyryeva, N. Kishimoto, N. Umeda, K. Kono, O.A. Plaksin and Y. Takeda. *Nuclear Instruments and Methods in Physics Research B, 953–958, 2004.*
19. Infrared spectroscopy analysis of physico-chemical modifications induced by heavy ions in ultra-high molecular weight polyethylene. V.C. Chappa, M.F. del Grosso, G. García-Bermúdez and R.O. Mazzei. *Nuclear Instruments and Methods in Physics Research B. 243(Issue1) 58–62. 2006.*
20. Infrared Transmission of Ion irradiated polymers. D.Fink, F.Hosoi, H.Omichi, T.Sasuga and L. Amaral. *Radiation Effects and Defects in solids, 132, 313–328, 1994.*
21. Chemical reactions and physical property modifications induced by keV ion beams in polymers. G. Marletta. *Nuclear Instruments and Methods in Physics Research B. 46, 295–305, 1990.*
22. Optical and electrical properties of some electron and proton irradiated polymers. R. Mishra, S.P. Tripathy, D. Sinha, K.K. Dwivedi, S. Ghosh, D.T. Khathing, M. Muller, D. Fink, W.H. Chung. *Nuclear Instruments and Methods in Physics Research B 168, 59–64, 2000.*
23. High energy ion beam irradiation of polymers for electronic applications D. Fink, P.S. Alegaonkar, A.V. Petrov, M. Wilhelm, P. Szimkowiak, M. Behar, D. Sinha, W.R. Fahrner, K. Hoppe and L.T. Chadderton. *Nuclear Instruments and Methods in Physics Research B. 236, 11–20, 2005.*
24. Surface modifications and nanoparticle formation by negative ion implantation of polymers. H. Boldyryeva, N. Kishimoto, N. Umeda, K.Kono, O.A. Plaksin and

- Y.Takeda. *Nuclear Instruments and Methods in Physics Research B*, 953-958, 2004.
25. Proceedings of the Indo German Workshop on Synthesis and Modifications of Nano-Structured Materials by Energetic Ion Beams, *Nuclear Instruments and Methods in Physics Research B*. 2006.
 26. An electron paramagnetic resonance study of PP and PP/SBS blends irradiated with gamma rays. P. Silva, C. Albano, R. Perera, J. González and M. Ichazo, *Nuclear Instruments and Methods in Physics Research B*. 226, 3, 320-326, 2004.
 27. Davenas J., Xu X. L., Boiteaux G. and Sage D. Relation between structure and electron properties of ion irradiated polymers. *Nuclear Instruments and Methods in Physics Research B*. 39, 754-763, 1989.
 28. Optically absorbing layers on ion beam modified polymers: A study of their evolution and properties. D. Fink, Muller, L.T. Chadderton, P. H. Cannington, R. G. Elliman and D. C. Mc Donald. *Nuclear Instruments and Methods in Physics Research B*. 32, 125-130, 1988.
 29. Poly (methyl methacrylate) sensitivity variation versus the electronic stopping power at ion lithography exposure. G. M. Mladenov and B.Emmoth. *Applied Physics Letter*. 38, 1000-1004, 1960.
 30. Ion implantation, a method for fabricating light guides in polymers. J. R. Kulish, H. Franke, A.Singh, R. A. Lessard and E. J. Knystautas. *Journal of Applied Physics*. 63, 2517-2521, 1988.
 31. Micromechanical properties of electron irradiated PVDF-TrFE copolymers. F.Macchi, B. Daudin, J. Hillairet, J. Lauzier, J.B. N'Goma, J.Y. Cavaille and J. F. Legrand. *Nuclear Instruments and Methods in Physics Research B*. 46, 334-337, 1990.
 32. Improved surface properties of polymer materials by multiple ion treatment. E.H. Lee, M.B. Lewis, B. J. Blan and L. K Mansur. *Journal of Material Research*. 6, 610-628, 1991.
 33. Changes in the optical energy gap and ESR spectra of proton-irradiated unplasticized PVC copolymer and its possible use in radiation dosimetry. A.A. Abdel-Fattah, H.M. Abdel-Hamid, R.M. Radwan. *Nuclear Instruments and Methods in Physics Research B*. 196, 279-285, 2002.
 34. Electron spin resonance investigation on Polycarbonate irradiated with U ion. M.I Chipara and J. Reyes Romero. *Nuclear Instruments and Methods in Physics Research B*. 185, 77-82, 2001.
 35. Pyrolytic effects induced by energetic ions in polymers. T. Steckenreiter, E. Balanzat, H. Fuess, C. Trautmann. *Nuclear Instruments and Methods in Physics Research B*. 151, 161-168, 1999.

36. Ion beam induced changes of the refractive index of PMMA. J. P. Biersack. and R. Kallweit. *Nuclear Instruments and Methods in Physics Research B.* 46, 309-312, 1990.
37. Study of chemical, optical and thermal modifications induced by 100 MeV silicon ions in a polycarbonate. A. Srivastava, T.V. Singh, S. Mule, C.R. Rajan, S. Ponrathnam. *Nuclear Instruments and Methods in Physics Research B.* 192, 402-406. 2002.
38. Polymers: Chemistry & Physics of Modern Materials. J.M. Cowie. Intertext Books Billings, Worcester, Great Britain. 283, 1973.
39. Proceedings of the 14th International Conference on Ion Beam Modification of Materials. *Nuclear Instruments and Methods in Physics Research B.* 242 (Issues 1-2) 2006.
40. Fundamental Aspects and Technological Applications. E.H. Lee. Chapter 17 in *Polyimides*, in: K. Mittal, M Ghosh (Eds.), Marcel Dekker, 471-503, 1996.
41. Ion beam lithography using single ions. A. Alves, P. Reichart, R. Siegele, P.N. Johnston and D.N. Jamieson. *Nuclear Instruments and Methods in Physics Research B.* 202, 412-420. 2006.
42. Radiation induced modification on thermal properties of PADC Detector. D. Sinha and K.K. Dwivedi. *Radiation Measurements.* 36, 713-718, 2003.
43. Effects of talc and gamma irradiation on mechanical properties and morphology of isotactic polypropylene/talc composites. M. Denae, V. Musil, I. Sijmit, F. Ranogajec. *Polymer Degradation and Stability.* 82, 263-270, 2003.
44. The effect of gamma radiation on the properties of polypropylene blends with styrenebutadiene-styrene copolymers. R. Perera, C. Albano, J. Gonzalez, P. Silva, M. Ichazo. *Polymer Degradation and Stability.* 85, 741-750, 2004.
45. E.H. Lee, G.R. Rao, L.K. Mansur, *TRIP* 4, 229, 1996.
46. J.N. Randall, D.C. Flanders, N.P. Economou, J.P. Donnelly, E.I. Bromley, *Applied Physics Letter.* 42, 457-465. 1983.
47. T.M. Hall, A. Wagner, L.F. Thompson. *Applied Phys. Lett.* 53, 3997, 1982.
48. A. Chapiro. Radiation Chemistry of Polymeric Systems, Wiley Publications, 1962.
49. Production of single-pore membranes for the measurement of red blood cell deformability. H. G. Raggkamp, H. Kiewewetter, R. Spohr, U. Daur and L. C. Busch. *Biomedizinische Technik.* 26, 167-169, 1981.
50. Production and use of nuclear tracks: Imprinting structure on solids. B. E. Fischer and R. Spohr. *Rev. Mod. Phys.* 55, 907-948, 1983.
51. Fission track dating of Bed I, Olduvai Gorge. R. L. Fleischer, P. B. Price, R. M. Walker and L.S.B. Leakey. *Science.* 148, 72-74, 1965.

52. Fission track ages and track annealing behaviour of some micas. R. L. Fleischer, P. B. Price, E. M. Symes and D.S. Miller. *Science*.143, 349-351, 1964.
53. Characteristics of fission tracks in Zircon: Applications to Geochronology and cosmology. S. Krishnaswami, D.Lal, N. Prabu and D. Mac Dougall. *Earth Planet. Science. Letters*. 22, 51-59, 1973.
54. Ternary fission produced in Au, Bi, Th and U with Ar Ions. V. P. Pereygin, N. H. Shadieva, S. P. Tretyakova, A.H. Boos and R. Brandt. *Nuclear. Physics. A* 127, 577-585, 1969.
55. Direct determination of the life time of excited compound nuclei by angular distribution measurements of fission fragments emitted from single crystals. W. M. Gibson and K.O. Nielson. *Phys. Rev. Letters*. 24, 114 -117, 1970.
56. Dielectric plastic as high exposure gamma-ray detectors. A.L. Frank and E. V. Benton. *Radiation Effects*., 269-272, 1970.
57. The Effect of gamma dose on the alpha response of CR-39. T. Portwood and D. L. Henshaw. *Nuclear. Tracks*. 12, 105-108, 1986.
58. Gamma ray dosimetric studies on CR-39 detectors. A. Joseph and K. M. Varier. *Indian Journal of Pure and Applied Physics*. 33, 406-409, 1995.
59. R. Shweikani, S. A. Durrani. and T. Tsuruta. Effects of gamma irradiation on the bulk and track etching properties of Cellulose Nitrate (Daicel 6000) and CR-39 plastics. *Nuclear. Tracks Radiation Measurements*. 22, 153-156, 1993.
60. Y. Komaki, N. Ishikawa and T. Sakurai. Effect of Gamma rays on etching of heavy ion tracks in Polyimide. *Radiation Measurements*. 24, 193-196, 1995.
61. Effect of high gamma dose on the PADC properties. F.Abu-Jarad, A.M. Hala, M. Farhat and M. Islam. *Radiation Measurements*. 28, 111 – 114, 1997.
62. Effect of high gamma doses on the etching behaviour of different types of PADC detectors, D. Sinha, R. Mishra, S.P. Tripathy, K.K. Dwivedi. *Radiation Measurements*. 33, 139-143, 2001.
63. The etching and structural studies of gamma irradiated induced effects in CR-39 plastic track recorder. S. Singh and S. Prasher. *Nuclear Instruments and Methods in Physics Research B*. 222 (Issue 4), 518-524, 2004.
64. Gamma-irradiation effects on track etching characteristics of polyester nuclear track detector Chhavi Agarwal, P. C. Kalsi, A. Ramaswami. *Radiation Effects and Defects in Solids*. Volume 161, No. 2, 2006. pp. 131 – 133.
65. Gamma-ray-induced modifications in microscopic glass slide used as a track detector. Surinder Singh and Amanpreet Kaur Sandhu. *Radiation Effects and Defects in Solids* Volume 161, No. 4, 235 – 239, 2006.
66. Proceedings of the 22nd International Conference on Nuclear Tracks in Solids, *Radiation Measurements Volume 40, Issues 2-6, Pages 125-794, November.2005.*

Chapter - 2

CHAPTER-2

TYPES OF RADIATION AND THEIR INTERACTION WITH MATTER

2.1. TYPES OF RADIATION:

Radiations are broadly classified into two categories:

(a) Charged particles

(b) Neutral radiations

The charged particle radiations include heavy charged particles like heavy ions, fission fragments, α -particles and protons and light charged particles like the electrons and positrons. Neutral radiations consist of neutrons and electromagnetic radiations namely gamma rays and X-rays.

2.1.1. Charged Particles:

[a] Electrons and Positrons: - energy is in the range of 10 eV to few MeV and velocity is in the range of 10^9 to 10^{10} cms^{-1} .

[b] Alpha particles and Protons: energy is in the range of 1 MeV to few MeV and velocity is in the range of 10^8 - 10^9 cms^{-1} .

[c] Fission fragments: energy is in the range of 60 MeV to 100 MeV, velocity is in the range of 10^7 to 10^8 cms^{-1} and a charge state of +20 to +22.

[d] Accelerated Particles: Accelerators are the most versatile heavy ion sources which provide monoenergetic, monoisotopic and highly parallel beams of practically all

ions. An extremely wide range of areal flux of 10^0 - 10^{12} cm^{-2} and ion energies of 10^0 - 10^3 MeV/u is attainable depending on the type and size of the accelerator.

2.1.2. Neutral and Uncharged Radiations:

[a] Electromagnetic radiations: - X-rays have energy upto 100 keV and gamma rays have energy ranging from 20 keV to 10 MeV.

[b] Neutrons: - energy is in the range of 0.025 eV to a few MeV.

2.2. INTERACTIONS OF RADIATION WITH MATTER:

Charged particles interact with matter through coulombic forces. On the other hand, in case of radiations that do not have charge, interaction is a two step process. First they undergo a reaction/interaction to produce charged particles to which kinetic energy is transferred and these particles then interact through coulombic forces.

2.2.1. Heavy Charged Particle: Heavy charged particles interact with matter through a series of binary collisions with the electrons of the atoms and molecules via columbic interaction and produce ionisation and excitation in the medium (or absorber). According to the law of conservation of momentum, the maximum kinetic energy (T_e) which can be imparted to the electron by a charged particle of mass M and energy E in a single collision is given as

$$(T_e)_{\max} = 4m_0(E/M) \quad (2.1)$$

Thus a proton of energy 5 MeV can transfer a maximum of 10keV energy to the electron. Due to small loss in energy per collision, heavy charged particles generally travel in a straight path in a medium.

2.2.2. Electrons: Like heavy charged particles, electrons also lose their energy in a stopping medium by collisional losses through coulombic interactions. In electron collisions, the incident electron can lose up to one half of its energy in a single collision. The mean deflection of an incident electron as a result of an ionisation or radiation collision is also large compared to a heavy particle. In addition the electron also suffers scattering due to elastic collision with the nuclei and electrons of the target atoms, resulting in further deflection from their direction of incidence. Electrons also lose their energy by emission of Bremsstrahlung. High speed charged particles passing close to the nucleus of an atom may be decelerated and radiate electromagnetic radiation. The energy loss due to emission of Bremsstrahlung will be greatest for light particles and stopping materials of higher atomic number.

2.2.3. Electromagnetic Radiation: Electromagnetic radiations like X-rays and gamma rays lose their energy in a stopping material through the following three processes -

[a] Photoelectric Effect:- In this process, a photon is absorbed in the medium and the energy is transferred to the atom. This energy if transferred to one of the electrons (normally tightly

bound electrons), then the velocity of that electron will be too high to remain in the orbital, thus resulting in its emission. The difference between the incident photon energy (E_γ) and the ionization energy of the electron (E_b) appears as the kinetic energy (E_e) of the ejected electron.

$$E_e = (E_\gamma - E_b) \quad (2.2)$$

The probability of emission of K electrons is higher than the other electrons provided the energy of the photon is higher than the threshold energy required for its ejection.

[b] Compton Scattering: In this process the photon interacts with an electron which may be loosely bound or free. The incoming photon is deflected through an angle θ , with respect to its original direction and a fraction of its energy is transferred to the electron (Figure.2.1).

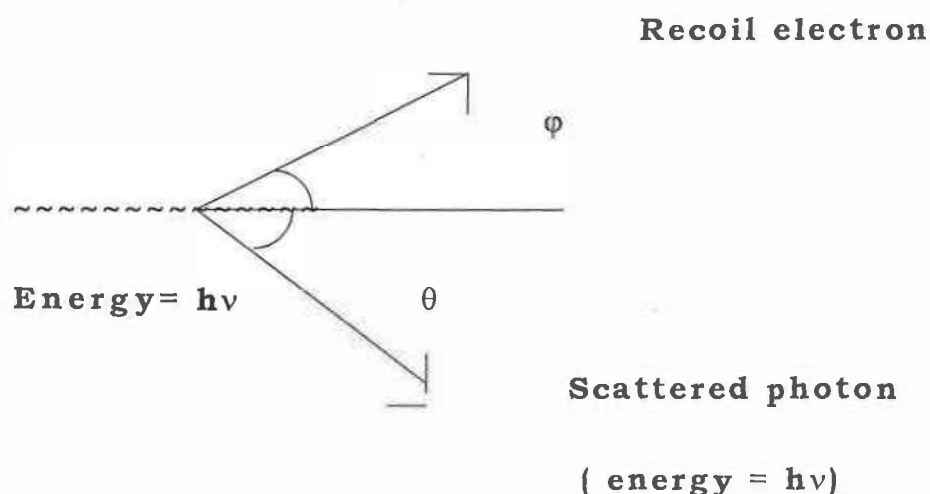


Fig. 2.1 The Compton effect

The outgoing photon energy is given by,

$$h\nu' = h\nu/[1+\{(h\nu/m_0c^2)(1-\cos\theta)\}] \quad (2.3)$$

The electron energy ($E_a = h\nu - h\nu'$) is zero at $\theta = 0$ and maximum ($\geq h\nu - m_0c^2/2$) at $\theta = 180$. Since electrons in the entire energy region between $E = 0$ and $\geq h\nu - m_0c^2/2$ are produced, a continuous response of the detector is obtained. Therefore, this interaction is not very useful for detection. Compton Scattering predominates for photon energies between 1 and 5 MeV in high Z materials and over a wide range of energies in low Z materials.

[c] Pair Production :- This process involves the complete absorption of a photon in the vicinity of an atomic nucleus with the formation of an electron- positron pair. This interaction occurs mainly in the coulomb field of the nucleus of the absorbing material. The conservation of energy is given by the equation

$$h\nu - 2m_0c^2 = E_{e+} + E_{e-} \quad (2.4)$$

where E_{e+} and E_{e-} are kinetic energies of the positron and electron respectively, and m_0 is the rest mass of the positron or electron.

2.2.4. Neutrons: Neutrons do not directly produce ionisation in matter. However they interact with nuclei of atoms of the absorbing medium through different nuclear reactions and

thus, interact with matter by elastic and inelastic scattering and nuclear reactions.

2.3. INTERACTION OF RADIATION WITH POLYMERS:-

The interaction of radiation with a polymer and the subsequent events can be chronologically divided into three distinct periods : energy absorption, establishment of thermal equilibrium, and the establishment of chemical equilibrium[1].

2.3.1. Energy Absorption: There are three modes of energy absorption: viz., electron displacement (ionisation and excitation), atomic displacement, and generation of impurity atoms as a result of nuclear reactions. For non-relativistic particles, the probability of energy transfer through a nuclear reaction is small compared to other modes of energy transfer[1]. Even if such an event does occur, it is quite discrete and obvious. Thus it need not be discussed with the other, more nearly continuous energy loss mechanisms. Except at very low velocities of the incident charged particle, the energy transfer via atomic displacement can also be neglected. However, the possibility of a 'displacement' spike occurring in last few microns of a heavy particle path can not be discounted at this time. Thus, the primary mechanism for energy absorption in polymeric systems is electronic displacement. This takes place in the time period of less than 10^{-15} seconds.

2.3.2. Thermal Equilibrium: The second phase, lasting for approximately 10^{-12} to 10^{-9} seconds, involves the transport and disposition of absorbed energy by molecular motion. During this phase thermal equilibrium within the solid is established. Again there are three alternatives: energy can be emitted as luminescence, it can be dissipated as heat, or energy can be stored as potential energy in the form of chemically reactive species. The exact path followed depends strongly on the structure of the molecule and the environmental conditions. A fraction of the energy emitted during luminescence can be in the form of short ultraviolet light which will be locally reabsorbed by the plastic. However, since the amount of energy involved in luminescence is generally of the order of only a few percent of the total, the photochemistry arising from this effect can be neglected. The great bulk of the energy ends up as heat. In case of slow, massive, very heavily ionising particles, such as fission fragments, the sudden deposition of a large amount of energy in a highly restricted space may for a period of 10^{-11} seconds, raising the local temperature in excess of several hundred degrees centigrade - the so-called 'thermal' spike concept [2]. Temperature in this range can activate certain atomic and electronic processes resulting in extensive atomic rearrangements and local chemical changes. Other damage spikes such as "plasticity", "displacement electron", [2] and "ion explosion" [3] have also been proposed.

2.3.3. Chemical Equilibrium: The duration of the third and final stage may be extended by diffusion processes and reaction rate may vary from a minimum of about 10^{-2} seconds upto years in certain solids. It involves the reduction of a small fraction of the energy which ends up as potential energy of the reactive species to a thermally stable level[1]. These species include electrons, excited molecules, ions and radicals. While the life time of excited molecules is short (10^{-9} to 10^{-8} s), measurable populations of the other species may persist almost indefinitely. This is because electrons are held in traps while ions and radicals are stabilized by the cage effect. The cage effect greatly enhances the probability of immediate recombination of the chemically reactive species inside the cage, while at the same time impeding reactions with molecules on the out side.

2.4. MECHANISM OF ION-MATTER INTERACTION

Ion interaction with polymers leads to both micro structural changes and macroscopic changes. The micro structural changes of polymers upon ion impact can be classified according to Table 2.4.1.[4] This table makes clear that polymer irradiation affects a multitude of parameters, nearly all of which are interconnected with each other in a delicate way. In general, their characterization requires more than just one technique, as all experimental methods are sensitive to different parametric dependencies of the same property. Irradiated polymers lead to significant macroscopic

changes. These changes are dependent on the dose and fluence of the radiation. It has been observed by several authors that due to irradiation, bulk properties of the polymers like density, surface, chemical resistance, optical, electrical, thermal properties etc. take place. Some of the important and relevant references have already been cited in Chapter-1.

2.5. FORMATION OF NUCLEAR TRACKS:

It is already a known phenomenon that the energetic charged particles create sub-microscopic damage trails in solid dielectrics such as glasses, plastics and inorganic crystals. These trails are of the order of 5 - 10 nm in diameter and are visible only at high magnification under an electron microscope. Due to the rapid fading characteristics of such latent tracks under the influence of high electron flux, it becomes difficult to make accurate measurements of any desired track parameter. With the help of suitable etching processes it is possible to enlarge and fix these trails into permanent tracks which could be easily observed under an optical microscope. Out of several track developing techniques, chemical etching is by far the most simple, accurate and widely used technique. The principle of chemical etching of nuclear tracks is based on the fact that the damage-trails are associated with large free energy, leading to a preferential etching along the track as compared to normal material when the detector is immersed

in any suitable chemical etchant. The speed with which the undamaged material of the detector is dissolved away by the etchant solution is known as bulk-etch rate (V_G). On the other hand, the rate of increase of track length with respect to etching time is defined as track-etch rate (V_T). The shapes of the etched tracks depend on the relative magnitude of the etch rates. In most plastic track detectors, one observes narrow conical tracks where as in glass detectors, shallow etch-pits are generally observed. SEM images of tracks observed after etching [5] are shown in Figure 2.2. In the past three decades an aura of excitement and fascination has been created in the field of nuclear tracks in solid dielectrics [6-15] partly because of its simple methodology but primarily because of the great diversity of its usefulness in scientific and technological domains which ranges from Anthropology[16], Geochronology[17,18]to Space research [17,18], from Geophysics [19], Superfluidity [20], Lithography[21] and Dosimetry [22] to Biomedical research [23] and from Gem diamond manufacturing [24] to Cancer therapy [25]. In addition to the broad range of applications of Solid State Nuclear Track Detectors (SSNTDs), the usefulness of these detectors In Nuclear Physics is particularly becoming more and more important. The study of heavy ion nuclear reactions [26,27], high resolution particle identification [28,29], ternary fission [30,31], measurement of reaction cross-section and life time [32-34], detection of short lived heavy nuclei [35], discovery of super

Table 2.1. Microstructural Changes in Properties of Ion-Irradiated Polymers

| Property | Experimental Techniques | Physical Informations obtained |
|--|---|---|
| Radical Formation | EPR | Unpaired spin density → degree of chemical reactivity |
| | Trapping of markers | Radical density, radical depth distribution |
| Destruction of existing chemical compounds | Chromatography | Mass of fragment → radiochemical inform. |
| | FTIR | Absorption frequency of functional groups → radiochemical inform. |
| | Luminescence | Degradation of luminescence spectra → radiochemical inform. |
| Formation of new com-Pounds | Chromatography | Mass of new compound → radiochemical inform. |
| | FTIR | Absorption frequency of functional groups → radiochemical inform. |
| | Mass Spectrometry | Mass of new compound → radiochemical inform. |
| Chain scissioning | Chromatography | Mass of scissioned compound → radiochemistry |
| | FTIR | Absorption frequency of functional groups → radiochemical inform. |
| | Mass Spectrometry | Mass of scissioned compound → radiochemistry |
| Property | Experimental Techniques | Obtained Informations |
| Cross-linking | Chromatography | Masses of new compounds → radiochemical inform. |
| | Residual matter after chemical dissolution Swelling by solvents | Fraction above gelation point → radiochemical information Remaining free volume → spatial information |
| | FTIR | Absorption frequency of functional groups → radiochemical informations |
| | Elasticity measurement DSC | Crosslink density Melting temperature → structural information |
| Free Volume Changes | Positron annihilation | Total free volume Microcavity size |
| | Marker uptake with different sizes of phosphorescent markers + tomography | Depth distribution of Total free volume V_{free} of cavities > d Alignment of pores |
| | SANS, SAXS DSC | 3D distribution of free volume Scattering intensities → Microcavity radius, size, surface, density Melting temperature → structural information |
| Crystallinity Changes | XRD AFM | Crystalline fraction Visualisation of crystalline domains |
| | FTIR | Characteristic bands for amorphisation and crystallinity |
| Cluster Formation | AFM | Visualisation of clusters |
| | SANS | Scattering intensities → |
| | SAXS | Cluster radius, size, density |
| | Conductivity studies | Cluster size, distance |

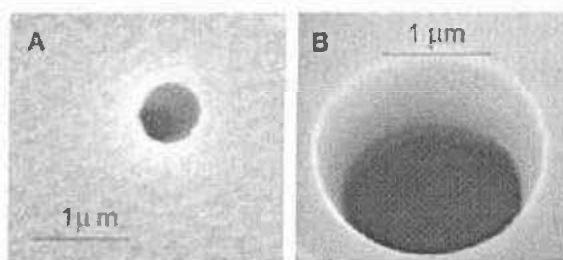


Fig. 2.2. Scanning electron microscopy (SEM) images of the etched side of a PET (A) and a Kapton foil (B), showing the large opening of a conical tracks (polymers were irradiated with under normal incidence with single heavy ions. Au for PET, and U for Kapton) of energy 11.4 MeV per nucleon) [5]

heavy elements [36], exotic decay [37,38], range and energy loss measurement in elemental and complex media [39-42], preparation of micro-filters [43-44], etc., involve extensive use of SSNTDs.

Experience shows that the track registration characteristics of polymeric Solid State Nuclear Track Detectors (SSNTDs) are greatly affected when exposed to high doses of gamma rays [45-55]. The modification in characteristics originates from the structural alterations by irradiation of polymers. Since polymeric solid state nuclear track detectors consist of long chain molecules, the net effect on the matrix due to irradiations is the production of many broken molecular chains, leading to a reduction in the average molecular weight of the substance. All these modifications change the track properties like bulk-etch rate, track-etch rate, etching efficiency etc.

In polymeric track detectors, only those charged particles with linear energy transfer (LET) above a critical value can create distinct etchable tracks. Atomic radiations

such as UV rays and X-rays, nuclear radiations like gamma rays and beta rays are low LET radiations. They mostly affect the physical and chemical properties of the polymeric films. Though they can not create any tracks, but they can affect etch rate values of detectors depending upon the absorbed dose. For track detectors exposed to high LET charged particles followed or preceded by low LET radiation exposure, both the bulk-etch rate and track-etch rate are found to vary in accordance with the absorbed doses of low LET radiations. Having a thorough knowledge about these effects are therefore necessary, when the track detectors are used for detecting charged particles in an atmosphere of intense low LET background radiation. Besides, it is useful in evaluating the dosimetric properties of track detectors.

2.5.1. Track registration criteria: The ability to predict which particle will produce latent (etchable) tracks in a given polymeric system is the basic requirement in the understanding and purposeful utilisation of detectors. In the past few years, several track registration criteria have been proposed. We will consider these criteria both in terms of their utility as well as the physical track formation mechanisms that are implied, and what distinguishes the latent track region from the unaffected bulk material. Also, the exact chemical and physical properties of the preferentially etchable region depends very strongly on the mass, charge and velocity of the track forming particles, on the chemical structure and physical state of the dielectric

material used during irradiation and the environmental conditions. However, in general it is expected that this region will have the properties listed in Table-2.2. The parameters which influence track etching can be separated into five broad categories :(1) The material parameters (which will include the chemical composition, molecular weight, crystallinity, solvent content, etc.);(2) the particle parameters (charge:Z, mass:M, velocity:V);(3) the irradiation

Table-2.2. Properties of the latent track region in the irradiated polymers

| |
|---|
| Reduced molecular weight |
| Increased number of polymeric chain ends |
| Increased solubility |
| Presence of new chemical species such as |
| a. free radicals |
| b. trapped gases (CO, CO ₂ , H ₂ , O ₂ etc.) |
| c. increased unsaturation |
| Reduced physical density |
| increased optical absorption, particularly in the UV region. |

environmental parameter (temperature, atmosphere, etc.); (4) the pre-etch storage parameters (atmosphere, temperature, etc.); and (5) the etching parameters (including type of etching solution, concentration, temperature, time etc.).

2.5.2. Theories used for track formation: Various authors have suggested that track formation should be related to a number of different parameters, such as total energy loss

rate, primary ionisation, restricted energy loss, etc. Once a certain track formation criteria is set up, it, which takes the form of a statement that tracks are formed in a medium when and only when, the chosen parameters exceed some critical value whatever be the bombarding particle. For a valid track formation, having parameters, (say) X , should be possible to draw a unique threshold value, X_c , separating the region of track etchability from that corresponding to non-etchability. In recent years, this view of track formation criteria has been modified somewhat in that, less emphasis is now placed on the threshold value of X . This is because experimental data have accrued [56,57] to show that the track etching rate (V_T) is a smoothly varying function of incident particle parameters. It is now usual to seek a parameter X such that $V_T(X)$ always has the same value (for a given combination of detector and etching conditions) at a given value of X , regardless of the combination of ionic charge and velocity that may lead to the X value in question.

The concept of 'thermal spike' was introduced as a mechanism by which energetic particles could produce considerable disruption of a crystal lattice. In this model the passage of an energetic particle is assumed to produce intense heating of a localised region (thermal spike concept) of the lattice. The region is therefore raised to a high temperature [2], from which it cools rapidly via heat conduction. As a result of this heating episode various

atomic processes are activated, and damage to the lattice is done.

Chadderton *et. al.* [58] and Chadderton and Torrens [59] have presented more detailed considerations of the manner in which the electronic excitation produced by the fission fragment is transferred to the lattice atoms. They found that, in metals, energy is lost by δ -rays primarily via electron-electron collisions down to very low electron energies, because the energy loss per collision is greater, and the relaxation time is shorter, than the electron-photon interactions. Thus the excitation is spread through out a large volume by the electrons before significant energy transfer to the lattice occurs; and therefore the peak temperature to which the lattice is raised in a metal is low. In insulators, on the other hand, electrons can interact readily with polar and acoustic modes of lattice vibration; and, indeed once the δ -ray energy falls below that equal to the band-gap i.e., several electron-volts release by the δ -rays of further electrons into the crystal's conduction band becomes impossible. Therefore, electron-photon collisions are expected to be the predominant energy loss process in insulators, and the excitation is communicated to the lattice more efficiently in such materials.

The nature of track formation appears to be distinctly different in polymers from what it is in inorganic solids. The damage along tracks in inorganic solids consists mainly of

displaced atoms. which can be explained by "ion explosion spike" model [3], is the use of a burst of ionisation along the path of a charged particle to create an electronically unstable array of adjacent ions which eject one another from their normal sites into interstitial positions.

REFERENCES:-

1. On the latent track formation in organic nuclear charged particle track detectors. E.V. Benton. *Radiation Effects*. 2, 273-280, 1970.
2. Radiation damage in solids. D.S. Billington and H. Jr Crawford. *Princeton University Press*. 1961.
3. The ion explosion spike mechanism for formation of charged particle tracks in solids. R. L Fleischer, P. B. Price and R. M. Walker. *J. Appl. Phys.* 36, 3645-3652, 1965.
4. "Fundamentals of Ion-Irradiated polymers" D. Fink, *Springer*, 2004.
5. Ion transport through asymmetric nanopores prepared by ion track etching Z. Siwy, P. Apel, D. Dobrev, R. Neumann, R. Spohr, C. Trautmann, K. Voss. *Nuclear Instruments and Methods in Physics Research B*. 208, 143 -148, 2003.
6. Examination of fission fragments tracks with an electron microscope. E.C.H. Silk and R.S. Branes. *Phil. Mag.* 4, 970-971, 1959.
7. R. L Fleischer, P. B. Price and R. M. Walker. "Nuclear Tracks in Solids, Principles and applications" *Univ. of California Press*, 1975.
8. Proceedings of the 15th Int. Conf. on SSNTD, *Nuclear Tracks and Radiation Measurements*. 19, 11-974, 1991.
9. Proceedings of the 19th International Conference on Nuclear Track in Solids. *Besancon, France*. 1998.
10. Proceedings of the 20th International Conference on Nuclear Tracks in Solids, *Portoroz, Slovenia* 2000.
11. Proceedings of the 21st International Conference on *Nuclear Tracks in Solids, Delhi*, 2002.
12. Towards new applications of ion tracks. J. H Zollondz and A. Weidinger. *Nuclear Instruments and Methods in Physics Research B*. 225, 2, 178-183, 2004.
13. Proceedings of the 22nd International Conference on Nuclear Tracks in Solids. *Radiation Measurements*. 40, 2-6, 125-794, 2005.

14. Science and technology with nuclear tracks in solids. P.B. Price. *Radiation Measurements*. 40, 2, 146-159, 2005.
15. Status of ion track technology—Prospects of single tracks R. Spohr *Radiation Measurements*. 40, 2, 191-202, 2005.
16. Fission track dating of Bed I R. L. Fleischer, P.B. Price, R.M. Walker and L.S.B. Leakley., Olduvai Gorge. *Science*. 148, 72-74, 1965.
17. Fission track ages and track annealing behaviour of some micas. R. L. Fleischer, P.B. Price, E. M. Symes. and D.S. Miller. *Science*. 143 349-351, 1964.
18. Characteristics of fission tracks in Zircon: Applications to Geochronology and cosmology. S. Krishnaswami, D.Lal, N. Prabu and D.Mac Dougall. *Earth Planet.Sci. Letters*. 22, 51-59, 1973.
19. Origin of fossil charged particle tracks in meteorite. R. L. Fleischer, P. B. Price., R. M. Walker and M. J. Maurette . *Geophysics. Research*. 72, 331-353, 1967.
20. Creation of quantized vortex rings in superfluid Helium. G. Gamota. *Physics. Review. Letters*. 31, 517-520, 1973.
21. Heavy ion Microlithography - a new tool to generate and investigate submicroscopic structures. B.E. Fischer and R.Spohr. *Nuclear Instruments and Methods in Physics Research B*. 168, 241-246, 1980.
22. Technological applications of Science: the case of particle track etching. R. L. Fleischer, H. W. Alter, S.C. Furman, P. B. Price and R. M. Walker. *Science*. 178, 255-263, 1972.
23. Production of single-pore membranes for the measurement of red blood cell deformability. H.G. Raggenkamp, H. Kiesewetter, R. Spohr, U.Daur and L. C.Busch. *Biomedizinische Technik*. 26, 167-169. 1981.
24. Boron content and profiles in large laboratory diamonds. R.M. Chrenko. *Nature*. 229, 165-167, 1971.
25. A sieve for the isolation of cancer cells and other large cells from the blood. S.Seal, *Cancer* 17, 637-643, 1964.

26. Multi-fragment decay relations induced by heavy ions and studied with mica track detectors. P. Vater, H.J. Beker, R. Brandt. and H. Freiesleben. *Nuclear Instruments and Methods in Physics Research B*. 147, 271-278, 1977.
27. Fragment correlations in the reaction 9.03 MeV/u $^{238}\text{U} + ^{\text{nat}}\text{U}$. R. Hagg, G. Fiedler, R. Ulbrich, G. Breitbach and P.A. Gottschalk. *Z. Physik. A*. 316, 183-193, 1984.
28. High resolution measurements of slowing cosmic rays from Fe to U. D. O'Sullivan, P.B. Price, E.K. Shirk, P.H. Flower, J.M. Kidd, E.J. Kodetich and Thorne R. *Phys. Rev. Letters*. 26, 463-466, 1971.
29. Isotopenanalyse on neiderenargetischen teilchen der elemente bor, kohlenstoff, stickstoff und sauerstoff aus der kosmischein strahlung in plastik-detektoren. Beaujean R. and Enge WZ. *Physik*. 256, 416-440, 1972.
30. Perelygin V. P., Shadieva N. H., Tretyakova S. P., Boos A. H. and Brandt R. Ternary fission produced in Au, Bi, Th and U with Ar Ions. *Nucl. Phys. A*. 127, 577-585, 1969.
31. Investigations on ternary photofission with track recorders of different sensitivity. Medeczky L. and Somogyi G. *Radiation Effects*. 5, 51-59, 1970.
32. Low-energy cross sections for $^{10}\text{B}(p,\alpha)^7\text{Be}$. Szabo J., Csikai J. and Varnagy M. *Nucl. Phys. A*. 195, 527-533, 1972.
33. Chemical separation of Khurchatovium. Zvara I., Belov V. Z., Chelnokov L. P., Domanov V. P., Hussonois M., Korotkin Yu. S., Schegolev V. A. and Shalayevsky M. R. *Inorg. Nucl. Chem. Letters*. 7, 1109-1116, 1971.
34. Direct determination of the life time of excited compound nuclei by angular distribution measurements of fission fragments emitted from single crystals. Gibson W. M. and Nielson K. O. *Phys. Rev. Letters*. 24, 114-117, 1970.
35. Synthesis and physical identification of the isotope of element 104 with mass number 260. Flerov G. N., Oganesyam Yu. Ts., Lobanov Yu. V., Kuznetsov V. I., Druin V. A., Perelygin V. P., Gavrilov K. A., Tretyakova S. P. and Plotko V. M. *Phys. Letters*. 13, 73-75, 1964.

36. Search for super heavy elements in natural and proton induced materials. Geisler F. H., Phillips P. R. and Walker R. M. *Nature*. 244, 428-429, 1973.
37. Barwick S. W., Price P. B. and Stevenson J. D. Radioactive decay of ^{232}U by ^{24}Ne emission. *Phys. Rev. C* 31 (1985), 1984-1986.
38. Price P. B., Stevenson J. D., Barwick S. W. and Bavan H. L. *Phys. Rev. Letters*. 54, 158-161, 1985.
39. Energy loss and mean ranges of ^{93}Nb in Nickel and Tantalum. Saxena A. and Dwivedi K. K. *J. Phys. D: Appl. Phys.* 23, 476-480, 1990.
40. Energy loss and mean ranges of ^{86}Kr and ^{197}Au in Tantalum. Dwivedi K. K., Srivastava A., Ghosh S., Sinha D., Saxena A. and Brandt R. *Radiat. Meas.* 26, 561-563, 1996.
41. Measurement of range and energy-loss of energetic ^{58}Ni and ^{197}Au Ions in Kapton. Srivastava A., Laldawngliana C., Sinha D., Ghosh S., Dwivedi K. K. and Brandt R. *Nucl. Sci. J.* 33, 85-93, 1996.
42. Mean ranges of ^{161}Dy in Hostaphan and Kapton. Ghosh S., Sinha D., Mawar A., Singh S., Srivastava A., Dwivedi K. K. and Brandt R. *Radiation Measurement*. 28, 41 - 44, 1997.
43. Development and characterization of polycarbonate microfilters. Dey M., Raju J., Ghosh S. and Dwivedi K.K. *Nucl. Tracks Radiat. Meas.* 22, 907-908, 1993.
44. On the development of polypropylene (PP) microfilters. Heise S., Vater P., Brandt R. Dwivedi K.K. and Dankmeyer C. *Nucl. Tracks Radiat. Meas.* 22 909-910, 1993.
45. Gamma ray dosimetric studies on CR-39 detector. Joseph A. and Varier K.M. *Indian Journal of Pure & Applied Physics*. 33, 406-409, 1995.
46. Effect of high gamma dose on the CR-39 properties. Abu-Jarad F., Hala A.M., Farhat M. and Islam M. *Radiation Measurements*. 28, 111-114, 1997.
47. Modifications of radiation detection response of PADC track detectors by Photons. D. Sinha, K.K. Dwivedi. *Radiation Physics and Chemistry*. Vol 53, 99-105, 1998.

48. Photon induced modifications of Triafol-BN and Triafol-TN polymeric detectors. D. Sinha, G.K. Sarkar, S. Ghosh, A. Kulukshetra, K.K. Dwivedi, D. Fink. *Radiation Measurements. Vol 29(6), 599-604, 1998.*
49. Structural modifications and track registration response of some gamma irradiated polycarbonate detectors. D. Sinha, S. Ghosh, K.K. Dwivedi, D. Fink. *Radiation Effects and Defects in Solids. Vol. 145, 45-56, 1998*
50. Effects of gamma irradiation on the bulk and track etching properties of Cellulose Nitrate (Daicel 6000) and CR-39 Plastics. Shweikani R., Durrani S.A. and Tsuruta T. *Nuclear Tracks Radiation Measurement 22, 153-156, 1993.*
51. Gamma Effect on Track properties of PADC Detector. D. Sinha, T. Swu, S.P. Tripathy, R. Mishra, K.K. Dwivedi. *Radiation Measurements. Vol. 36, 229 -231, 2003.*
52. The etching and structural studies of gamma irradiated induced effects in CR-39 plastic track recorder. Surinder Singh and Sangeeta Prasher. *Nuclear Instruments and Methods in Physics Research B. 222, 4, 518-524, 2004.*
53. Gamma-irradiation effects on track etching characteristics of polyester nuclear track detector. Chhavi Agarwal, P. C. Kalsi, A. Ramaswami. *Radiation Effects and Defects in Solids. 161, 2, 131 - 133, 2006.*
54. Gamma-ray-induced modifications in microscopic glass slide used as a track detector Surinder Singh and Amanpreet Kaur Sandhu. *Radiation Effects and Defects in Solids Volume 161, No. 4, 235 - 239, 2006.*
55. The optical, chemical and spectral response of gamma-irradiated Lexan polymeric track recorder Surinder Singh and Sangeeta Prasher. *Radiation Measurements. Volume 40, Issues 2, Pages 50-54, 2005.*
56. Track structure theory in radiobiology and in radiation detection. Katz R. *Nuclear Track Detection. 2, 1-28, 1978.*
57. Electron and alpha-particle damage in biotite mica: Implications of track formation mechanisms. Hashemi-Nezhad S. R., Bull R. K. and Durrani S. A. *11th Int. Conf. Solid State Nuclear Track Detectors, Bristol. Nucl. Tracks. 3, 23-6, 1981.*

58. On the electron microscopy of fission fragment damage. Chadderton L.T., Morgan D.V., Torrens I. McC., and Van Vliet D. *Phil. Mag.* 13, 185-195, 1966.
59. Fission damage in crystals. Chadderton L.T. and Torrens I. McC. *Methuen, London, 1969.*

Chapter - 3

CHAPTER-3**TECHNIQUES OF CHARACTERIZATION OF IRRADIATED POLYMERS**

In order to understand the modifications that take place in irradiated polymers, different techniques are used. The techniques are used to understand the chemical and physical changes that take place in irradiated polymers. In this chapter, a brief description about the techniques used is given. The techniques used are:

IR Spectroscopy

UV-VIS Spectroscopy

Thermogravimetric Analysis (TGA)

Differential Scanning Calorimetry (DSC)

X-ray Diffraction (XRD)

Track Technique

3.1 IR SPECTROSCOPY

On irradiation, polymers' properties are altered due to chemical changes and this radiochemical destruction process can be derived from the IR peak assignment [1-3]. Polymers having functional groups which exhibit strong absorption lines such as C=C, C=O, or aromatic groups are favourable for such studies. Polymers with long side chains or heavily branched ones are known to be especially radiation sensitive. On the other hand, the back bone structure is seen to be frequently preserved. Further, aromatic groups are known to reduce the polymer irradiation sensitivity, due to delocalization of the excited energy.

IR spectroscopy is one of the most important analytical techniques, which provides sufficient information in determining the

chemical identity and structure of a compound in question. This technique is based upon the fact that chemical substances show absorption of IR radiation only at marked selective and definite frequencies or wavelengths. After absorption of IR-radiation, the molecules vibrate in different modes producing absorption bands, called IR-absorption spectra. When spectra of any new compound is correlated peak-by-peak against the spectra of an authentic and known compound, it gives an excellent evidence for identity.

A complex molecule normally produces IR spectra in such a way that it indicates a large number of normal vibrations. Each normal mode involves displacement of all or almost all of the atoms in the molecule. In some of the modes, all the atoms may undergo approximately the same displacement, while in others the displacement of a small group of atoms may be much more vigorous. Thus, normal modes may be divided into two classes: (1) skeletal vibrations, which involve all the atoms to almost the same extent and (2) the characteristic group vibrations, which involve only small portions of the molecule, the remaining being more or less stationary.

Skeletal frequencies usually fall in the range of $1400-700\text{ cm}^{-1}$ and arise from linear or branched chain structures of the molecule. It is seldom possible to assign particular bands to specific vibrational modes but the whole complex of bands observed is highly typical of the molecular structure under examination. Further, changing a substituent (on the chain or on the ring) usually results in a marked change in the pattern of the absorption bands. Therefore, these bands in the IR region are referred to as the "finger print" because from the frequencies at which absorption takes place one can obtain information about structural moiety and functional groups present in

the molecule as a whole and with few exceptions, fall in ranges above and well below that of the skeletal modes.

For a molecule to absorb in the IR region, two very important conditions are – (a) correct wavelength of radiation and (b) electric dipole. IR spectra appear only if the vibration produces a change in the permanent electric dipole of a molecule. It is reasonable to suppose, then, that the more polar a bond the more intense will be the IR spectrum from the vibrations of that bond.

3.2 UV-VIS SPECTROSCOPY

The ultra-violet-visible (UV-Vis) spectroscopy in the region 2000-8000 Å (200 – 800 nm) is considered to be one of the physical methods mainly used for quantitative analysis and serves as a tool for structural elucidation. When a compound containing different groups and bonds is irradiated with an electromagnetic radiation in the UV region ($\lambda = 200 - 400$ nm) or visible region ($\lambda = 400 - 800$ nm), it is observed that only a part of the incident radiation is absorbed. The actual amount of radiation absorbed depends on the structure of the compound as well as the wavelength of the radiation. The energy of the radiation beam absorbed is used for the excitation of electrons in orbitals of lower energy to orbitals of higher energy. The amount of light absorbed at each wavelength in UV or visible range is measured with the help of a spectrophotometer. UV-VIS spectroscopy is based on the law governing absorption of electromagnetic radiation in matter, which states that – “the intensity of a beam of monochromatic light decreases exponentially with increase in concentration of absorbing substance”.

Although fine structure of rotation and sometimes vibration do

not appear in case of liquid or solid samples, but the position and intensity of a broad absorption band is observed. This is due to an electronic transition, which is characteristic of the molecular group involved. The wavelength at which maximum absorption (λ_{\max}) takes place is taken as the position of absorption. λ_{\max} is quoted either in Angstrom units ($1\text{\AA} = 10^{-10}\text{m}$) or in nanometers ($1\text{nm} = 10^{-9}\text{m}$), the latter being more commonly used. For practical reasons the electronic spectrum is divided into three regions: the visible region between 400 nm and 750 nm (or $25,000\text{cm}^{-1} - 13300\text{ cm}^{-1}$), the near ultra-violet between 200 nm – 400nm ($50,000 - 25,000\text{ cm}^{-1}$) and the far ultra-violet region, below 200 nm.

Electrons in most of the molecules fall into one of the three classes: σ -electrons (sigma-electrons), π -electrons (π -electrons) and n-electrons (non-bonding electrons). A single bond between atoms contains only σ -electrons. Examples of such bonds are found in C-C, C-H, O-H, etc. A multiple bond systems such as C=C, C \equiv C, C \equiv N, etc., contain π -electrons in addition to σ -electrons, while atoms to the right of carbon in the periodic table, such N, O and halogens, possess n-electrons. Generally, sigma electrons are most firmly bound to the nuclei and hence require greater amount of energy to undergo transitions, while the pi-electrons require lesser energy than sigma electrons. The n-electrons usually (but not invariably) require the least amount of energy.

Any material, on exposure to gamma radiation, results in alteration of physical or chemical properties. The changes strongly depend on the internal structure of the absorbing substances and on the intensity of gamma radiation. It is expected that the interaction of gamma rays with solids will cause electronic ionization (or excitation)

of the orbital electrons and possibly atomic displacements. The photo conduction electrons produced will go back and forth and become freely or loosely bound to trapping centers somewhere in the material structure. These new electronic configurations, in addition to the possible displacement of atoms would cause a change in the optical properties of the absorbed substances[4-6].

3.3 THERMOGRAVIMETRIC ANALYSIS (TGA)

Quantitative measurement of weight loss due to thermally induced transitions is called thermogravimetry or thermogravimetric analysis (TGA). During polymer decomposition, weight loss takes place following a definite pattern and thus, it is useful in characterizing polymer structure. TGA is mainly of two types viz: isothermal and non-isothermal. In the former, weight loss is recorded as a function of time at constant temperature. In the latter, temperature is increased at constant rate and weight loss is recorded as a function of temperature. This provides more useful information as it directly indicates the upper limits of thermal stability. It has been observed by several authors [7-9] that the thermal properties of polymers change to a significant extent upon irradiation. It is understood that a correlation exists between radiation exposure and polymer thermal stability. The gamma-ray irradiation is known to induce point defects and defect clusters [10]. The specific defects and defect clusters might be responsible for hardening of ionic crystals.

3.4 DIFFERENTIAL SCANNING CALORIMETRY (DSC)

Differential scanning calorimetry (DSC) is widely used to characterize the thermo - physical properties of polymers. DSC can measure important thermoplastic properties including melting temperature,

heat of melting, percent crystallinity, T_g or softening, crystallization, presence of recyclates/regrinds. Most DSC experiments on polymers are conducted by heating at temperature ranging from ambient conditions to above the melting temperature. Thermal susceptibility is one of the most important properties of organic polymers, because their physical and chemical properties can be easily altered by heat treatments. In DSC technique the sample and the thermally inert reference material are subjected to controlled heating and the energy liberated or absorbed by the sample during the transition state is measured i.e., when thermal transition occurs in the sample (chemically or physically), thermal energy is added either to the sample or the reference in order to maintain their temperature at the same degree. Since the energy transferred is exactly equivalent in magnitude to the energy absorbed or evolved in the transition, the balancing energy yields a direct calorimetric measurement of the transition energy. So, in short, we can say that DSC is a technique for the calorimetric measurement of transition energy released or absorbed as a function of temperature. DSC profiles of ion irradiated polymers have been studied by few authors[11-13] where in they have reported the change in polymer properties such as, glass transition temperature, melting point, percent crystallinity etc.

3.5 X-RAY DIFFRACTION

This is a study of the pattern of x-rays diffracted from the planes of a crystal by the atoms present in it. This method depends on the wave character of the x-rays and the regular spacing of planes in a crystal. The condition for diffraction of a beam of x-rays from a crystal is given by the Bragg's equation:

$$M\lambda = 2d \sin\theta \quad (3.1)$$

Where M = order of diffraction, λ = wavelength, d = distance between crystal planes, θ = angle of diffraction.

Every atom in a crystal scatters each x-ray beam incident upon it in all directions. The atoms in any crystal are arranged in a regular and repetitive manner distinctly from any other crystal and the scattering power of an atom for x-ray depends on the number of electrons it possesses. Furthermore, the intensities of the diffracted beams depend on the type of atoms in the crystal and the location of the atoms in the fundamental repetitive unit patterns. When both the direction and intensity are considered, no two substances can have absolutely identical diffraction. The diffraction pattern is thus a fingerprint of a crystalline compound, and the crystalline components of a mixture can be identified individually. XRD studies have been extensively used to understand the crystalline structure of the polymers [14-16]. Change in polymer crystallinity like amorphous to crystalline or vice versa can be easily understood by XRD techniques.

3.6 TRACK TECHNIQUE

Chemical modifications observed in irradiated polymeric materials have imparted the initial motivation for usage of polymers as track detectors. Only those charged particles with linear energy transfer (LET) above a critical value can create distinct etchable tracks in polymeric track detectors. Atomic radiations such as UV rays and X-rays, nuclear radiations such as gamma ray and nuclear particles like electrons are low LET radiations. They mostly affect the bulk-etch rate of the detector depending upon the absorbed dose. For track detectors exposed to high LET charged particles, preceded by low LET radiation exposure, both the track-etch rate and bulk-etch rate are

found to vary in accordance with the absorbed dose of low LET radiation. It is already an established fact that, when a heavy charged particle passes through a di-electric medium, it creates tracks. So the basic requirement for track study is the heavy ion source as well as dielectric solids (track detectors). The details of heavy ion sources are given below.

3.6.1. Heavy ion sources:

[a] Alpha particle sources: - Usually heavy nuclei ($A > 200$) are energetically unstable towards the spontaneous emission of α -particles. The probability of α - decay is governed by the mechanism of 'barrier penetration' and the half-life of most of the useful sources vary from a few days to many thousands of years. Most alpha-particle energies range from 4 to 6 MeV/U. Also, there exists a very strong correlation between alpha-particle energy and the half-life of the parent nucleus. Isotope (^{253}Es) with shortest half-life emits alpha-particles of highest energies ($E = 6.5$ MeV). Alpha particles lose their energy rapidly in materials and therefore, the alpha sources must be prepared in very thin layers in order to obtain more energetic ions. High energy alpha-particles can be obtained from accelerators which are described in section (C). In all our experiments, ^{252}Cf is used as the alpha particle source.

[b] Spontaneous Fission Sources: - Theoretically all heavy nuclei are unstable and undergo spontaneous fission forming lighter fragments. Spontaneous fission from transuranic nuclides is a very simple and useful way of obtaining heavy ions of about 1 MeV/u specific energy. The penetration depth of these fragments in solids is of the order of $10\mu\text{m}$. The most widely used source is ^{252}Cf which undergoes

spontaneous fission with a half-life of 2.65 years. The medium light and medium heavy fragments have masses 108.55 and 143.55 [17], kinetic energies 106.2 ± 0.7 MeV and 80.3 MeV [17] and the most probable charges obtained from Mukherji's prescription [18] are 42.55 and 55.45 respectively. The fragments have initial positive charge of +20, but as they interact with matter, additional electrons are picked up by the ions thus reducing their effective charges. Nuclear reactors are being routinely used to produce high flux (10^{10} cm⁻²) of induced fission fragments by exposing ²³⁵U foils at neutron outlet ports. The energy and mass distribution of the reactor generated fission fragments are nearly same as those obtained from radio-active sources. However better beam collimation could be achieved for induced fission fragments.

[c] Heavy ion accelerators :- Accelerators are the most versatile heavy ion sources which provide monoenergetic, monoisotopic and highly parallel beams of practically all ions. An extremely wide range areal flux (10^0 - 10^{12} cm⁻²) and ion energies (10^0 - 10^3 MeV/u) is attainable depending on the type and size of the accelerator. Accelerated heavy ion beams are quite useful for various nuclear experiments in elemental and complex media. In last two decades or so, particle accelerators have initiated research activities in the fields of heavy ion interactions with matter [19-25].

3.6.2. Methods and formulations associated with track study

[a] Bulk-etch rate (V_G) :- The bulk-etch rate (V_G) is defined as the speed with which the undamaged material of the detector is dissolved away by the etchant solution under a given etching condition. There are three different methods of determining V_G .

[i] Track diameter method: - The initial damage formed in the detector is very small and is about 5-10 nm. When this is etched in a suitable etchant, the etch rate along the surface is normal while along the track it is too fast. Thus, for a detector irradiated perpendicular to the surface, the etching rate will be very fast along the track while it will be normal along the surface. Thus we can find out the rate of increase of track diameter with etching time. If D is the track diameter (μm) at a etching time t (h), the bulk etch rate (in $\mu\text{m/h}$) is given by

$$V_G = (D/2t) (\tan\theta + \sec\theta) \quad (3.2)$$

where θ is the cone angle. For any cone angle less than 5° , the term $(\tan\theta + \sec\theta)$ may be approximated as unity. Therefore, we can write,

$$V_G = D/2t \quad (3.3)$$

[ii] Thickness method: - This method is based on the rate of decrease of thickness of the material with etching, assuming same rate of etching for both the surfaces of the detector. If X_i be the initial thickness, and X_f the thickness after a certain interval of time t , then V_G is given by

$$V_G = (X_i - X_f) / 2t \quad (3.4)$$

[iii] Gravimetric Technique: - This method is based on the measurement of the weight lost by a sample foil of known area after it is etched in the etchant solution of known concentration for a given period of time at a given temperature. If m grams is the loss in weight of the detector after an etching time t (in hours), then the bulk-etch rate (in $\mu\text{m/h}$) is given as

$$V_G = \Delta m / 2s\rho t \times 10^4 \quad (3.5)$$

where ρ is the density of the detector foil in g/cm^3 , and 's' is the surface area of the foil in cm^2 .

[b] Track-etch rate (V_T) :- The rate of increase of track length with respect to etching time is defined as track etch rate (V_T). Assuming that, over a small portion of the track, V_T remains almost constant, the track etch rate (V_T) may be determined by measuring the small increase in track length Δl (in μm) in short etching time Δt (in h) from the equation

$$V_T = \Delta l / \Delta t \quad (\mu\text{m/h}) \quad (3.6)$$

For our purpose the bulk-etch rate (V_G) is calculated from track diameter method where as for track-etch rate (V_T), can also be derived from the following equations [26]

$$V_G = D_{ff}/2t, \quad V_T = V \times V_G, \quad \text{where } V = 1+x^2/1-x^2 \quad (3.7)$$

$x = D_{ff}/D_\alpha$, where D_{ff} is the diameter of fission tracks and D_α is the diameter of alpha tracks.

There are some other terms associated with track studies like etching efficiency and critical angle which can be determined from the equations given below.

$$\text{etching efficiency } \eta(\%) = (1 - V_G/V_T) \times 100 \quad (3.8)$$

$$\text{Critical angle } \theta_c = \text{Sin}^{-1}(1/V) \quad (3.9)$$

REFERENCES

1. Infrared transmission of Ion irradiated polymers. D. Fink, F. Hosoi, H. Omichi, T. Sasuga and L. Amaral. *Radiation Effects and Defects in Solids*. 132, 313-328, 1994.
2. Infrared spectroscopy analysis of physico-chemical modifications induced by heavy ions in ultra-high molecular weight polyethylene. V.C. Chappa, M.F. del Grosso, G. García-Bermúdez and R.O. Mazzei. *Nuclear Instruments and Methods in Physics Research B*. 243, 58-62, 2006.
3. Swift heavy ion induced amorphisation and chemical modification in polycarbonate. Y. Sun, Z. Zhu, Z. Wang, Y. Jin, J. Liu, M. Hou, Q. Zhang. *Nuclear Instruments and Methods in Physics Research B*. 209, 188-193, 2003.
4. Study of chemical, optical and thermal modifications induced by 100 MeV silicon ions in a polycarbonate. A. Srivastava, T.V. Singh, S. Mule, C.R. Rajan, S. Ponrathnam. *Nuclear Instruments and Methods in Physics Research B*. 192, 402-406, 2002.
5. Optical and electrical properties of some electron and proton irradiated polymers. R. Mishra, S.P. Tripathy, D. Sinha, K.K. Dwivedi, S. Ghosh, D.T. Khathing, M. Muller, D. Fink, W.H. Chung. *Nuclear Instruments and Methods in Physics Research B*. 168, 59-64, 2000.
6. Spectroscopic and Thermal studies of Gamma-irradiated Polypropylene films. D. Sinha, T. Swu, S.P. Tripathy, R. Mishra, K.K. Dwivedi. *Radiation Effects and Defects in Solids*. 158 (No. 7), 531-537, 2003.
7. Mechanical, thermal and morphological behaviour of the polystyrene/polypropylene (80/20) blend, irradiated with gamma-rays at low doses (0-70 kGy) C. Albano, J. Reyes, M. Ichazo, J. Gonza'lez, M. Herna'ndez, M. Rodr'iguez. *Polymer Degradation and Stability*. 80, 251-261, 2003.
8. Radiation-induced modification on thermal properties of different nuclear track detectors. D. Sinha, K.K. Dwivedi. *Radiation Measurements*. 36, 713-718, 2003.
9. Study of chemical, optical and thermal modifications induced by 100 MeV silicon ions in a polycarbonate. A. Srivastava, T.V. Singh, S. Mule, C.R. Rajan, S. Ponrathnam. *Nuclear Instruments and Methods in Physics Research B*. 192, 402-406, 2002.
10. "Fundamentals of Ion-Irradiated Polymers" by D. Fink, Springer, 2004.
11. An electron paramagnetic resonance study of PP and PP/SBS blends irradiated with gamma rays. Pedro Silva, Carmen Albano, Rosstela Perera, Jeanette Gonz'alez and Miren Ichazo. *Nuclear Instruments and Methods in Physics Research B*. 226, 3, 320-326, 2004.

12. Electron spin resonance investigation on Polycarbonate irradiated with U ion. M.I Chipara and J. Reyes Romero. *Nuclear Instruments and Methods in Physics Research B*. 185, 77-82, 2001.
13. Gamma induced modifications of Polycarbonate polymer. D.Sinha, K.L.Sahoo, U.B.Sinha, T.Swu, A. Chemseddine, D.Fink. *Radiation Effects and Defects in Solids*. 159, 10, 587-595, 2004.
14. Swift heavy ion induced amorphisation and chemical modification in polycarbonate Y. Sun, Z. Zhu, Z. Wang, Y. Jin, J. Liu, M. Hou, Q. Zhang. *Nuclear Instruments and Methods in Physics Research B*. 209, 188-193, 2003.
15. Damage process induced by swift heavy ion in polycarbonate. Y. Sun, Z. Zhu, Z. Wang, J. Liu, Y. Jin, M. Hou, Y. Wang, J. Duan. *Nuclear Instruments and Methods in Physics Research B*. 212, 211-215, 2003.
16. Proceedings of the Sixth International Symposium on Swift Heavy Ions in Matter, *Nuclear Instruments and Methods in Physics Research B*. 245 (Issue 1), 2006.
17. Fragment energy correlation measures for ^{252}Cf spontaneous fission and ^{235}U thermal-neutron fission. Schmit H. W., Neiler J. H. and Walter F. J. *Physics Review*. 14, 146-152, 1966.
18. Nuclear charge distribution in fission. S. Mukherji. *Nuclear Physics.A* 129, 297-301, 1969.
19. Energy loss and mean ranges of ^{86}Kr and ^{197}Au in Tantalum. K.K Dwivedi, A. Srivastava, S. Ghosh, D. Sinha, A. Saxena and R. Brandt. *Radiation Measurements*. 26, 561-563, 1996.
20. Chemical modification of polycarbonate induced by 1.4 GeV Ar ions. Y. Wang, Y. Jin, Z. Zhu, C. Liu, Y. Sun, Z. Wang, M. Hou, X. Chen, C. Zhang, J. Liu and B. Li. *Nuclear Instruments and Methods in Physics Research B* 164, 420-424 2000.
21. High energy ion beam irradiation of polymers for electronic applications D. Fink, P.S. Alegaonkar, A.V. Petrov, M. Wilhelm, P. Szimkowiak, M. Behar, D. Sinha, W.R. Fahrner, K. Hoppe and L.T. Chadderton. *Nuclear Instruments and Methods in Physics Research B*. 236, 1, 11-20, 2005.
22. Ion-solid interactions: current status, new perspectives D. Fink and L.T. Chadderton. *Radiation Effects and Defects in Solids*. 160 (Number 3-4), 67 - 83 2005.
23. Electrical conductivity studies of swift heavy ion modified PVC and PVC-PANI composite. A. Srivastava, V. Singh, A. Chandra, K. Witte, U.W. Scherer and T.V. Singh. *Nuclear Instruments and Methods in Physics Research B*. 244, 277-280, 2006.
24. Change of hydrogen concentration after ion beam irradiation on polyimide films with 100-400 °C annealing. M. Watamori. *Nuclear Instruments and Methods in Physics Research B*. 249, 159- 161, 2006.

25. Proceedings of the Indo German Workshop on Synthesis and Modifications of Nano-Structured Materials by Energetic Ion Beams, *Nuclear Instruments and Methods in Physics Research B*. 2006.
26. R Shweikani, S. A. Durrani and T. Tsuruta. Effects of gamma irradiation on the bulk and track etching properties of Cellulose Nitrate (Daicel 6000) and CR-39 plastics. *Nucl. Tracks Radiation Measurements*. 22, 153-156, 1993.

Chapter - 4

CHAPTER-4

EXPERIMENTAL TECHNIQUES

4.1 PREPARATION OF DETECTORS: In the present investigation six different types of polymers are used viz; Polyvinylchloride (PVC), Polypropylene (PP), Polycarbonate (PC) and three types of Polyallyldiglycolcarbonate(PADC). Polyallyldiglycolcarbonates (PADC) which are used in this thesis are generally known and used as nuclear track detectors. Three types of PADC track detectors have been studied. They are PADC (Persshore), PADC(Homalite) and PADC(Trastrak). Some of the important properties and chemical structures of these detectors are listed in Tables 4.1 & 4.2. A brief description about these polymeric materials is given below.

[a] Polyvinylchloride [1,2]: - There are two methods for the production of the monomer vinyl chloride: one is cracking ethylene dichloride in vapour phase and the other is by reacting acetylene with hydrogen chloride, in presence of a catalyst. Industrial polymerisation of vinylchloride is carried out either in suspension or emulsion. The emulsion system has the advantage that polymerisation can be done at low temperature (say, 20°C) whereas higher temperatures (50°C-80°C) are required for suspension and bulk polymerisation. Since the monomer is a gas at these temperatures, polymerisation has to be conducted in a pressure reactor or an autoclave. Structurally, the PVC molecule is partially syndiotactic and does not have a completely regular

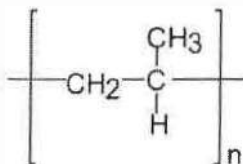
structure. That is why PVC has low crystallinity. The polymer molecules are either linear or slightly branched.

PVC is one of the cheapest and most widely used plastics globally. It is used for the large scale production of cable insulations, equipment parts, pipes, laminated materials and in fibre manufacturing. PVC is thermally not very stable and beyond 200°C it degrades, with the evolution of HCl. This is further attended by the formation of conjugated double bonds along the chain, which will result in the discolouration of the polymer. To avoid such discolouration, a suitable stabilizer is added to the polymer. The usual stabilizers are alkali earth oxides, organometallic salts, epoxy compounds or amine type compounds.

PVC as such is a horn-like material and difficult to process. It is therefore compounded with plasticizers. Depending on the plasticizer's percentage, fully rigid to highly flexible finished products can be obtained. In many cases, the plasticizer content may be up to 30% by weight of the polymer.

PVC is insoluble in alcohols, water and hydrocarbons. Acids and alkalis have practically no effect on PVC, at least upto 20°C. PVC however, dissolves in ketones, chlorinated hydrocarbons and some other organic solvents. A mixture of acetone and carbon disulfide is found to be an excellent solvent for PVC.

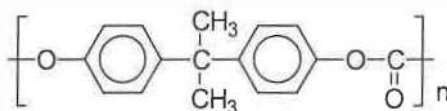
[b] Polypropylene[1,2]:- The polypropylene polymer can be represented as follows :



Polypropylene is perhaps the lightest known industrial polymer. It is produced by the polymerisation of propylene using the famous Ziegler-Natta catalysts. Polypropylene can be prepared in isotactic, syndiotactic or atactic forms. The isotactic polymer melts at 208°C and is highly crystalline. The polymer molecules are essentially linear and take up configurations leading to helical structures. Being highly crystalline, polypropylene exhibits high stiffness, hardness and tensile strength. Its high strength to weight ratio makes it very useful industrially. It is insoluble at room temperature in many of the known solvents. However, polypropylene, on heating above its melting point, can be dissolved in aromatic and chlorinated hydrocarbons. It is resistant to many chemicals such as acids, alkalis, and oils, but less resistant to oxidation compared to polyethylene. Components made of polypropylene are used in appliances such as refrigerators, radios, and TVs. It is also used for producing package films, pipes, storage tanks, seat covers, monofilaments, and ropes.

[c] Polycarbonate: - Polycarbonates [2-5] are polyesters of carbonic acid. Although carbonic acid itself is not a stable

compound, its derivatives (Phosgene, urea, carbonates) are commercially available. The reaction of phosgene with bisphenol A was developed into commercial production by Farbenfabriken Bayer in Germany.



Bisphenol A polycarbonate

While any dihydroxy compound, in principle, forms a polycarbonate with phosgene, only bisphenol-A has gained commercial importance. This is due to a combination of low monomer cost and unusually good polymer properties.

Polycarbonate melts at around 265°C and has very high impact strength. It is resistant to water and many organic compounds but alkalies slowly hydrolyse it. It is a transparent plastic. Many useful articles such as safety goggles, safety shields, telephone parts and machinery housings can be made from this plastic.

[d] The polyallyldiglycolcarbonate detectors :- PADC is a highly cross-linked thermoset polymer prepared by the polymerisation of a liquid monomer diethyleneglycol bis allyl carbonate [6].

4.2. IRRADIATION OF DETECTORS: One set of each polymer containing seven samples are prepared by cutting out several pieces of the size $3 \times 3 \text{ cm}^2$ from the commercially available large sheets. They are then washed thoroughly with soap solution and then with deionised water. The clean samples are dried inside vacuum desiccators and then kept in covered plastic boxes.

Gamma exposures are done using a ^{60}Co gamma source, having a dose rate of 3.0 Gy/h . The gamma exposures are done at room temperature in the dose range of $10^1 - 10^6 \text{ Gy}$. There is about 8% error associated with 10 Gy of gamma dose where as higher doses are accurate within 1%. For track studies, the PADC detectors are irradiated with gamma source first. After the gamma exposures are done, the detectors are then exposed to fission fragments and alpha particles. For this, a ^{252}Cf source having half-life of 2.65 years and activities 5.7×10^3 fission/minute and 1.84×10^5 alpha particles/minute is used as a source of fission fragments and alpha particles. All the seven samples of each set of PADC detectors are exposed at normal incidence to the fission fragments for about 7-10 minutes for sufficient detection of charged particles. For 90° irradiation, the samples are nicely fixed to one side of the collimator and then placed at a distance of 1 cm away from the Cf-source with the other side of the collimator facing the source. Then the exposures are done for around seven to ten minutes. The irradiation is done inside a desiccator in air. Upon completion

of exposure, the samples are collected and kept separately in plastic boxes for analysis.

4.3. CHEMICAL ETCHING FOR TRACK DEVELOPMENT:- Chemical etching of PADC detectors is done one set at a time. Before etching, the detectors are washed with soap solution to remove all the greasy substances and the contaminants from the surface. They are then dried between layers of soft filter paper and later dried in a vacuum desiccator. The detectors are then etched with 6N NaOH solution at different temperatures. One pristine sample is also etched each time for comparative study. The accuracy in the maintenance of temperature is $\pm 1^{\circ}\text{C}$. After every etching the detectors were washed in running water followed by 2-3 washings with distilled water.

4.4. MEASUREMENT OF TRACK PARAMETERS: Etched track diameters in each of the detectors are measured with the help of a "Leitz" optical microscope fitted with special objectives of 40X. After every etching, washing and drying, the samples are mounted on a special holder and viewed under the microscope. About 20-25 tracks are measured for each detector to find out the most probable track diameters. The error involved in the measurement of track diameter is $\pm 0.43 \mu\text{m}$. In all measurements we have considered the systematic errors only (i.e. $\pm 0.43 \mu\text{m}$). Since the samples are exposed to both fission fragments and alpha particles from a ^{252}Cf source, difference in the sizes of the tracks allows one

to distinguish between alpha tracks and fission fragment. Fission fragments tracks are larger in diameter as compared to alpha tracks.

TABLE - 4.1

| Properties of PADC(Pershore) PADC(Trastrack) and PADC(Homalite) | | | |
|---|-------------------------|-------------------------|-------------------------|
| Properties | PADC(Homalite) | PADC(Pershore) | PADC(Trastrack) |
| Composition | $C_{12}H_{18}O_7$ | $C_{12}H_{18}O_7$ | $C_{12}H_{18}O_7$ |
| Density (g/ml) | 1.32 | 1.32 | 1.32 |
| Thickness(μm) | 1000 | 1500 | 650 |
| Uniformity | Good | Good | Good |
| Clarity | Good | Good | Good |
| Surface view | Optical grade | Optical grade | Optical grade |
| Colour | Colourless | Colourless | colourless |
| Molecular weight | 274 | 274 | 274 |
| Manufactures | Homalite | Pershore | Trastrack |
| Chemical name | Allyldiglycol carbonate | Allyldiglycol carbonate | Allyldiglycol carbonate |

TABLE - 4.2

| Properties of Polyvinylchloride, Polypropylene and Polycarbonate | | | |
|--|------------------------|------------------------|-------------------|
| Properties | Polyvinylchloride | Polypropylene | Polycarbonate |
| Composition | $C_2H_3Cl_1$ | C_3H_6 | $C_{16}H_{14}O_3$ |
| Density (g/ml) | 0.9 | 0.9 | 1.20 |
| Thickness(μm) | 100 | 80 | 100 |
| Uniformity | Good | Good | Good |
| Clarity | Good | Good | Poor |
| Surface view | Optical grade | Optical grade | Optical grade |
| Colour | Colourless | Colourless | colourless |
| Manufactures | commercially available | commercially available | Bayer AG, FRG |
| Chemical name | polyvinyl chloride | polypropylene | polycarbonate |

4.5. DETERMINATION OF BULK-ETCH RATE AND TRACK-ETCH RATE:

Bulk-etch rates are determined by the track diameter method based on the formula $V_G = D/2t$, where D is the track diameter of the fission fragments and t is the etching time. The details about etch-rates are given in Chapter-3. The track-etch rate (V_T) is obtained by measuring both fission fragment track diameters and the alpha track

diameters and using the standard relation given by Durrani[9].

$$V_T = V_G [(1+x^2)/(1-x^2)] \quad (4.5.1)$$

Where V_G is the bulk-etching rate ($\mu\text{m/h}$), $x = D_f/D_\alpha$, is the ratio of the diameter D_α (μm) of the alpha particles track to D_f (μm) diameter of the fission fragments track.

4.6. IR SPECTRA :- For IR studies, irradiated samples along with the pristine are cut into small pieces of $1.0 \times 1.0 \text{ cm}^2$. The spectra were then recorded by a Nicolet (Impact 410) Fourier-transforming instrument (FTIR). Some IR spectra were also recorded using an Equinox 55, Bruker IR spectrophotometer. The spectra were recorded in the range $4000\text{-}500 \text{ cm}^{-1}$ in the solid state keeping air as the reference.

4.7. UV - VIS SPECTRA: UV - VIS spectra of the pristine and irradiated samples were recorded for these materials using Beckman DU-650 spectrophotometer. For such measurements the samples were cut into small pieces of $0.5 \times 1.5 \text{ cm}^2$. For each set of detectors there were seven samples including the pristine one. The samples were put vertically inside a quartz-shell and the absorption spectra were recorded in the range $200\text{-}800 \text{ nm}$ keeping air as the reference.

4.8. THERMOGRAVIMETRIC STUDY: TGA studies were performed by using PERKIN-ELMER instrument. Here again the polymers

were cut into small pieces ($0.25 \times 0.25 \text{ cm}^2$) and kept on a thermo balance. The samples are then heated up to the required temperature at a constant heating rate. This heating rate was $20^\circ\text{C}/\text{min}$ for all the samples. The detectors were heated up to a very high temperature, so that in the process of heating, they lost most of their weight. Heating temperature varied from one polymer to other polymer. This heating resulted in the TG-curve, in which weight loss was recorded as a function of temperature.

4.9. DSC STUDY: The DSC studies were carried out using Pyris 1, Perkin-Elmer instrument under high-purity argon atmosphere. The DSC is calibrated using pure indium and zinc standards giving an accuracy of $\pm 0.3^\circ$ for the temperature and 0.2 mW for the heat flow measurements. The measurements are done keeping the heating rate speed of $20^\circ\text{C}/\text{min}$.

4.10. XRD study: XRD measurements are carried out using a conventional diffractometer (Siemens, Bruker axs) equipped with a graphite monochromator crystal with Cu $K\alpha$ radiation (wave length 0.15405 nm) performed at 40 kV and 40 mA. The diffraction pattern was recorded in the 2θ range from 8 to 60° with scanning speed of 0.2° per minute. The instrument broadening is corrected using a Si single crystal as a reference for calculating the pattern peak width.

REFERENCES

1. "Polymer Science". Gowariker V.K., Viswanathan N.V. and Sreedhar J., *New Age International(P) Limited, 1999.*
2. Polymer Chemistry. Charles E. Carraher Jr. Fourth Edition, 2002.
3. Christopher W.F. and Fox D.W. "Polycarbonates", Reinhold, *New York, 1962.*
4. "Chemistry and Physics of Polycarbonates". Schrell H. *Wiley-Interscience, New York, 1964.*
5. Vernaleken H. in "Interfacial Synthesis" (F. Millie) and C.E. Carreher, Jr., Eds.), *Marcel Dekker, New York, 1975.*
6. The polymer physics on CR-39 - the state of understanding. Radiat. Stejny J. *Prot. Dosim. 20, 31-36, 1987.*
7. On the quantitative analysis and effects of internal temperature fluctuations during cure of the polycarbonate CR-39. Turner T.W., Clapham V.M., Fewes A.P. and Henshaw D.L. *Proc. 11th Int. Conf. SSNTD'S, 141-144, 1981. Bristol, Pergamon Press, Oxford.*
8. Status of development in the field of CR-39 track detectors. Somogyi G. *Proc. 11th Conf. SSNTD'S, 101-113, 1981. Bristol, Pergamon Press, Oxford.*
9. Effects of Gamma Irradiation on the bulk and track etching properties of Cellulose Nitrate (Daicel 6000) and CR-39 plastics. Shweikani R., Durrani S.A. and Tsuruta T. *Nuclear Tracks Radiation Measurements. 22, 153-156, 1993.*

Chapter - 5

CHAPTER 5

Results and Discussions

Gamma Photon Induced Modification of Polymers is dealt in this chapter. This chapter consists of four parts and each part deals with one type of polymer. The chapters are as follows:

Part 1 – Gamma Radiation Effects on Polyvinylchloride

Part 2 - Gamma Radiation Effects on Polypropylene

Part 3 - Gamma Radiation Effects on Polycarbonate

Part 4 - Gamma Radiation Effects on PADC Detectors

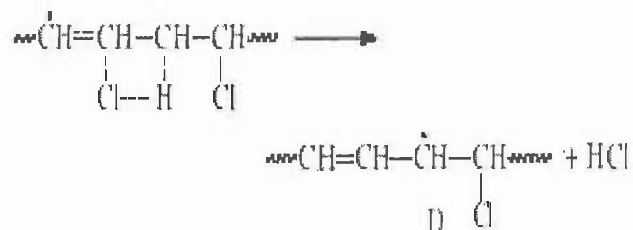
PART-1

GAMMA RADIATION EFFECT ON POLYVINYLCHLORIDE

This part of the work has been published in

Radiation Effects and Defects in Solids. Vol. 158, No.8, 593-598, 2003.
(Taylor & Francis publications)

Amongst the three radiation-induced polymeric radicals, "B" continues the process by way of a four centre reaction, in which HCl is formed and acts as a catalyst.



This chain reaction can proceed until the occurrence of a termination step. The gamma and electron beam irradiation-induced formation of main-chain unsaturated polyene groups in PVC has been observed by some authors earlier [6-8]. In addition to the cross linking there are chain scission and other side reactions, mostly of a deleterious character and their importance depends on the radiation conditions and additives [9]. For this kind of polymers, the prevailing side reaction is a dehydrochlorination process [10]. Radiation also causes polyenyl radical formation, a species which can react with oxygen giving rise to peroxy radicals. On the basis of polyenyl [11, 12] and peroxy radical EPR signals reported in literature [13, 14], the effects of irradiation on polyvinyl chloride (PVC) have been investigated by several researchers over a period of time [14-16]. In this part of the thesis chapter, work on gamma irradiation on PVC polymer in the dose range of 10^1 to 10^6 Gy has been discussed. The experimental details along with results are thoroughly analysed and discussed.

5-1-2 INVESTIGATION PROCEDURE

Studies on gamma photon induced modifications in Polyvinylchloride (PVC) polymer have been reported in this part of the

chapter. To monitor the chemical and structural changes caused by gamma radiation, FT-IR and UV-VIS spectroscopic studies, TGA and DSC studies of pristine and irradiated PVC have been performed. Polyvinylchloride film of thickness 100 μm and density of 0.9 g ml^{-1} is used for the irradiation. The film of sizes 2.5 x 2.5 cm^2 are cut and then washed thoroughly with soap solution and deionised water. The clean samples are dried and irradiated with various gamma doses (10^1 – 10^6 Gy) from a gamma source of ^{60}Co with a dose rate of 3.0 k Gy/h. The exposure time varies from 12 s to nearly 14 days in order to deliver the required doses. UV-VIS spectra of the polymers are recorded using a Beckman (DU-650) spectrophotometer. Absorbances at different wavelengths are measured for finding out the optical band gap (E_g). The optical band gap is determined by using Tauc's plot [17]. FT-IR spectra of the irradiated and pristine polymer are recorded in the solid state using a Nicolet Impact instrument. TGA and DSC studies are performed using a Perkin-Elmer instrument. For TGA studies, the samples are heated in air to a high temperature between 630°C to 690°C at a constant heating rate of 20°C min^{-1} . This heating results in weight loss, which is recorded as a function of temperature. On the other hand for DSC, the samples are heated up to a temperature of 490°C in nitrogen atmosphere.

5-1-3 RESULTS AND DISCUSSIONS

Physically Observable Changes: It has been observed for Polyvinyl Chloride polymer that due to gamma exposure, the colour of the film changes. This change is visible above the dose of 10^4 Gy. At the dose of 10^5 Gy, the polymeric film turns little blackish brown. However at the dose of 10^6 Gy, it turns dark brown. But there is no apparent change in colour, till the dose of 10^4 Gy.

UV-Vis spectra of pristine and gamma irradiated PVC films is shown in Figure.5.1.1. Even though the spectra of irradiated polymers at different doses are taken, spectra only from the dose of 10^4 Gy onwards are shown in the figure. Since there is practically no change in the UV-VIS spectra till the dose of 10^3 Gy, the spectra are not shown. The spectra indicate that only when the dose exceeds 10^3 Gy, the absorbance increases gradually with dose till 10^5 Gy. But at the dose of 10^6 Gy, the absorption spectrum totally changes.

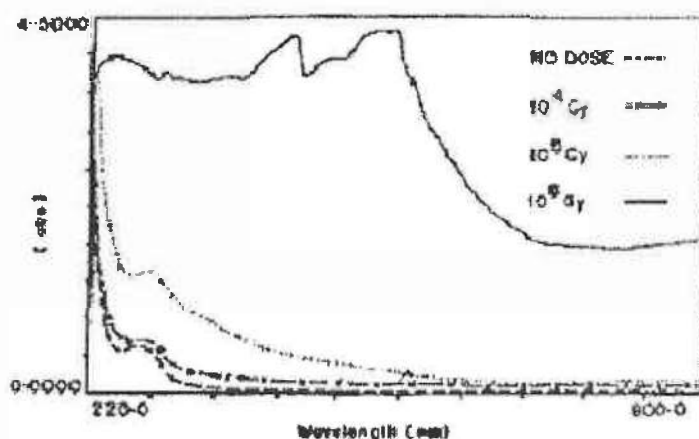
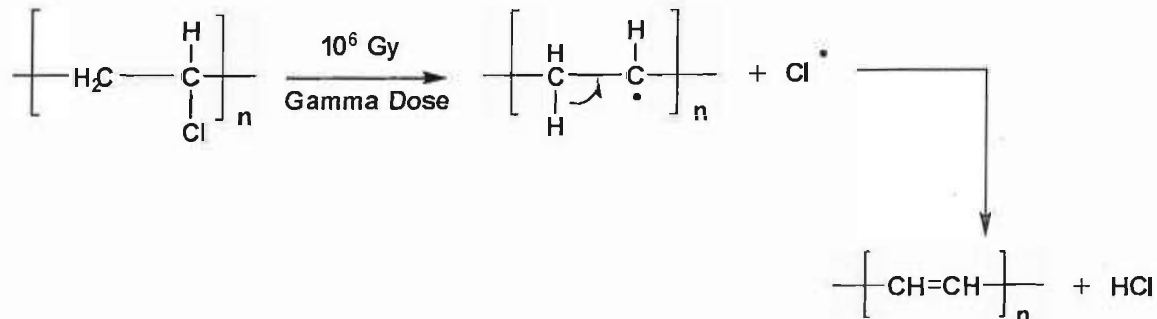


Fig. 5.1.1. UV-Vis spectra of polyvinylchloride film exposed to different gamma doses.

The spectrum at the dose of 10^6 Gy shifts towards longer wave-length region. Moreover, one notices in Figure.5.1.1 that the polyvinylchloride polymer gives a small absorption peak in the region of around 260 nm. This peak is probably due to the $n-\sigma^*$ transition of C-Cl bond of PVC molecule. This peak remains unaffected up to a dose of 10^5 Gy. Only at the dose of 10^6 Gy, this peak disappears. Mechanistically, this can be possible only if scissioning of C-Cl bonds in the polymer takes place. The probable mechanism for the scissioning of the C-Cl bond might be as follows:



Though the scissioning of the C-Cl bonds takes place at the dose of 10^6 Gy, still the UV-VIS spectra show a very little existence of the said peak. This brings the understanding that even though most of the C-Cl bond in the polymer breaks, still some amount of C-Cl bond does exist after the irradiation also. At the same time there are formation of unsaturated polyene groups (-C=C-) in the film. The appearance of the fine structure at the highest dose is indicative of the polyene group's existence. Of course the appearance of the fine structures is not very

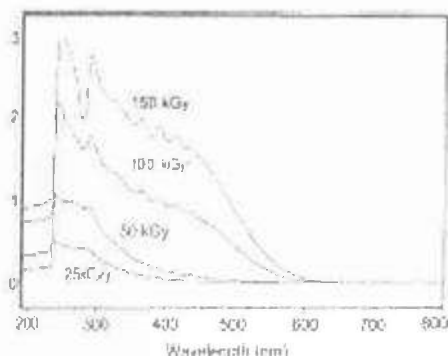


Fig. 5.1.2. UV-Vis spectra of gamma irradiated PVC powder [14]
Show the appearance of fine structure

distinct, but there is definitely a tendency for the formation of such a fine structure. Irradiation of PVC induces dehydrochlorination of the polymer chains (i.e. loss of H-Cl) producing -C=C- bonds. Probably due to less concentration of the polyene formed the fine structure is not

very apparent. Such fine structure peaks associated with polyene chain formations, having double bond numbers between 3 and 14 have also been reported earlier by Baccaro et. al. [14] for PVC powder irradiated with gamma radiation (Figure 5.1.2). It is also observed in Figure 5.1.1 that with increasing gamma dose, the absorption edge of the UV-VIS spectra shifts towards the higher wavelength region. The reason for the shift of the spectra towards longer wave-length region is due to increase in unsaturation in the polymer film. One of the reasons for the increase in unsaturation is due to formation of unsaturated polyene groups ($-C=C-$) in the polymer matrix.

The study of the optical absorption, particularly the absorption band edge, is more useful method for investigating optically induced transitions rather than providing information about both the band structure and optical energy gap in the materials. The study of the optical absorption, and the absorption band edge, involves investigating optically the induced transitions, providing information about the structure and optical energy. Electronic transitions between conduction bands in the non-crystalline materials start at the absorption edge which corresponds to the minimum energy difference E_g between the lowest conduction band and the highest valence band. If these extremes lie at the same point in K-space, then the transitions are called direct. Otherwise, the transitions are possible only when phonon-assisted and are called indirect. The value of the energy gap, which is a characteristic of the whole absorption band, is related to the basic chemical properties of the material. It is a fact that the optical band gap of a molecule changes with the change in saturation in a molecule. With increasing pi- bonds and non-bonding electrons in a molecule, the band gap (the difference between bonding and

nonbonding orbital) also decreases. So in an effort to find out change in optical band gap, absorbance of the spectra is measured at different wavelengths. Since the absorption edge is known to be correlated with the optical band gap (E_g) via Tauc's relation [17], the value of absorption is measured in the absorption edge region of the spectra. The absorption values at different wavelengths are then put in Tauc's equation and by applying the formula the band gap of the pristine and irradiated polymers are measured. For the pristine polymer the band gap value is 2.68 eV, where as for polymers irradiated with a dose of 10^6 Gy it becomes 1.43 eV. At present it is not yet clear whether the shift of the absorption edge always can be unambiguously interpreted by structural modifications in terms of unsaturation; however the emergence of unsaturation under irradiation is meanwhile a well-established fact. The values of the optical band gap differences are listed in Table 5.1.1. A significant increase in optical band gap takes place when the dose is higher than 10^3 Gy.

Table 5.1.1. Difference in Optical Band Gap (E_g) in Gamma irradiated PVC

| <i>Gamma dose (Gy)</i> | <i>Difference optical band gap ΔE_g (eV)</i> |
|------------------------|---|
| No dose | 2.68 |
| 10^1 Gy | 2.68 |
| 10^2 Gy | 2.68 |
| 10^3 Gy | 2.68 |
| 10^4 Gy | 2.31 |
| 10^5 Gy | 1.85 |
| 10^6 Gy | 1.43 |

The IR spectra of the PVC polymer before and after irradiation do not give any significant information. Some of the characteristics peaks (at 2958 cm^{-1} for $\nu_{\text{as}}\text{ CH}_3$), (at 2885 cm^{-1} for $\nu_{\text{s}}\text{ CH}_3$), (at 1461 cm^{-1} for

δ_s CH₂), (at 1380 cm⁻¹ for δ_s CH₃) are totally unchanged after the gamma exposure. There is no indication about appearance of new peaks also. Even though there is dehydrochlorination of the polymer chain (i.e. loss of H-Cl), at the same time, formation of -C=C- bonds takes place in the film, IR spectra can not detect the chemistry going on in the polymer due to irradiation. This might be due to the detection limit of the instrument or may be due to low concentration of the identified bonds/groups. The dehydrochlorination process is considered as the main structural change upon irradiation as witnessed by the decrease in intensity of the absorption band at about

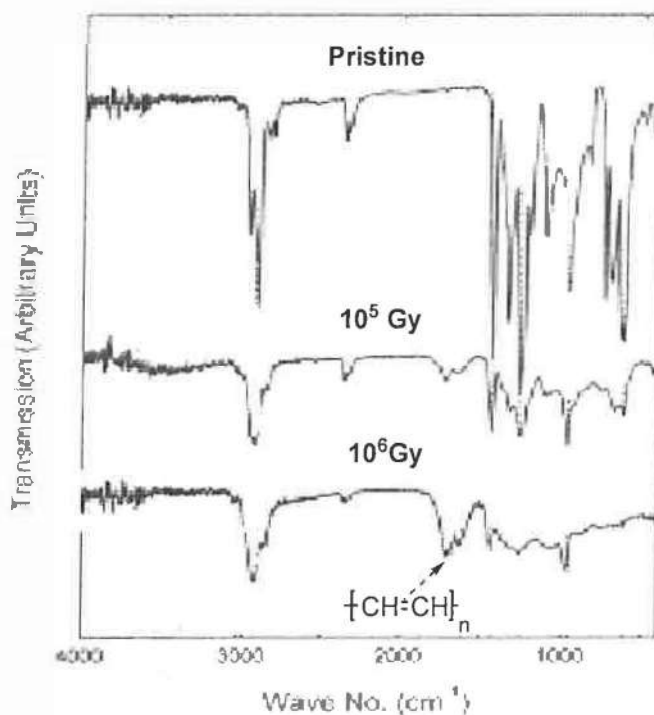


Fig. 5.1.3. FT-IR spectra of gamma irradiated PVC polymer

700 cm⁻¹ (characteristic of C-Cl bond stretching) [15] with the increase of H⁺ ion beam fluence. The dehydrochlorination leads to formation of C=C bonds, is confirmed by the appearance of IR absorption band at

1620–1680 cm^{-1} (characteristic of C=C stretching) [15]. Evelyn *et. al.* [16] has reported the effect of 4.0 MeV alpha particles, at fluences of 1×10^{14} and 5×10^{15} on PVC polymer. In our present study also, it has been observed that due to gamma exposure, the intensity of the absorption bands for the C-H stretching vibrations (3100–3000 cm^{-1} region) and the C-H bending vibrations (900–675 cm^{-1} region) get reduced for the PVC polymer as shown in Fig.5.1.3.. The changes are apparent at dose higher than 10^5 Gy. There is clear indication in the spectra about the formation of C=C bond and at the same time decrease of C-Cl bond taking place due to ion irradiation at the higher doses.

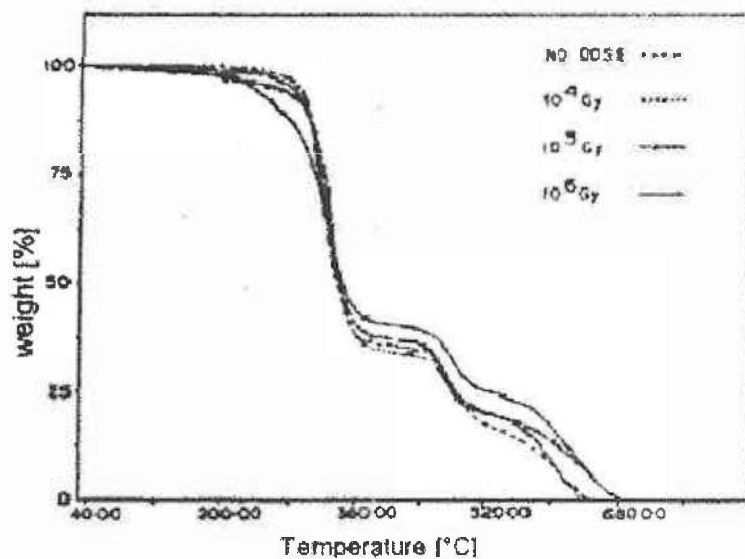


Fig.5.1.4. TGA thermograms of pristine and gamma irradiated polyvinylchloride with different doses.

Thermogravimetric response curves of pristine and irradiated PVC polymers are shown in Figure.5.1.4. It is evident from the thermogram that the thermal stability of the polymer is influenced by gamma exposure. The decomposition starts around 255°C for the pristine polymer. With increasing gamma dose also, this

decomposition temperature remains almost same. But at the dose of 10^6 Gy, the decomposition of the film starts at much lower temperature i.e. around 225°C . This lowering of the decomposition temperature may be due to the scissioning of C-Cl bonds in the polymer. Scissioning of the C-Cl bonds makes degradation processes easier and faster and so the decomposition takes place at much lower temperature. It is also significant to note that complete weight loss of the pristine PVC takes place at around 640°C . Gamma irradiation does not change the stability of the polymer till the dose of 10^3 Gy. But when the dose is higher than 10^3 Gy, this complete weight loss temperature starts increasing. It increases upto 647°C for the dose of 10^4 Gy. It further increases with increasing dose. For the gamma dose of 10^5 and 10^6 Gy, complete weight loss takes place at around 675°C (Figure.5.1.4). The first derivative TG curve of irradiated PVC polymer at the dose of 10^6 Gy, is shown in Fig.5.1.5. The curve shows three distinct decomposition steps for the irradiated PVC polymer. The first step of weight loss starts around 255°C and finishes around 360°C . During this step around 60% of the polymer weight is lost. The evolution of HCl takes place during this step. The second step of weight loss starts around 445°C and continues till 540°C . The third step starts at 540°C and continues until all material has vanished. It is apparent from the first derivative spectrum (shown by the dotted line in Figure.5.1.5) that the first and second weight loss peaks are very sharp whereas the third step is broad. On the other hand the weight loss during the third step process is comparatively slower as compared to the first and second steps.

The DSC thermograms of pristine and irradiated polymer show the exothermic behavior of the PVC polymer. A very sharp exothermic peak can be seen in the thermogram Figure 5.1.6. This exothermic

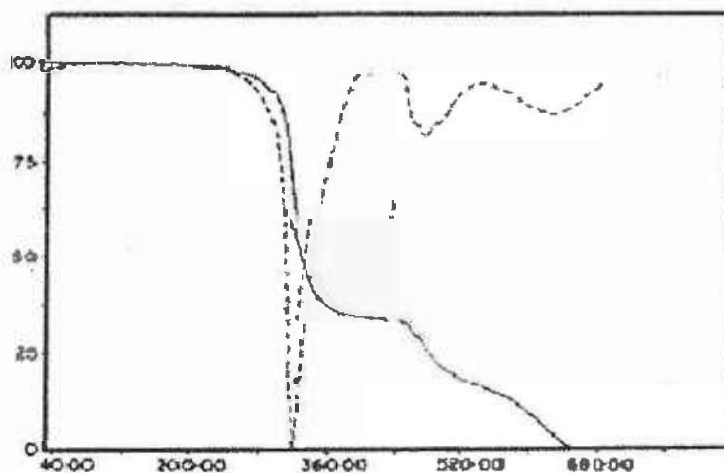


Fig.5.1. 5. First derivative TGA curve (dotted line) of polyvinylchloride film shows three distinct decomposition patterns. The solid line shows the general TGA curve for the PVC polymer.

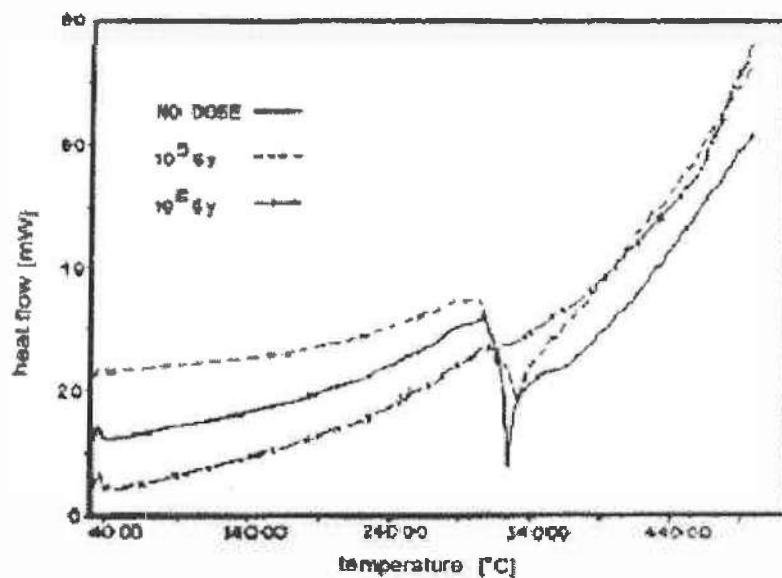


Fig.5.1.6. DSC thermograms of pristine and gamma irradiated PVC polymer show the disappearance of the exothermic peak at the dose of 10^6 Gy.

peak in the temperature range of 310°C to 320°C , is due to the evolution of HCl from the polymer matrix. The amount of heat involved for this thermal transition for the pristine PVC polymer is around

1060 J/g. Exposure to gamma radiation dose not alter the exothermic behaviour of the polymer till the dose of 10^4 Gy, which indicates that the thermal bulk property of the polymer is not altered. But at a higher radiation dose, i.e. at 10^5 Gy, the intensity of the exothermic nature of the polymer decreases and as a result the heat involved for the release of HCl decreases and is found to be 600 J/g. This decrease may be due partial scissioning of the C-Cl bonds of the polymer. At an even higher dose (10^6 Gy), the exothermic behaviour of the polymer disappears, probably due to the complete scissioning of the C-Cl bonds and hence the exothermic peak does not appear in the thermogram.

CONCLUSIONS

On the basis of the present results, it has been concluded that

- due to the gamma exposure at a dose higher than 10^3 Gy, optical band gap for the PVC polymer decreases. This decrease continues till the dose of 10^6 Gy. The decrease in band gap is more significant at higher gamma doses.
- the decrease in optical band gap is due to the increase in unsaturation in the polymer matrix due to the formation of $-C=C-$ groups.
- polymer exposed to the gamma dose of 10^6 Gy, undergoes scissioning of the C-Cl bonds.
- this scissioning of the C-Cl bond reduces the thermal stability of the irradiated PVC polymer and the irradiated polymer decomposes at temperatures lower than those ones for the pristine polymer.
- the heat evolved due to the decomposition of the polymer decreases to a large extent at the dose of 10^5 Gy indicating the fact that the scissioning of the C-Cl bond starts at this dose.
- at the highest dose of 10^6 Gy, the exothermic behaviour of the polymer disappears due to the complete scissioning of C-Cl bonds.

REFERENCES

1. G. de Hollain, *Mater. Appl.* 5 1980.
2. E.D. Owen, Degradation and Stabilisation of PVC, *Elsevier Applied Science Publishers, New York, 1984.*
3. L. Costa, V. Brunella, P. Bracco, Irradiation effects on poly(Vinyl Chloride), *World Scientific Edition, 2006 (in press).*
4. E.J. Lawton, J.S. Balwit, *J. Phys. Chem.* 65, 815, 1961.
5. Chapiro, *J. Chem. Phys.* 53, 895, 1956
6. Radiation Chemistry of Polymeric Systems. Chapiro, *High Polymers, Vol. 15, Inter Science Publishers, New York, 1962.*
7. M. Dole, The Radiation Chemistry of Macromolecules, *Vol. 1, Academic Press, New York, 1972.*
8. M. Dole, The Radiation Chemistry of Macromolecules, *Vol. 2, Academic Press, New York, 1973.*
9. Charlesby, *Radiat. Phys. Chem.* 9, 17, 1977.
10. W.A. Salmon, L.D. Loan, *J. Appl. Polym. Sci.* 16 (1972) 671.
11. R. Salovey, J.P. Luongo, W.A. Yager, *Macromolecules* 2 (2) (1969) 198.
12. B.R. Loy, *J. Polym. Sci. L* (1961) 245.
13. Z. Kuri, H. Ueda, S. Shida, *J. Chem. Phys.* 32, 2, 371, 1960
14. γ -irradiation of poly(vinyl chloride) for medical applications. S. Baccaro, V. Brunella, A. Cecilia, L. Costa. *Nuclear Instruments and Methods in Physics Research B* 208. 195–198, 2003.
15. Changes in the optical energy gap and ESR spectra of proton-irradiated unplasticized PVC copolymer and its possible use in radiation dosimetry. A.A. Abdel-Fattah *, H.M. Abdel-Hamid, R.M. Radwan. *Nuclear Instruments and Methods in Physics Research B.* 196, 279–285, 2002.
16. Ion beam modification of PES, PS and PVC polymers. A.L. Evelyn, D. Ila, R.L. Zimmerman, K. Bhat, D.B. Poker, D.K. Hensley, C. Klatt, S. Kalbitzer, N. Just,

- C. Drevet. *Nuclear Instruments and Methods in Physics Research B*, 148, 1141-1145, 1999.
17. J. Tauc, R. Grigorovici, and A. Vancu. *A. Phys. Stat. Sol.*, 15, 627, 1966.

PART-2

GAMMA RADIATION EFFECT ON POLYPROPYLENE

This part of the work has been published in

Radiation Effects and Defects in Solids, Vol. 158, No.7, 531-537, 2003.
(Taylor & Francis publications)

PART-2

5-2-1 INTRODUCTION

Among the synthetic polymers, polypropylene (PP) has occupied a prominent position because of its low cost, inert nature, good mechanical properties and weathering resistance. Synthetic polymers often experience modifications in their properties due to radiation. The degradation induced by exposure to different types of radiation on polypropylene polymer has been a subject of extensive investigation for last few years. Unfortunately polypropylene experiences a complex degradation process under gamma exposure in the presence of air [1] and this considerably limits its use because most of its valuable physical and chemical properties are lost during the degradation. The direct consequence is that the material crumbles into pieces. To avoid this undesirable degradation, additives are introduced in to the polymer to make it resistant against gamma oxidation. The effect of gamma irradiation on PP has been investigated in bulk [2, 3] using different techniques. Lacoste *et. al.* [4] have found that all gamma radiation induced decomposition products accumulate progressively, with tert-hydroperoxide being the dominant degradation product. Tidjani and Watanabe [1] have studied the dose dependent effects of gamma irradiation on physical and chemical changes of PP film. They have reported that due to gamma irradiation, formation of carbonyl, hydroperoxide and hydroxyl groups are formed. Rajulu *et al.* [5] also indicated the possibility of ketonic group formation in Si irradiated PP polymer. Perera *et. al.* have reported that from the shape of the calorimetric melting curve, valuable information of the thermal history and structural characteristics of the gamma irradiated PP polymer [6] can be obtained. Figure.5.2.1. displays the melting endotherms of pure

PP irradiated at 25, 50 and 100 kGy dose gamma rays, as observed by Perera *et. al.* [6]. Those endotherms show well-defined peaks whose melting peak temperatures and enthalpy values are similar, indicating that the crystallinity content is un-effected by the radiation, no matter what the radiation dose is (25, 50 or 100 k Gy).

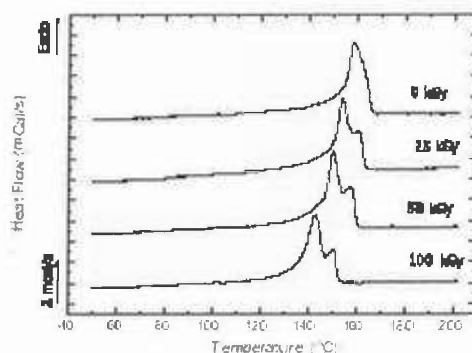


Fig. 5.2.1. DSC melting thermograms of pure PP irradiated at different doses [6]

It can be seen in the above figure that the unirradiated PP presents just one melting peak, whereas the PP irradiated at the different doses has two melting peaks. The intensity of the appearance of these peaks increases with increasing dose. Exposure to radiation and subsequent damage that takes place in the matrix depends on types of radiation and their dose/energy/exposure time etc. It is not expected that all the radiation will have same effect. Duplication or multiplication of melting peaks can be attributed to structural reasons. Multiple endotherms are observed in a wide variety of semicrystalline polymers and can arise from segregation effects, among other parameters. The fact that two peaks whose resolutions increase with the radiation dose, are present in melting thermograms suggests that two different and well-defined crystalline populations with different lamellar thickness coexist, one thicker with more perfect

crystals melting at higher temperatures, and the other one thinner, with less perfect crystals melting at lower temperatures. This difference in crystalline populations can then be attributed to the decrease in the molecular weight of the PP, due to chain scission brought about by the radiation [7, 8]. It is not expected that all radiations will have the same effect. For example, Mishra *et. al.* [9] have reported based on FT-IR spectral analysis that, the isotactic nature of PP was not destroyed due to electron irradiation which is shown in Figure 5.2.2. Peaks due to symmetric and asymmetric stretching, scissoring or bending and wagging of CH₃ and CH₂ groups are observed in the IR spectra of both pristine as well as irradiated PP. The increase in absorbance of the CH₂ wagging vibration due to irradiation indicates an increase in chain length of hydrocarbon due to addition of more CH₂ groups, which might be due to some cross-linking induced by electron irradiation in the polymer [9].

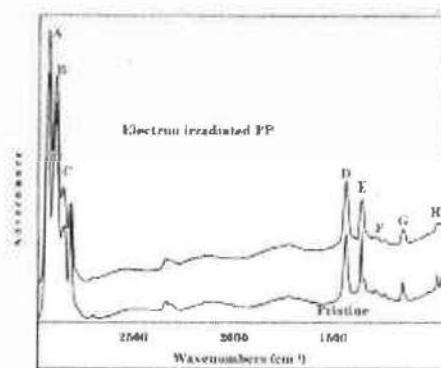


Fig. 5.2.2. Fourier transform infrared spectra of the pristine and 2 Mev electron irradiated PP[9]

Albano *et. al.* have reported [10] in Figure. 5.2.3.(b), about the deterioration of the PP fracture surface as a result of gamma irradiation (60 kGy) as compared with Figure 5.2.3.(a) of the non-

irradiated PP film. A more lamellar-like morphology is observed in the case of irradiated polymer.

The changes produced by radiation while passing through the polymer causes atomic displacements or electronic ionizations of the orbital electron [11]. This new electronic configuration which subsequently arises, causes a change in the molecular structure of the polymer, thus, causing a change in the optical band-gap (E_g) of the polymer. The optical band - gap can be found from the shift of the absorption edge from UV towards the visible region under irradiation.

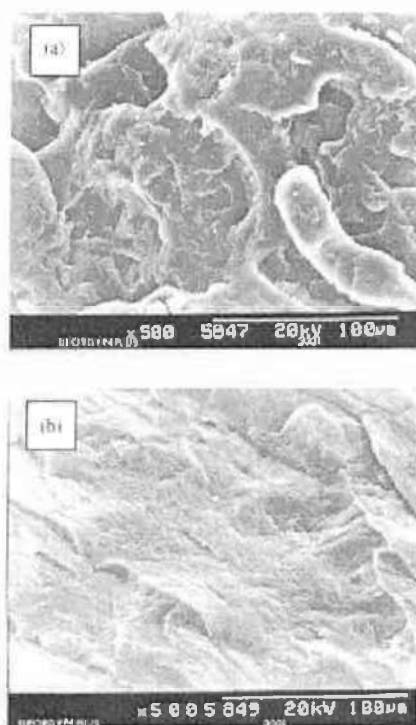


Fig. 5.2.3. SEM micrographs of the PP at different radiation doses: (a) pristine (b) 60 kGy [10]

This can be correlated with the optical band-gap (E_g) by the Tauc's expression [12]: $\omega^2\varepsilon_2 = (h\omega - E_g)^2$, where $\varepsilon_2(\lambda)$ is the imaginary part of the complex refractive index i.e. the optical absorbance, and λ is the

wavelength. E_g is usually derived from the plot ϵ_2/λ versus $1/\lambda$. The intersection of the extrapolated spectrum with the abscissa yields the gap wavelength (λ_g), from which the gap energy is derived to be $E_g = hc/\lambda_g$.

The results of studies of optical properties in ion irradiated PP have been reported [13, 14], in which it was found that the band-gap is reduced after irradiation. In this thesis also the different aspects of the work on optical band gap have been studied and a comparison is made on the changes in band gap due to gamma irradiation.

It is an established fact that due to gamma exposure, the thermal stability of polymers changes to a great extent. Even in our earlier studies [15, 16] it has been observed that due to gamma exposure thermal stability of polymeric track detectors like Triafol-BN (Cellulose Acetate Butyrate) and PADC (Polyallyl diglycol carbonate) are modified to a significant extent. In the present work also thermo gravimetric analysis (TGA) of the irradiated PP polymer has been carried out. Spectroscopic techniques like UV-VIS, FT-IR have also been used to investigate the structural modifications in irradiated PP polymer. Based on the spectral data, modifications in some of the properties have been investigated

5-2-2 INVESTIGATION PROCEDURE:

Seven samples of isotactic PP film (thickness = 8 nm and density = 0.9 g cm^{-3}) of sizes ($3 \times 3 \text{ cm}^2$) are prepared. These are then washed thoroughly with soap solution and de-ionised water. The clean samples are dried and irradiation is done with various gamma doses ranging from 10^1 – 10^6 Gy). The exposure time varies from 12 seconds to nearly 14 days in order to deliver the required doses. The errors in doses range from 8% for low dose (10 Gy) to about 1% for high doses.

UV-VIS spectra of the irradiated and pristine polymers are recorded using a Beckman (DU-650) spectrophotometer. Films of sizes 0.5 x 1.0 cm² sizes are cut and used for this study. The UV-VIS spectra are then recorded by putting the individual pieces inside a quartz-shell. The absorption spectra for the film are then recorded in the wavelength region 200–800 nm. All the spectra are taken keeping air as the reference. In order to make the Tauc's plot, absorbance is measured at different wavelengths in the absorption edge region. FT-IR spectra of the irradiated and pristine polymers are recorded in the solid state. The spectra are taken using a Nicolet Impact 410 Fourier transforming instrument in the range between 4000 cm⁻¹ to 400 cm⁻¹. Handling of the film irradiated at the highest dose is done very carefully because the film becomes fragile at this dose.

Thermogravimetric studies are performed using a Perkin-Elmer instrument. For this study, the samples are cut into very small pieces (0.25 x 0.25 cm²) and then put on a thermo-balance. The samples are heated to high temperature at a heating rate of 20^oC min⁻¹. This heating results in weight loss, which is recorded as a function of temperature in the TGA thermogram

5-2-3 RESULTS AND DISCUSSIONS

Physically Observable Changes: There are no visible changes observed in the polymer irradiated with gamma dose up to the dose of 10⁴ Gy. But at the higher dose of 10⁵Gy, the polymer becomes light yellow. The intensity of the colour increases at the highest dose (10⁶Gy). Again at this dose the film becomes very brittle. This change in colour is possibly due to formation of free and trapped radicals in the polymer.

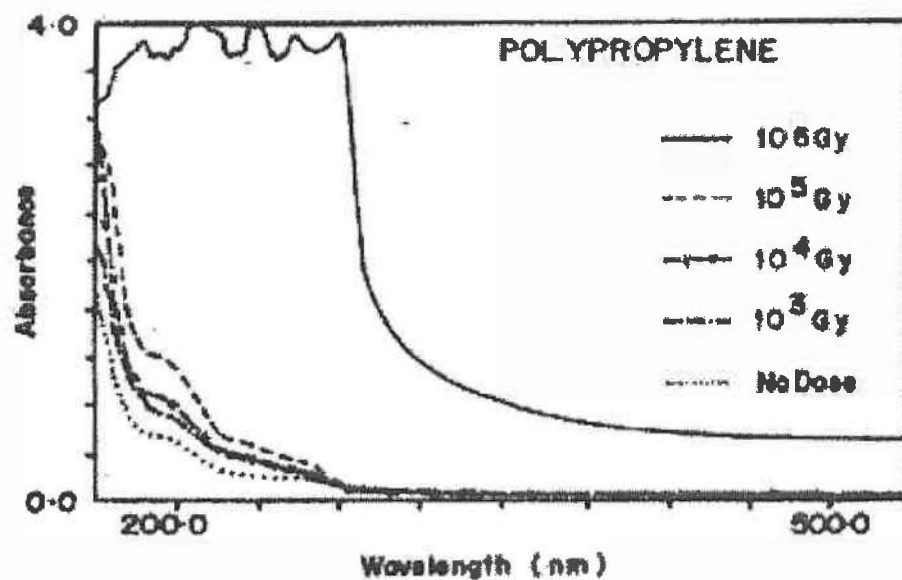


Fig.5.2.4. UV-Vis spectra of Polypropylene film exposed to different gamma doses.

Figure 5.2.4. shows the uv-vis spectra of pristine and irradiated polypropylene polymer. In the figure, the respective spectra for the different films irradiated with different doses have overlapped and shown together so that a dose dependent comparative study becomes easier. Of-course there is virtually no difference in the UV-VIS spectra of pristine and polymer irradiated samples till the dose of 10^2 Gy. So two uv-vis spectra, one corresponding to 10^1 Gy and other to 10^2 Gy are not shown in the figure for better clarity. A shoulder at 220 nm as evident from the spectra could be due to the presence of some antioxidant. Till the dose of 10^5 Gy, this shoulder remains intact but at the dose of 10^6 Gy, this shoulder disappears. So, probably any antioxidant present is destroyed at this dose. Destruction of the antioxidant favours oxidation and thus, the polymer becomes brittle. Moreover, it is also observed that with increasing dose the absorption edge shifts to higher wavelength region. These changes are significant above the gamma dose of 10^2 Gy. The shift of the spectra towards

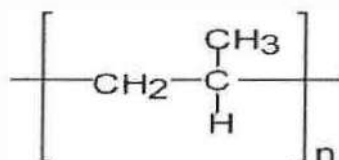
higher wavelength region is due to an increase in unsaturation in the system.

The absorption edge is correlated with the optical band-gap (E_g) via Touc's relation [12]. Applying this formula, we get the band gap of 4.6 eV for pristine PP. This band-gap remains almost the same till 10^2 Gy of gamma dose. Then, it slowly starts decreasing with increasing dose and at the highest dose the decrease in band gap becomes very significant (2.1 eV). Table 5.2.1 gives the change in optical band-gap with changing gamma dose.

Table 5.2.1 Variation in Optical Band Gap of Polypropylene with increasing gamma dose

| Gamma dose (Gy) | Band gap (eV) |
|-----------------|---------------|
| No Dose | 4.59 |
| 10^1 Gy | 4.58 |
| 10^2 Gy | 4.56 |
| 10^3 Gy | 4.07 |
| 10^4 Gy | 4.03 |
| 10^5 Gy | 3.90 |
| 10^6 Gy | 2.07 |

The FT-IR spectra of pristine and irradiated PP are shown in Figure 5.2.5. The spectra shown are only of the pristine film and the one irradiated with the highest dose of 10^6 Gy. Some of the characteristics peaks of polypropylene polymer are given in Table 5.2.2. The structure of Polypropylene is presented below:



The bands at 1165 cm^{-1} , 997 cm^{-1} and 977 cm^{-1} (3/1 helix) indicates that the polymer is isotactic, implying that the methyl group is located on one side of the plane of the carbon atom chain. Upon irradiation, it is noticed that many of the characteristic bands totally disappear at the highest dose. This disappearance of IR peaks due to irradiation clearly indicates that there is a destruction of the polymer matrix. The complete absence of the characteristic isotactic bands at 1165 cm^{-1} and 997 cm^{-1} indicates that the isotactic arrangement of the polymer is no longer present. The peaks D and E disappear completely and peaks A and B disappear partially. So, the C-H bonds of methylene and methyl groups get ruptured at the dose of 10^6 Gy .

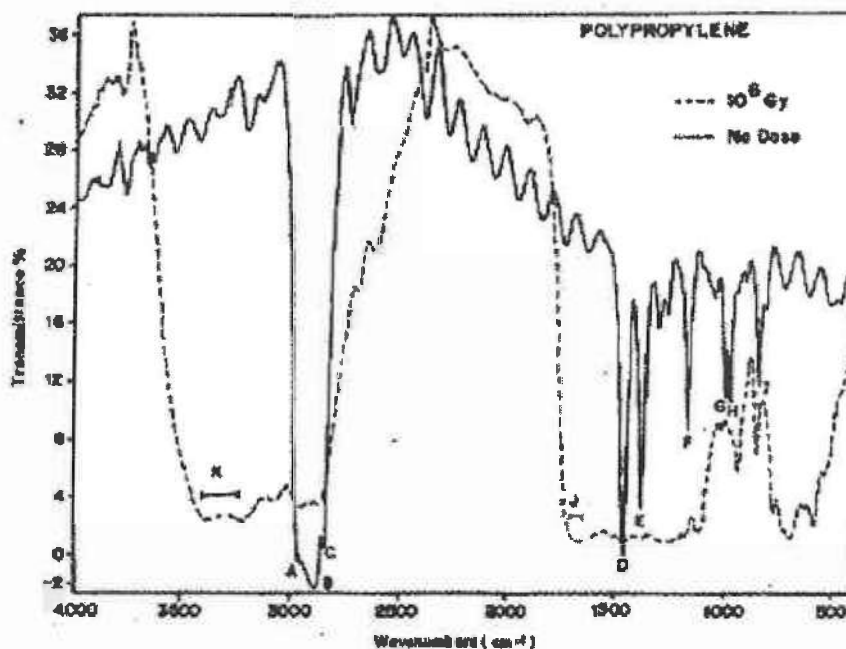


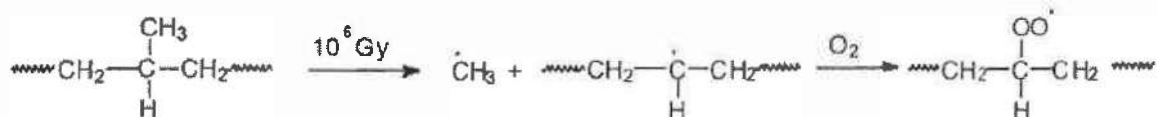
Fig.5.2.5. FT-IR spectra of pristine and gamma irradiated Polypropylene

Table 5.2.2: Assignment of IR Absorption Peaks

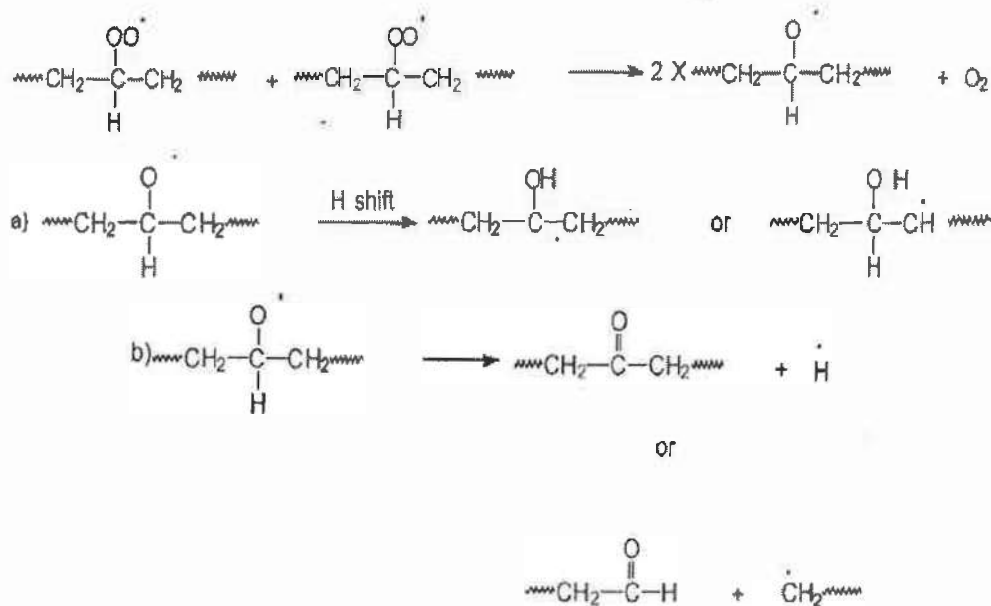
| Peak Name | Wave Number [cm^{-1}] | Interpretation |
|-----------|----------------------------------|--------------------------------------|
| A | 2958 | ν_{as} CH ₃ |
| B | 2885 | ν_{as} CH ₃ |
| C | 2838 | ν_{as} CH ₂ |
| D | 1461 | δ_{as} CH ₂ |
| E | 1380 | δ_{as} CH ₃ |
| F | 1165 | isotactic bonds |
| G | 997 | isotactic bonds |
| H | 977 | isotactic bonds |
| I | 843 | $\nu_{\text{C-H}}$ |
| J | 1670-1690 | ν_{s} C=O |
| K | 3300-3415 | ν_{s} O-H |

Interestingly no new sharp peak has been observed due to gamma exposure. Only one broad band around $3300\text{cm}^{-1} - 3415\text{cm}^{-1}$ appears in the spectra, which is the characteristic bond of alcoholic group (O-H stretching). This indicates that, some alcoholic groups are formed in the irradiated polymer. One can notice in the spectra that there is a slight shoulder developed in the wavelength region 1670cm^{-1} to 1690cm^{-1} which may be due to the formation of some C=O groups. Probably because of very low concentration of this C=O functional group in the irradiated polymer, a shoulder appears rather than a peak. The mechanism for the formation of alcoholic or ketonic (C=O) groups is not very clear. Gamma degradation process involves initiation, propagation, and termination stages. The initiation reaction may take place on different sites of the PP chain [1]. When energy is absorbed from gamma rays, it causes scissioning of a covalent backbone. Since the isotactic arrangements as well as the C-H bond of methylene breaks, so out of several preferred initiation routes

proposed by Tidjani and Watanabe [1], the most probable mechanism may be as follows:



Afterwards, propagation occurs by unzipping or by radical abstraction of neighbouring H atom [1]. The result of this is that radical is transferred to another chain or further down the same chain. So a possible mechanism for the formation of alcohol or C=O is presented below.



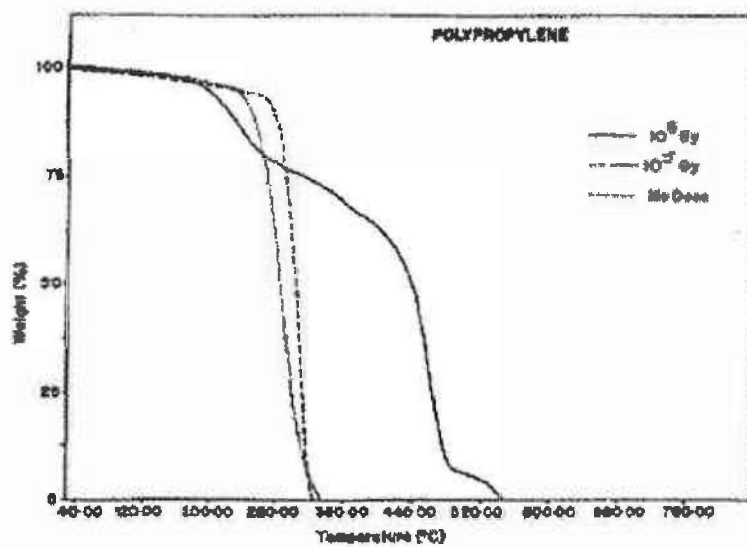


Fig.5.2.6. TGA thermogram of pristine and gamma irradiated Polypropylene

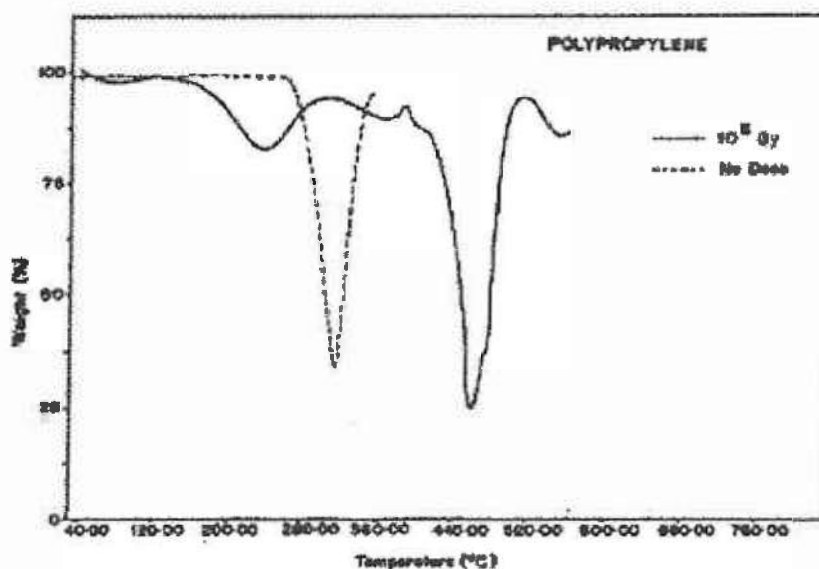


Fig. 5.2.7. First derivative TGA curve of pristine and gamma irradiated Polypropylene film.

TGA study reveals some informative results. Up to the dose of 10^5 Gy, the decomposition of the polymer starts at around 260–270°C and finishes at around 330–335°C (Figure.5.2.6). But at the dose of 10^6 Gy, decomposition starts at much lower temperature, i.e., around

178°C and continues up to about 550°C. The decomposition pattern of the polymer irradiated at the dose of 10⁶ Gy is totally different from the other ones.

Figure 5.2.7, which is the first derivative TG curve, shows that the polymer decomposes in four different steps. The first step of decomposition takes place in the temperature range of 175°C–292°C in which around 20% weight of the polymer is lost. Second step takes place from 292°C to 392°C. Again third step of weight loss (58% of the polymer weight) takes place in the temperature range between 392°C–489°C. The last and final step of weight loss starts from 489°C and finishes around 550°C where the remaining weight (around 7%) is lost. The third step of weight loss (58%) is probably due to the decomposition of C₂H₂. We are exactly not in a position to explain the actual decomposition mechanism, but from this study it is clear that due to gamma exposure the thermal property of PP changes drastically and it indicates an increase in the thermal resistance of the polymer at the highest dose. At this occasion it is worthwhile to note that an enhanced polymeric resistance against thermal decomposition also shows up after irradiation with 20 to 800 keV light ions (He to Ne) at elevated fluences (up to 10⁶cm⁻²) of e.g., photoresist, [17, 18]. Though high-fluence irradiation destroys the original polymeric structure quite efficiently, it also leads to the formation of radiation defects (radicals, excess internal free volume) that acts as traps for diffusing polymeric decomposition products, thus preventing their escape from the matrix. Further, depending on the polymer's chemistry, also cross-linking might take place that would help stabilizing the remaining structure. The thermal polymer stabilization after ion irradiation is shown to be an effect of electronic – not of nuclear – energy transfer [17, 18]. As it

is known that PP is a candidate that undergoes preferentially cross-linking after irradiation, and as the primary effect of gamma irradiation onto matter is the production of energetic electrons, it is obvious that a limited polymer stabilization should also take place after gamma irradiation, as is observed in this work.

CONCLUSIONS

On the basis of the present study it is concluded that:

- due to gamma exposure at the dose of 10^6 Gy, oxidation takes place by removing antioxidants present in the film
- random destruction of the polymeric chain takes place with the probable formation of alcoholic and ketonic groups
- band-gap decreases with increasing dose
- due to gamma exposure at the dose of 10^6 Gy, the thermal resistance of the polymer increases and it decomposes in four different steps.

REFERENCES

1. Tidjani, A. and Watanabe, Y. *J. Appl. Polym. Sci.*, 60, 1839, 1996.
2. Mayo, F. R. *Macromolecules*, 11, 942, 1978.
3. Decker, C. and Mayo, F. R. *J. Appl. Polym. Sci.*, 11, 2877, 1973.
4. Lacoste, J., Vaillant, D. and Carlsson, D. J. *J. Appl. Polym. Sci.*, 51, 313, 1993.
5. Rajula, A. V., Reddy, R. L., Avasthi, D. K. and Asokan, K. *Radiation Effects and Defects in Solids*, 152, 57, 2000.
6. The effect of gamma radiation on the properties of polypropylene blends with styrenebutadienestyrene copolymers. R. Perera, C. Albano, J. Gonza' lez, P. Silva, M. Ichazo. *Polymer Degradation and Stability* 85, 741-750, 2004.
7. Polypropylene: structure, blends and composites, vol. I. New York: Varga J. In: Karger-Kocsis J, editor. *Chapman & Hall*; p. 56-115, 1995.
8. Phillips R.A, Wolkowicz MD. In: Moore EP, editor. *Polypropylene handbook*. New York: *Hanser*, 113-176, 1996.
9. Electron induced modification in polypropylene. R. Mishra, S.P. Tripathy, K.K. Dwivedi, D.T. Khathing, S. Ghosh, M.Muller and D. Fink. *Radiation Measurements*. 33, 845-850, 2001.
10. Mechanical, thermal and morphological behaviour of the polystyrene/polypropylene (80/20) blend, irradiated with g-rays at low doses (0-70 kGy). C. Albano, J. Reyes, M. Ichazo, J. Gonza' lez, M. Herna' ndez, M. Rodrı' guez. *Polymer Degradation and Stability*. 80, 251-261, 2003.
11. Higazy, A. A. and Hussein, A. *Radiation Effects and Defects in Solids*. 133, 225, 1995.
12. Touc, J., Grigorovici, R. and Vancu, A. *Phys. Stat. Sol.*, 15, 627, 1966.
13. Mishra, R., Tripathy, S. P., Sinha, D., Dwivedi, K. K., Ghosh, S., Khathing, D.T., Mu' ller, M., Fink, D. and Chung, W. H. *Nucl. Instr. Meth. B*, 168, 59, 2000.
14. Fink, D., Chung, W. H. and Wilhelm, M. *Radiation Effects Defects in Solids*. 133, 209, 1995.

15. Sinha, D., Sarker, G. K., Ghosh, S., Kulshreshtha, A., Dwivedi, K. K. and Fink, D. *Radiat. Meas.*, 29, 599, 1998.
16. Sinha, D. and Dwivedi, K. K. *Radiat. Phys. and Chem.*, 53, 99, 1998.
17. Sias, U. S., Sanchez, G., Kaschny, J. R., Amaral, L., Behar, M. and Fink, D. *Nucl. Instr. Meth. B*, 134, 35, 1998.
18. Sias, U. S., Sanchez, G., Kaschny, J. R., Amaral, L., Behar, M. and Fink, D. *Nucl. Instr. Meth. B*, 141, 187, 1998.

PART-3

GAMMA RADIATION EFFECT ON POLYCARBONATE

This part of the work has been published in

Radiation Effects and Defects in Solids. Vol. 159, page 587-595, 2004.
(Taylor & Francis publications)

PART-3**5-3-1 INTRODUCTION**

Polycarbonate resins can be divided in two structural classes: aliphatics, which are not extensively used as thermoplastics, and aromatics, which have notable applications as engineering thermoplastics. Polybisphenol A carbonate is the most widely used aromatic polycarbonate. It is a condensation polymer in which benzene rings plus quaternary carbon atoms form bulky stiff molecules that promote rigidity and strength. The bulky chains crystallize with great difficulty, so the polymer is normally amorphous with excellent characteristics such as optical clarity, heat stability and mechanical properties. These properties make it an ideal material for outdoor applications. However, on exposure to radiation, the physical and chemical properties of the polymer are modified to a significant extent [1-3].

Sun *et.al.* (2003) have reported that irradiation by 15.14 MeV/amu Xe^{136} and 11.4 MeV/amu U^{238} suffers serious degradation in polycarbonate polymer because of subsequent bond scission and cross-linking[4]. The results show that aromatic ether and methyl groups are more sensitive to irradiation than the para-substituted phenyl and there are similar damage cross-sections for the bands having the same functional group. Dissociation of alkyne and alkene groups are induced by the irradiation. XRD measurements show a decrease in the main XRD peak intensity. Progressive amorphisation process of polycarbonate (known as Makrofol-kg) with increasing fluence is also traced by XRD measurements. Amorphisation occurs with the largest radius in the latent track, and the formation radius of

alkyne is larger than the destruction radius of a chemical group. Figure.5.3.1 shows the XRD spectra of Xe ion irradiated polycarbonate polymer [4]. Similarly Wang *et. al.* (2000) have reported that alkyne end groups are produced by the irradiations of 1.4 GeV Ar ions in Polycarbonate[5]. It has been observed by Srivastava *et. al.* (2002) that polycarbonate does show substantial modification in its chemical, optical and thermal characteristics when it is bombarded with 100 MeV silicon ions[6]. The role of chemical modification comes out very

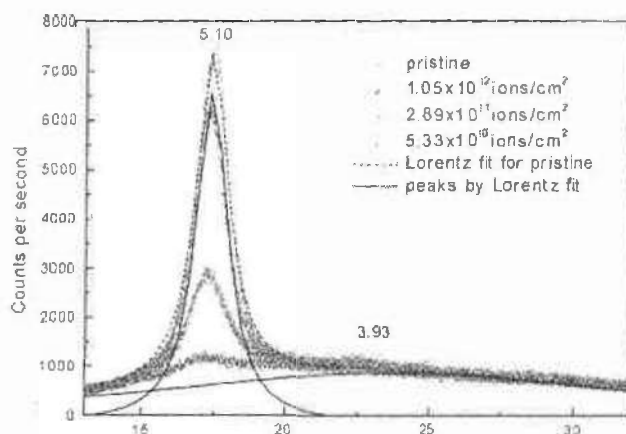


Fig. 5.3.1. XRD spectra of Makrofol kg irradiated with Xe ions at 7.62 keV/nm at different fluence [4]

clearly in terms of the breaking of the C-O single bond of carbonate and formation of phenolic O-H bond with the phenoxy radical presumably abstracting a hydrogen ion from the neighboring isopropyl group. Figure 5.3.2 shows the IR spectra of polycarbonate polymer after irradiation by heavy ions [6].

A gradual decrease in the glass transition temperature from 141.1 °C to 137.9 °C to 132.4 °C, respectively is observed by the authors with the increase in the total ion fluence from 3.5×10^{11} ions to 6.9×10^{11} ions to 3.5×10^{12} ions, respectively. This decrease in the

glass transition temperature is generally due to the increase in molecular mobility as a result of scissioning of the polymer chains[6].

Most of the studies reported so far are on swift heavy ions induced modification on polycarbonate polymer. Work on gamma radiation effect on polycarbonate is not very common. Keeping this in mind, gamma effect on polycarbonate polymer has been investigated and thus the results are reported in this part of the thesis.

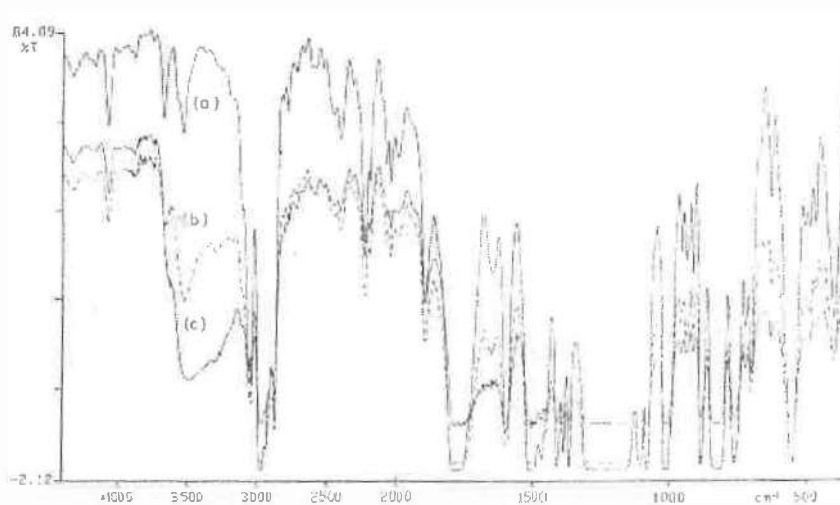


Fig. 5.3.2. FT-IR spectra of virgin and irradiated polycarbonate films: (a) virgin, (b) irradiated with the total ion fluence of 6.9×10^{11} ions, (c) irradiated with the total ion fluence of 7.0×10^{12} ions [6]

5.3.2. INVESTIGATION PROCEDURE

Polycarbonate polymer (Figure.5.3.3) manufactured by Bayer AG, FRG, of thickness 100 μm (semi transparent) and density 1.20 g cm^{-3} are used for this experiment. A set of seven samples each having sizes of $2 \times 2 \text{ cm}^2$ is made from commercially available sheets. They are thoroughly washed and dried. The samples are then irradiated with gamma radiation starting from 10^1 Gy up to 10^6 Gy . A ^{60}Co source having a dose rate of 3.0 kGy h^{-1} is used for the gamma exposure.

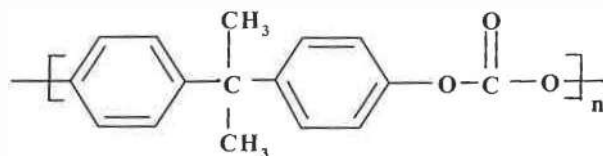


Fig.5.3.3. Structure of polycarbonate

After the irradiation, different analytical techniques like FT-IR, DSC and XRD are applied to understand the modifications that take place in the polymer. These measurements are carried out long after the irradiation. Hence the results represent the stable stationary state of the irradiated foils where the metastable defects if any are expected to have annealed and the radiation enhanced oxidation, if any, would have been completed.

FT-IR measurements are carried out using an Equinox 55, Bruker IR spectrophotometer. The measurement is done in the wave number range 500 to 4000 cm^{-1} keeping air as the reference. XRD measurements are carried out with a conventional diffractometer (Siemens, Bruker axis) equipped with a graphite monochromator crystal with Cu $K\alpha$ radiation (wave length 0.15405 nm) performed at 40 kV and 40 mA. The diffraction pattern is recorded in the 2θ range from 8 to 60° with scanning speed of 0.2° per minute. The instrument broadening is corrected using a Si single crystal as a reference for calculating the pattern peak width.

The thermal analysis of the polymers is carried out using DSC (Pyris 1, Perkin-Elmer) under high purity argon atmosphere. The DSC is calibrated using pure indium and zinc standards, giving an accuracy of $\pm 0.3^\circ\text{C}$ for the temperature and ± 0.2 mW for the heat flow

measurements. All the polymer samples are heated in the range of 40°C to 250°C keeping the heating speed of 20°C/min.

5.3.3. RESULTS AND DISCUSSIONS

The FT-IR spectrum of the pristine polycarbonate polymer is shown in Figure.5.3.4. For better understanding of the IR spectrum, assignments of the major peaks of the polymer are given in Table 5.3.1. Figure.5.3.5 shows the IR spectra for the pristine and polymer irradiated at gamma dose of 10^5 Gy. As there are no visible changes taking place till the gamma dose of 10^4 Gy, the respective spectra for the lower doses are not shown.

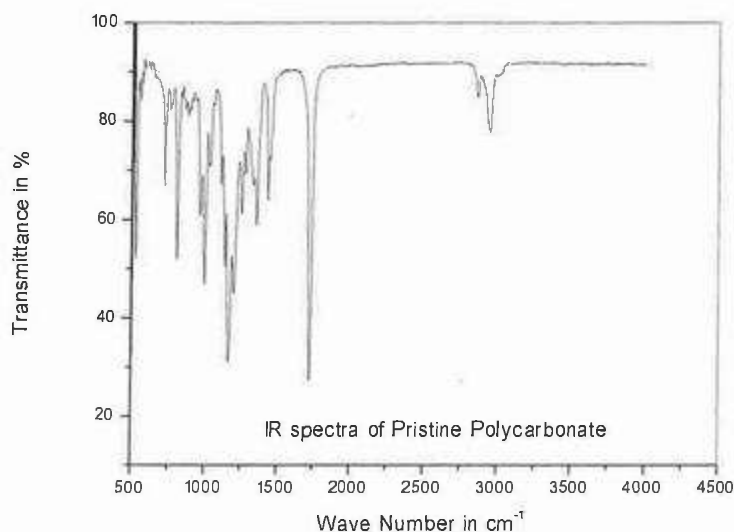
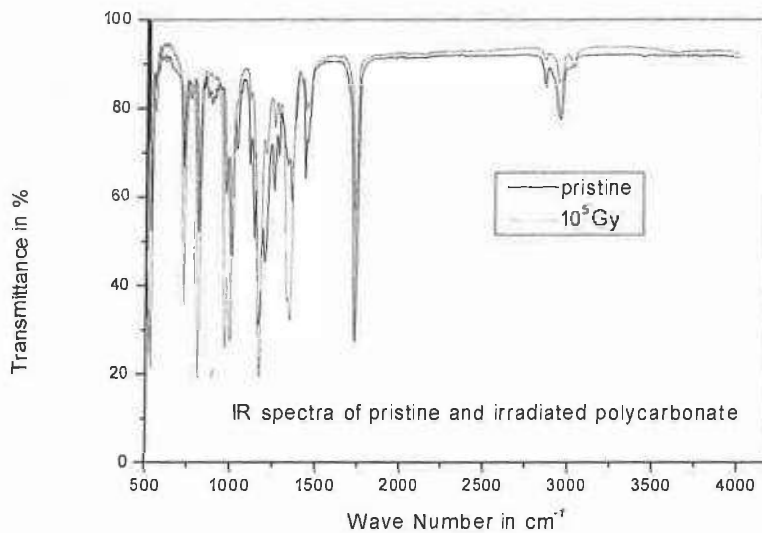


Fig.5.3.4. FT-IR spectra of pristine polycarbonate Polymer

It is clear from Figure 5.3.5 that the peak intensities and positions for some of the major bands change drastically due to gamma exposure at a dose of 10^5 Gy. Even though the peak intensities are changed at the dose of 10^5 Gy, the spectra clearly indicate that neither total destruction nor formation of new peaks take place at this dose.

Table 5.3.1. Major absorption bands for pristine polycarbonate polymer (PC)

| | |
|-----------------------|--|
| 2950 cm^{-1} | $\nu_{\text{as}}\text{CH}_3$ |
| 2864 cm^{-1} | $\nu_{\text{s}}\text{CH}_3$ |
| 1725 cm^{-1} | $\nu\text{C}=\text{O}$ |
| 1434 cm^{-1} | $\nu\text{C}-\text{O}$ (aromatic) |
| 1206 cm^{-1} | $\nu(\text{C}-\text{O}-\text{C})$ (aromatic) |
| 1166 cm^{-1} | $\nu(\text{C}-\text{O}-\text{C})$ (aromatic) |
| 1143 cm^{-1} | $\nu(\text{C}-\text{O}-\text{C})$ (aromatic) |
| 999 cm^{-1} | $\nu(\text{C}-\text{H})$ (aromatic) |

**Fig.5.3.5.** FT-IR spectra of gamma irradiated polycarbonate polymer

The intensity of peaks corresponding to $\text{C}=\text{O}$ bonds (1725cm^{-1}), aromatic $\text{C}-\text{O}$ bonds (1434cm^{-1}), $\text{C}-\text{O}-\text{C}$ bonds (1206cm^{-1}), and $\text{C}-\text{H}$ bonds of CH_3 group (2968cm^{-1} and 2874cm^{-1}), aromatic $\text{C}-\text{H}$ bonds (999cm^{-1}) decreases. This decrease in intensities of the peaks is generally due to lesser concentration of the respective bonds. This signifies that scissioning of these bonds takes place at this dose. When the dose becomes as high as 10^6Gy , the changes become very apparent. At this dose, most of the major peaks almost disappear (see Figure 5.4.6) and also at the same time a strong peak appears at 1063cm^{-1} .

The carbonyl peak shifts from 1725 cm^{-1} to 1599 cm^{-1} . This shift towards lower frequency of carbonyl bond is probably due to the decrease of the bond order of the C=O bond. Because of irradiation, scissioning of chains takes place and as a result the free radical density- or in other words, the electron density- in the polymer matrix increases. This increase in electron density is responsible for the decrease of the C=O bond order which subsequently lowers the absorption of the carbonyl groups. Again one can see that a distinct broad band appears around 3500 cm^{-1} at the dose of 10^6 Gy . This broad band is due to the formation of phenolic groups (-OH groups) in the polymer matrix.

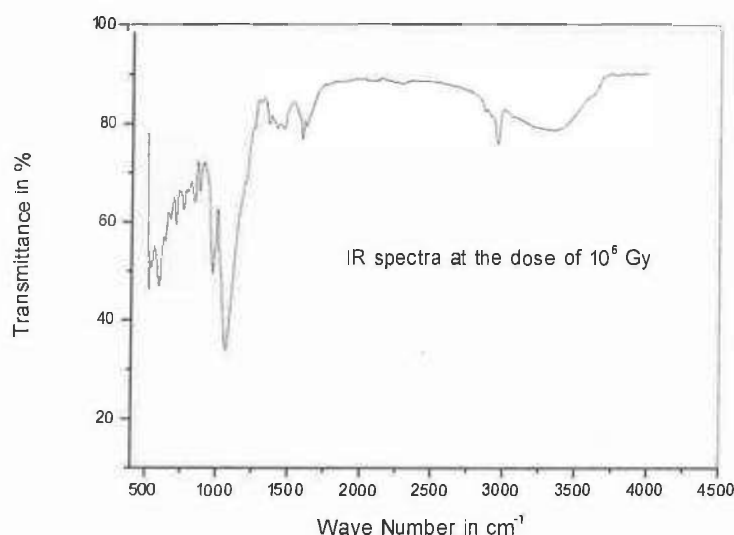


Fig.5.3.6. IR spectra of gamma irradiated polycarbonate at the dose of 10^6 Gy

It is evident from the IR spectrum of the polymer irradiated with 10^6 Gy that due to gamma exposure, the ester linkage breaks and probably ester radicals are formed (see the mechanism of Figure.5.3.7). These ester radicals might further decompose and result in the release

of CO₂, thus leading to the formation of oxygen radicals. The oxygen radicals once formed, can easily pick up hydrogen radicals (which are formed due to cleavage of C-H bonds) and form phenolic groups. Similar broad peaks due to phenolic group formation have also been observed by other authors for polycarbonate polymers irradiated with heavy ions [3 - 5]. Though different authors have given different explanations of the IR results, so far no mechanism has been proposed to explain the chemical modifications that take place in the polymer due to gamma irradiation. Here, we propose the probable mechanism in an effort to explain the chemical changes that might have taken place in the polymer. The mechanism is proposed keeping in mind the IR results. It can be graphically described by Figure.5.3.7.

The DSC thermograms of the pristine and irradiated polycarbonate polymers are shown in Figure.5.3.8. The thermograms are obtained within the temperature range of 40°C to 250°C, with a heating speed of 20°C/min. The thermogram for the polymer irradiated at 10¹ Gy of gamma dose is not shown in the figure. This is because, at this dose, there is practically no change taking place. From Figure.5.3.8 we can understand that the glass transition temperature (T_g) of the irradiated polymers decreases with increasing gamma dose from 151.8°C for the pristine polymer to 140°C for the dose of 10⁶ Gy. This decrease in T_g is significant above 10⁴ Gy. Figure.5.3.9 shows the change in T_g due to gamma exposure. This decrease in T_g is probably due to the increase in molecular mobility as a result of scissioning of the polymer chains. It is a known fact that below T_g, molecules do not have segmental motion, and so portions of the molecule may not wiggle around but may only be able to vibrate slightly. At T_g, the molecules can start segmental motion.

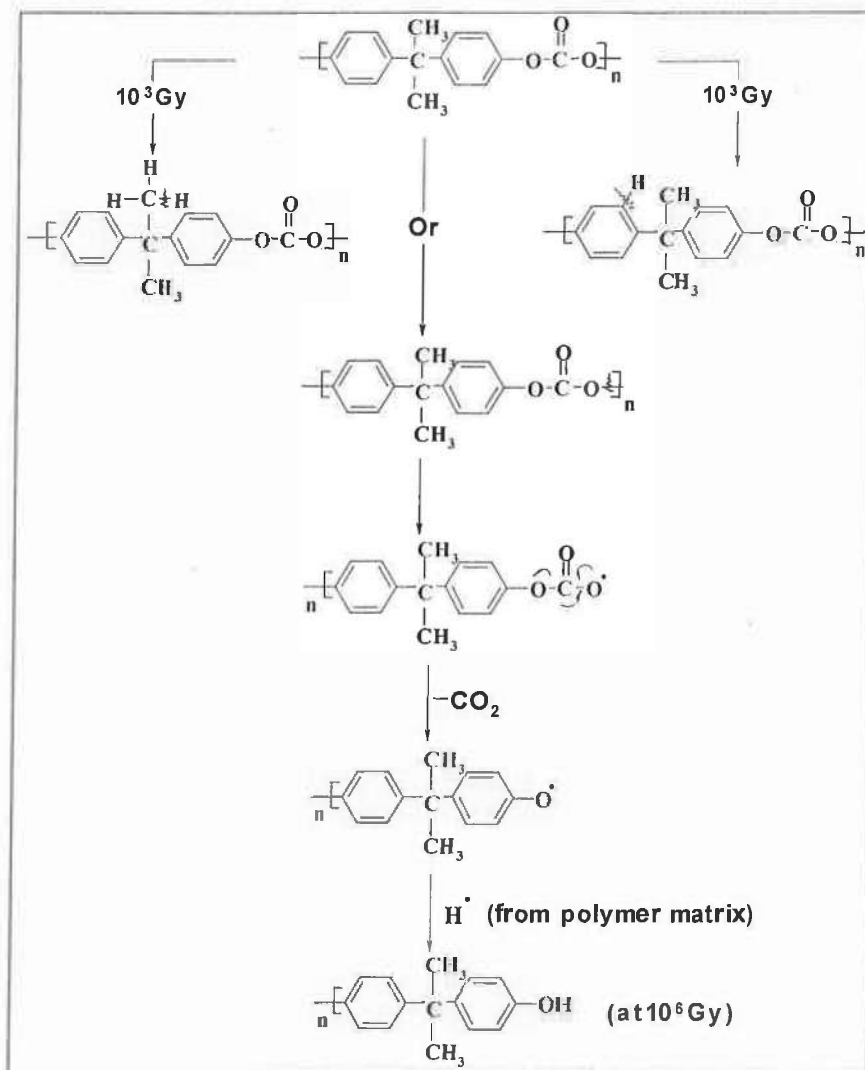


Fig.5.3.7. Mechanism of the chemical changes taking place in polycarbonate polymer

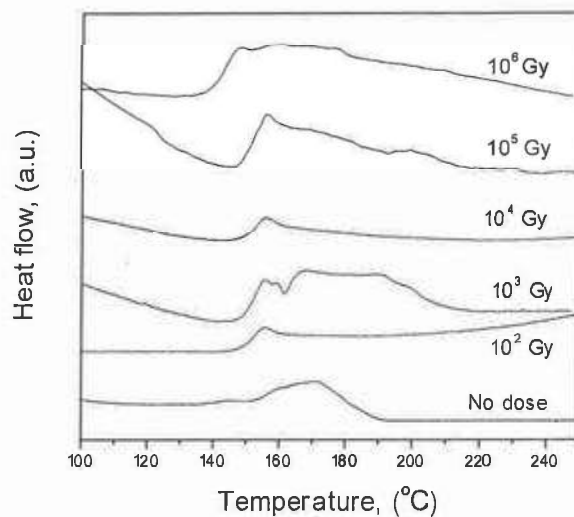


Fig.5.3.8. DSC thermogram of gamma irradiated polycarbonate polymer

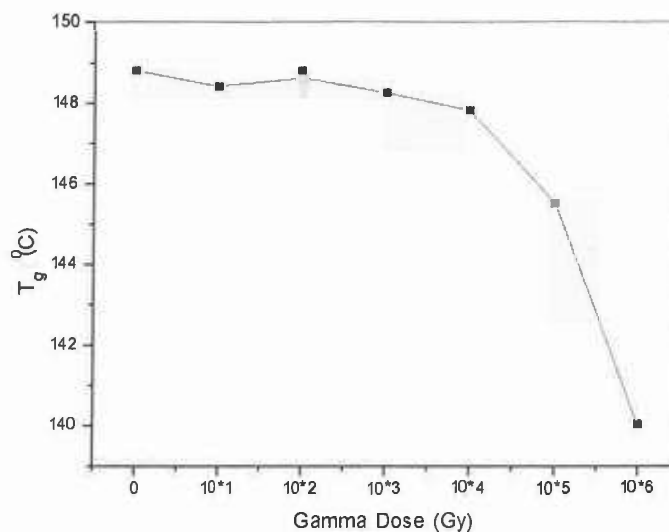


Fig.5.3.9. Dose dependent variation of T_g for gamma irradiated polycarbonate polymer

Gamma irradiation causes scissioning of the molecular chains and this leads to decrease in the average molecular length of the polymer chain. This decrease in polymer chain length accelerates the mobility of the molecular chains, as a result the glass transition temperature of the polymer decreases.

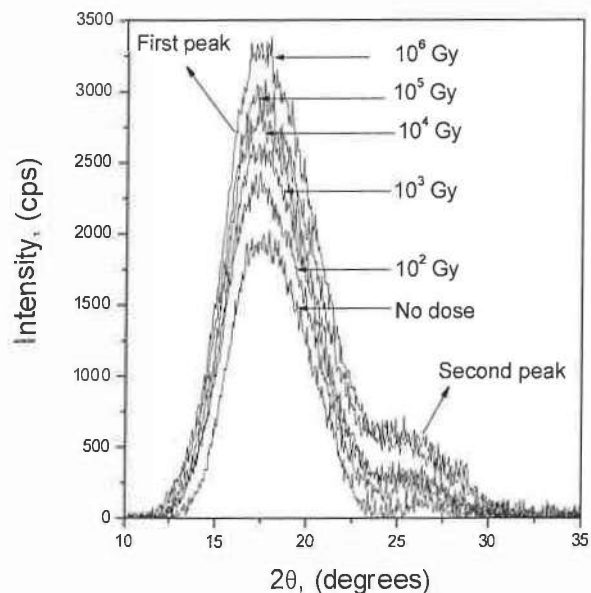


Fig.5.3.10. XRD spectra of gamma irradiated polycarbonate polymer

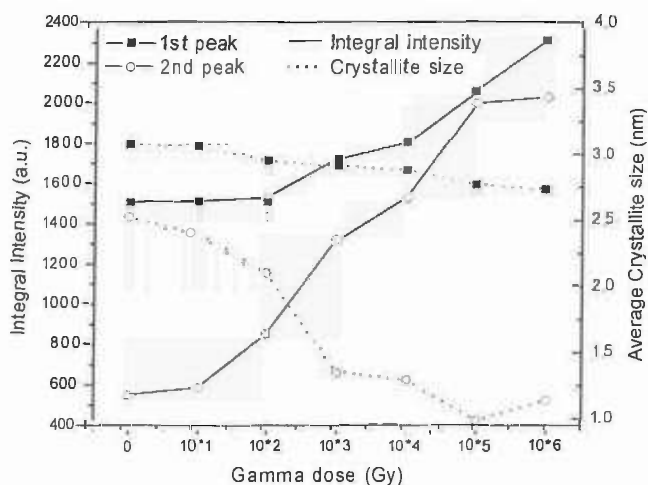


Fig.5.3.11. Dose dependent variation of integral intensity and average crystallite size for gamma irradiated polycarbonate. For the second peak, both the values of integral intensity and average crystallite size have to be multiplied by a factor of 4.5 and 0.3, respectively.

Fig.5.3.10 shows the XRD spectra of the pristine and gamma irradiated polycarbonate polymer. The XRD figure indicates the presence of two types of nano crystalline zones which are dispersed in

an amorphous matrix. With increasing gamma dose, the intensity of both the peaks increases. These results reflect that the amorphous character of the polymer decreases and crystallinity increases with increase in dose. This may be due to scissioning of the polymer chains, by which the polymer undergoes some spatial rearrangement. The small fragments may rearrange themselves towards new crystalline zone. From the XRD peaks we have calculated the integral intensity and the half width full maxima (FWHM) values. The integral intensity of the XRD peak increases due to irradiation. Many authors [7, 8, and 9] have used the half width full maxima (FWHM) value to calculate the crystal size according to Scherrer's formula [10];

$$D = \frac{0.88\lambda}{w \cdot \cos\theta}$$

where λ is the X-ray wave length (0.154056 nm), w is the full width at half maximum and θ is the Bragg angle. We found that due to gamma irradiation the crystal size decreases from 3.07 nm (for the pristine sample) to 2.73 nm (irradiated at 10^6 Gy) for the first peak and from 8.4 nm (pristine sample) to 3.8 nm (irradiated at 10^6 Gy) for the second peak, respectively. Figure 5.3.11 shows the change in integral intensity and in average crystallite size of the irradiated polymers for both the peaks. It is interesting to note that in both the cases the crystal size decreases and the integral intensity increases due to irradiation. The trend of increase or decrease of these values reflects the fact that a similar type of morphological change is taking place in both cases.

It is expected that due to decrease in crystal size, the corresponding integral intensity should decrease. But the observed

value of integral intensity increases. This increase indicates an increase of the overall crystallinity in the polymer matrix which means that part of the amorphous regions become crystalline. Hence we deal here with the secondary radiation induced crystallinity (SRIC) effect as reported by Fink [11]

CONCLUSIONS

On the basis of the present results, we can conclude that

- due to gamma exposure, polycarbonate polymer forms phenolic group at the dose of 10^6 Gy. This phenolic group forms due to cleavage of ester bonds.
- with increasing dose the polymer becomes more crystalline.
- the average crystallite size decreases due to gamma exposure.
- due to scissioning of the polymeric chains, the mobility of the chains increases, and as a result the glass transition temperature (T_g) of the polymer decreases. The decrease of T_g is very apparent at higher doses.
- significant modifications are possible only above the dose of 10^4 Gy.

REFERENCES

1. Non-linear effect of cluster irradiation on chemical modification of polycarbonate. K. Hirata, Y. Saitoh, K. Narumi, Y. Nakajima, Y. Kobayashi. *Nuclear Instruments and Methods in Physics Research B* 193, 816, 2004.
2. Infrared transmission of ion irradiated polymers. D. Fink, M. Müller, L.T. Chadderton, P.H. Cannington, R.G. Elliman and D.C. McDonaldt. *Radiation Effects Defects in Solids*, 132, 313, 1994.
3. Chemical modifications induced in bisphenol A polycarbonate by swift heavy ions. F. Dehaye, E. Balanzat, E. Ferain and R. Legras. *Nucl. Instr. Meth.B* 209, 103, 2003.
4. Swift heavy ion induced amorphisation and chemical modification in polycarbonate. Y. Sun, Z. Zhu, Z. Wang, Y. Jin, J. Liu, M. Hou and Zhang, Q. *Nucl. Instr. Meth. B* 209, 188, 2003.
5. Chemical modification of polycarbonate induced by 1.4 GeV Ar Ions. Yanbin Wang, Yunfan Jin, Zhiyong Zhu, Changlong Liu, Youmei Sun, Zhiguang Wang, Mingdong Hou, Xiaoxi Chen, Chonghong Zhang, Jie Liu, Baoquan Li. *Nucl. Instr. Meth. B* 164, 420-424, 2000.
6. Study of chemical, optical and thermal modifications induced by 100 MeV silicon ions in a polycarbonate film. A. Srivastava, T.V. Singh, S. Mule, C.R. Rajan and S. Ponrathnam. *Nucl. Instr. Meth. B* 192, 402, 2002.
7. The damage process induced by swift heavy ion in polycarbonate. Youmei Sun, Zhiyong Zhu, Zhiguang Wang, Jie Liu, Yunfan Jin, Mingdong Hou, Ying Wang, Jinglai Duan. *Nucl. Instr. Meth. B* 212, 211-215, 2003.
8. Chemical modifications of polymer films induced by high energy heavy ions. Z. Zhu, Y. Sun, C. Liu, J. Liu and Y. Jin. *Nucl. Instr. Meth. B* 193, 271, 2002.
9. Physical changes associated with gamma doses of Pm-555 solid-state nuclear track detector. S.A. Nouh. *Radiation Measurements*. 38, 167, 2004.
10. X-ray Diffraction Procedure for Polycrystalline and Amorphous Materials. H.P. Klug and L.E. Alexander. *Wiley, New York*, 1974.
11. Fundamentals of Ion-Irradiated Polymers. D. Fink. *Springer*, 2004.

PART-4

GAMMA RADIATION EFFECT ON PADC DETECTORS

Part of this work has been published in

Radiation Measurements, Vol.36, Page 229-231, 2003
Elsevier Publications

PART-4**5-4-1 INTRODUCTION**

Since its inception about 40 years ago, the field of track detection using solid state nuclear track detectors (SSNTDs) is being constantly developed. Track detectors are being increasingly used in various fields like Biomedical, Environmental, Anthropology, Space research and Nuclear sciences [1-6]. For newer and more innovative applications of these detectors a systematic study on the effects of external factors on their physical and chemical properties is essential. It is well known that unlike charged particles gamma rays are a highly penetrating form of electromagnetic radiation. They do not lose energy at every interaction with the atoms constituting the material they pass through. The energy loss of gamma rays occurs either through collisions with atomic electrons or through scattering as a photon of a longer wave length or through producing electron-positron pairs. Thus gamma ray does not have a specific range in matter as charged particles do.

Experimental evidence shows that the track registration characteristics of plastic Solid State Nuclear Track Detectors (SSNTDs) are greatly affected when exposed to high doses of gamma rays [7-10]. The action of electromagnetic radiation is known to be one of the major sources of altering the properties of the materials they pass through. The changes are strongly dependent on the internal structure of the absorbing substances and the radiation gamma doses. It may

be expected that the interaction of gamma-rays with solids cause electronic ionisation (or excitation) of the orbital electrons and possibly atomic displacements. Since polymeric solid state nuclear track detectors consist of long chain organic molecules, the net effect on the material is the formation of many broken molecular chains, leading to a reduction in the average molecular weight of the substance. Such radiation induced modifications of polymeric materials does influence their track properties [7-14].

Polyallyldiglycol carbonate (PADC generally referred as CR-39 in the literature, is a class of plastic detectors which has been most widely used in many fields of science and industry. This detector is mostly used as charged particle detection. The application of the track detector is dependent on the type of radiation which the detector is influenced by. It is now a text book story that track properties of this detectors are influenced by gamma radiation, and in this context, PADC detectors have been especially studied by Frank and Benton, [15]; Khan et al., [16]; Akber et al., [17]; Portwood and Henshaw, [18]; Sharma et al., [19]; Shweikani et al., [20]; Abu-Jarad et al., [21]; Sinha and Dwivedi, [22]. It has been observed by most of the workers that due to gamma exposure etch-rates increases. The increase in etch rates is due to scissioning of the molecular chain of the track detectors.

Recently Singh and Prasher [10] have reported that due to gamma exposure etch rates of CR-39 (Pershore) increase at doses higher than 50,000 krad. Figure 5.4.1, Figure 5.4.2 and Table 5.4.1 gives the values of these etch rates as reported by Singh and Prasher[10].

Table 5.4.1. The variation of the bulk etch rate V_B , the track etch rate V_T and sensitivity S with gamma dose in case of CR-39 plastic track detector [10]

| Gamma dose (krad) | V_B ($\mu\text{m}/\text{h}$) | V_T ($\mu\text{m}/\text{h}$) | S (V_T/V_B) |
|-------------------|----------------------------------|----------------------------------|-------------------|
| 0 | 2.02 | 13.03 | 6.45 |
| 50 | 0.65 | 13.82 | 21.26 |
| 100 | 0.80 | 19.17 | 24.77 |
| 1000 | 1.06 | 31.72 | 29.92 |
| 50,000 | 83.28 | 152.27 | 1.83 |
| 100,000 | 306.66 | 408.10 | 1.33 |

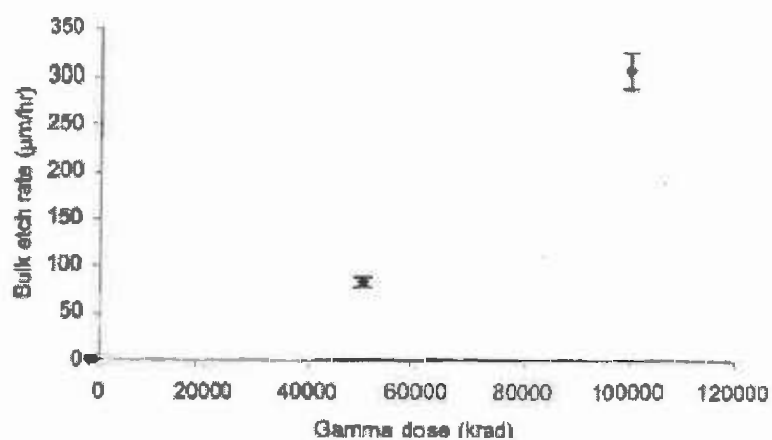


Fig.5.4.1. Bulk etch rate versus gamma dose in case of CR-39 [10].

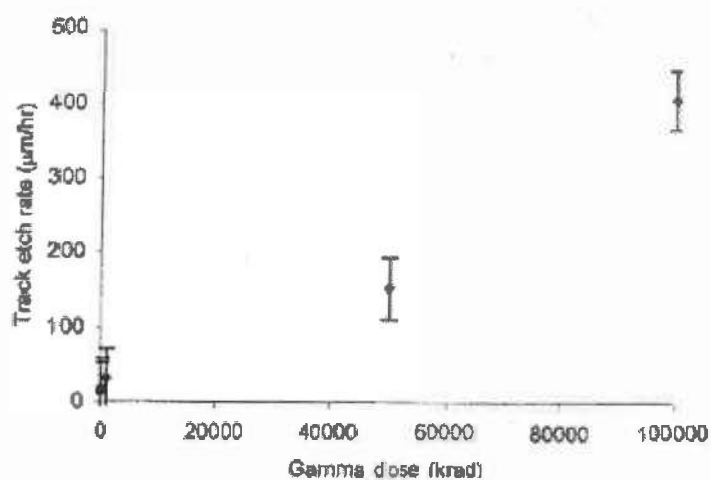


Fig. 5.4.2. Track etch rate versus gamma dose in case of CR-39 [10].

It is observed that most of the authors have limited their studies to within the doses of a few Mrad (less than 2×10^5 Gy). Only Abu-Jarad *et al.* [21] have studied the effect of gamma doses up to as high as 5×10^5 Gy on PADC (Persshore) detector. However, Sinha and Dwivedi [22] had earlier reported the effect of even higher doses of gamma radiation (10^6 Gy) on PADC (American Acrylics) detector. They have reported that bond scissioning of polyalyl chains containing diethyleneglycol lead to increase in etch-rates at dose of 10^6 Gy [22].

This particular part of the thesis is the study of gamma radiation effect on track properties of other types of PADC detectors like PADC - Homalite, PADC-Persshore and PADC-Tastrack. However the work reported here is restricted to only track studies of these detectors. A comparison has been made of the effects of different doses of gamma radiation on the etching characteristics of different types of PADC detectors. The variations in etch-rates, etching efficiency, etch-rate ratio and critical angle with gamma doses are determined and compared.

5.4.2 INVESTIGATION PROCEDURE

The PADC detectors used in this study are classified on the basis of their make as (a) Homalite - PADC (HL), (b) Persshore - PADC (PS) and (c) Tastrack - PADC (TT). The thickness of these sheets vary between 500 and 1500 μ m. Seven samples of each type of PADC detectors are prepared from the commercially available sheets and subjected to various doses of gamma rays ($10^1 \pm 10^6$ Gy) at room temperature from a ^{60}Co gamma source having a dose rate of 3 kGy/h. Two sets of samples, thoroughly washed and dried of sizes $2 \times 2 \text{ cm}^2$, are prepared from the commercially available sheets. One set of samples is first exposed at

normal incidence to alpha and fission fragments for 5 mins from a ^{252}Cf source. The pre-exposed samples along with the unexposed second set of samples are then irradiated with various doses of gamma radiation. Subsequent to the gamma exposure, the second set is exposed to ^{252}Cf source for alpha and fission fragment detection. The first and the second sets are respectively referred to as the post-gamma and pre-gamma sets. After exposure to the fission fragments, alpha and gamma radiation, the detectors are etched in 6 N NaOH solution at two different temperatures i.e. at 60°C and 65°C . The track diameters of the incident fission fragments and alpha particles are measured using Leitz Optical Microscope. Since the etch rates of PADC detectors irradiated at the dose of 10^6 Gy is observed to be very high, the detectors are etched for a shorter time (3 –10 min) as compared to the etching time (2 –4 h) of those exposed to lower doses of gamma radiation.

The bulk-etch rate (V_G), track-etch rate (V_T), are determined from the following expressions [20]

$$V_G = D_{ff}/2t, \quad V_T = V \times V_G,$$

where $V = 1+x^2/1-x^2$ $x = D_{ff}/D_\alpha$, where D_{ff} is the diameter of fission tracks, D_α is the diameter of alpha tracks.

There are some other terms associated with track studies like etching efficiency, critical angle, etch-rate ratio which are also determined from the equations given below.

$$\text{Etching efficiency } \eta (\%) = (1 - V_G/V_T) \times 100$$

$$\text{Critical angle } \theta_c = \sin^{-1}(1/V)$$

$$\text{Etch-rate ratio } S = V_T/V_G$$

5.4.3 RESULTS AND DISCUSSIONS

The bulk and track-etch rates of different types of PADC detectors are given below. It is observed that in almost all the cases, the etch-rate starts increasing at a dose higher than 10^4 Gy. This increase in etch-rates is observed in both pre- and post-gamma exposed detectors. Since the etch-rate increase is generally due to scissioning of the molecular chain, it may be assumed that scissioning of the molecular chain starts at a dose of 10^4 Gy. The possible route of gamma-induced scission of PADC chain is by the cleavage of polyallyl linkage with diethylene glycol segments, as reported earlier (Sinha and Dwivedi, 1998) [22]. With increasing radiation dose, the intensity of chain scission increases. It is also observed that post-gamma exposure of detector has more effect than pre-gamma exposure. The increase in etch-rate values for post gamma exposed samples is due to deposition of additional energy at the latent damage trails already created by fission tracks. Tables 5.4.2 to 5.4.7 give the values of both bulk-etch rates and track-etch rates for different PADC detectors.

Table.5.4.2 Bulk-etch rate(V_G) in $\mu\text{m/h}$ for gamma irradiated PADC-Homalite detector

| Temperature | No dose | 10^1 Gy | 10^2 Gy | 10^3 Gy | 10^4 Gy | 10^5 Gy | 10^6 Gy |
|------------------------|-----------------|-----------------|-----------------|-----------------|-----------------|-----------------|-----------------|
| 65 $^{\circ}$ C(pre) | 1.61 \pm 0.05 | 1.63 \pm 0.05 | 1.63 \pm 0.05 | 1.63 \pm 0.05 | 1.63 \pm 0.05 | 1.80 \pm 0.05 | 17.30 \pm 3.5 |
| 65 $^{\circ}$ C(post) | 1.61 \pm 0.05 | 1.61 \pm 0.05 | 1.64 \pm 0.05 | 1.65 \pm 0.05 | 1.69 \pm 0.05 | 2.07 \pm 0.05 | 20.70 \pm 3.5 |
| 60 $^{\circ}$ C (pre) | 0.69 \pm 0.03 | 0.72 \pm 0.03 | 0.72 \pm 0.03 | 0.72 \pm 0.03 | 0.72 \pm 0.03 | 0.75 \pm 0.03 | 9.33 \pm 1.2 |
| 60 $^{\circ}$ C (post) | 0.69 \pm 0.03 | 0.69 \pm 0.03 | 0.68 \pm 0.03 | 0.70 \pm 0.03 | 0.70 \pm 0.03 | 0.76 \pm 0.03 | 11.20 \pm 1.2 |

Table.5.4.3 Track-etch rate(V_T) in $\mu\text{m/h}$ for gamma irradiated PADC-Homalite detector

| Temperature | No dose | 10^1Gy | 10^2Gy | 10^3Gy | 10^4Gy | 10^5Gy | 10^5Gy |
|-----------------------------|-----------------|-----------------|-----------------|-----------------|-----------------|-----------------|-----------------|
| $65^0\text{C}(\text{pre})$ | 2.42 ± 0.05 | 2.41 ± 0.05 | 2.41 ± 0.05 | 2.40 ± 0.05 | 2.43 ± 0.05 | 2.65 ± 0.05 | 28.87 ± 3.5 |
| $65^0\text{C}(\text{post})$ | 2.42 ± 0.05 | 2.43 ± 0.05 | 2.46 ± 0.05 | 2.49 ± 0.05 | 2.53 ± 0.05 | 3.74 ± 0.05 | 61.90 ± 3.5 |
| $60^0\text{C}(\text{pre})$ | 0.92 ± 0.03 | 0.95 ± 0.03 | 0.95 ± 0.03 | 0.97 ± 0.03 | 0.96 ± 0.03 | 0.98 ± 0.03 | 15.80 ± 1.2 |
| $60^0\text{C}(\text{post})$ | 0.92 ± 0.03 | 0.95 ± 0.03 | 0.95 ± 0.03 | 0.94 ± 0.03 | 0.99 ± 0.03 | 1.12 ± 0.03 | 31.60 ± 1.2 |

Table.5.4.4. Bulk-etch rate(V_G) in $\mu\text{m/h}$ for gamma irradiated PADC-Persshore detector

| Temperature | No dose | 10^1Gy | 10^2Gy | 10^3Gy | 10^4Gy | 10^5Gy | 10^6Gy |
|-----------------------------|-----------------|-----------------|-----------------|-----------------|-----------------|-----------------|-----------------|
| $65^0\text{C}(\text{pre})$ | 2.42 ± 0.05 | 2.40 ± 0.05 | 2.43 ± 0.05 | 2.48 ± 0.05 | 2.52 ± 0.05 | 4.00 ± 0.05 | 26.60 ± 3.5 |
| $65^0\text{C}(\text{post})$ | 2.42 ± 0.05 | 2.42 ± 0.05 | 2.44 ± 0.05 | 2.44 ± 0.05 | 3.20 ± 0.05 | 6.20 ± 0.05 | 31.50 ± 3.5 |
| $60^0\text{C}(\text{pre})$ | 1.50 ± 0.03 | 1.50 ± 0.03 | 1.52 ± 0.03 | 1.50 ± 0.03 | 2.62 ± 0.03 | 4.20 ± 0.03 | 15.60 ± 1.2 |
| $60^0\text{C}(\text{post})$ | 1.50 ± 0.03 | 1.50 ± 0.03 | 1.50 ± 0.03 | 1.58 ± 0.03 | 3.12 ± 0.03 | 5.90 ± 0.03 | 22.40 ± 1.2 |

Table.5.4.5 Track-etch rate(V_T) in $\mu\text{m/h}$ for gamma irradiated PADC-Persshore detector

| Temperature | No dose | 10^1Gy | 10^2Gy | 10^3Gy | 10^4Gy | 10^5Gy | 10^6Gy |
|-----------------------------|-----------------|-----------------|-----------------|-----------------|-----------------|------------------|-----------------|
| $65^0\text{C}(\text{pre})$ | 3.80 ± 0.05 | 3.80 ± 0.05 | 3.80 ± 0.05 | 3.90 ± 0.05 | 3.98 ± 0.05 | 6.68 ± 0.05 | 46.20 ± 3.5 |
| $65^0\text{C}(\text{post})$ | 3.80 ± 0.05 | 3.80 ± 0.05 | 3.80 ± 0.05 | 3.90 ± 0.05 | 5.36 ± 0.05 | 10.50 ± 0.05 | 55.20 ± 3.5 |
| $60^0\text{C}(\text{pre})$ | 2.13 ± 0.03 | 2.14 ± 0.03 | 2.16 ± 0.03 | 2.20 ± 0.03 | 3.82 ± 0.03 | 6.95 ± 0.03 | 26.50 ± 1.2 |
| $60^0\text{C}(\text{post})$ | 2.13 ± 0.03 | 2.14 ± 0.03 | 2.14 ± 0.03 | 2.24 ± 0.03 | 4.44 ± 0.03 | 9.37 ± 0.03 | 38.30 ± 1.2 |

It is observed that there is an increase in etch-rate ratio value for both PADC-Persshore and PADC-Trastrack detector at the highest dose of 10^6Gy . For example, for the Persshore

detector, an increase of around 11% in etch-rate for both pre and post gamma exposed samples takes place at an etching temperature of 65°C. But at a lower etching temperature of 60°C, the etch-rate is increased by around 20% for both pre and post gamma exposed PADC-Pershire detectors. Similarly for PADC-Trastrack an increase etch-rate ratio of around 10% is observed for both pre and post-gamma cases at both etching temperatures at the highest dose. Whereas for PADC-Homalite detector, the result is quite different, and in this case the increase in etch-rate is much more in post-gamma exposed samples.

This increase in case of post-gamma exposed samples is observed at both etching temperature of 65°C and 60°C. An increase of around 10% in etch-rate value is observed for pre-gamma exposed samples, etched at 65°C whereas an increase of around 30% is seen to take place when the etching temperature is 60°C in the pre-gamma condition. However the value of etch-rate increases by around 95% for post-gamma exposed samples at an etching temperature of 65°C and an increase of 110% takes place at an etching temperature of 60°C. These results clearly indicate that the etch-rate ratio for PADC-Homalite detector is much higher than the PADC-Pershire and PADC-Trastrack detector. Since the etch-rate is the ratio between track-etch rate and bulk-etch rate, it is obvious from this result that the damage along the track is much more pronounced in case of PADC-Homalite detector as compared to PADC-Pershire and PADC-Trastrack detectors. Moreover etching along the track is more effective when the detector is etched at lower temperature of 60°C.

Table.5.4.6 Bulk-etch rate(V_G) in $\mu\text{m/h}$ for gamma irradiated PADC-Tastrack detector

| Temperature | No dose | 10^1 Gy | 10^2 Gy | 10^3 Gy | 10^4 Gy | 10^5 Gy | 10^6 Gy |
|--------------------------|-------------|-------------|-------------|-------------|-------------|-------------|-------------|
| 65 ⁰ C(pre) | 4.50 ± 0.05 | 4.50 ± 0.05 | 4.50 ± 0.05 | 4.52 ± 0.05 | 4.80 ± 0.05 | 5.88 ± 0.05 | 37.00 ± 3.5 |
| 65 ⁰ C(post) | 4.50 ± 0.05 | 4.50 ± 0.05 | 4.50 ± 0.05 | 4.54 ± 0.05 | 6.00 ± 0.05 | 8.82 ± 0.05 | 43.00 ± 3.5 |
| 60 ⁰ C (pre) | 2.50 ± 0.03 | 2.50 ± 0.03 | 2.52 ± 0.03 | 2.56 ± 0.03 | 2.80 ± 0.03 | 3.80 ± 0.03 | 21.00 ± 1.2 |
| 60 ⁰ C (post) | 2.50 ± 0.03 | 2.50 ± 0.03 | 2.52 ± 0.03 | 2.54 ± 0.03 | 3.00 ± 0.03 | 5.60 ± 0.03 | 26.20 ± 1.2 |

Table.5.4.7 Track-etch rate(V_T) in $\mu\text{m/h}$ for gamma irradiated PADC-Tastrack detector

| Temperature | No dose | 10^1 Gy | 10^2 Gy | 10^3 Gy | 10^4 Gy | 10^5 Gy | 10^6 Gy |
|--------------------------|-------------|-------------|-------------|-------------|-------------|--------------|-------------|
| 65 ⁰ C(pre) | 6.75 ± 0.05 | 6.72 ± 0.05 | 6.75 ± 0.05 | 6.78 ± 0.05 | 7.40 ± 0.05 | 9.40 ± 0.05 | 61.00 ± 3.5 |
| 65 ⁰ C(post) | 6.75 ± 0.05 | 6.72 ± 0.05 | 6.75 ± 0.05 | 6.78 ± 0.05 | 9.20 ± 0.05 | 13.80 ± 0.05 | 67.00 ± 3.5 |
| 60 ⁰ C (pre) | 3.70 ± 0.03 | 3.72 ± 0.03 | 3.74 ± 0.03 | 3.76 ± 0.03 | 4.32 ± 0.03 | 5.90 ± 0.03 | 33.60 ± 1.2 |
| 60 ⁰ C (post) | 3.70 ± 0.03 | 3.72 ± 0.03 | 3.74 ± 0.03 | 3.78 ± 0.03 | 4.68 ± 0.03 | 8.74 ± 0.03 | 41.40 ± 1.2 |

Table.5.4.8 Etch- rate ratio S (V_T/V_G) in $\mu\text{m/h}$ for PADC-Homalite Detector

| Temperature | No dose | 10^1 Gy | 10^2 Gy | 10^3 Gy | 10^4 Gy | 10^5 Gy | 10^6 Gy |
|--------------------------|---------|-----------|-----------|-----------|-----------|-----------|-----------|
| 65 ⁰ C(pre) | 1.50 | 1.47 | 1.47 | 1.47 | 1.49 | 1.58 | 1.66 |
| 65 ⁰ C(post) | 1.50 | 1.49 | 1.50 | 1.51 | 1.50 | 1.80 | 2.99 |
| 60 ⁰ C (pre) | 1.33 | 1.32 | 1.32 | 1.34 | 1.34 | 1.36 | 1.70 |
| 60 ⁰ C (post) | 1.33 | 1.34 | 1.36 | 1.37 | 1.41 | 1.47 | 2.82 |

Table.5.4.9 Etch- rate ratio $S (V_T/V_G)$ in $\mu\text{m/h}$ for PADC (Persshore) Detector

| Temperature | No dose | 10^1 Gy | 10^2 Gy | 10^3 Gy | 10^4 Gy | 10^5 Gy | 10^6 Gy |
|--------------------------|---------|-----------|-----------|-----------|-----------|-----------|-----------|
| 65 ⁰ C(pre) | 1.57 | 1.58 | 1.56 | 1.57 | 1.58 | 1.67 | 1.74 |
| 65 ⁰ C(post) | 1.57 | 1.57 | 1.56 | 1.59 | 1.67 | 1.69 | 1.75 |
| 60 ⁰ C (pre) | 1.42 | 1.42 | 1.42 | 1.41 | 1.46 | 1.65 | 1.70 |
| 60 ⁰ C (post) | 1.42 | 1.42 | 1.42 | 1.42 | 1.42 | 1.59 | 1.71 |

Table.5.4.10 Etch- rate ratio $S (V_T/V_G)$ in $\mu\text{m/h}$ for PADC-Trastrack Detector

| Temperature | No dose | 10^1 Gy | 10^2 Gy | 10^3 Gy | 10^4 Gy | 10^5 Gy | 10^6 Gy |
|--------------------------|---------|-----------|-----------|-----------|-----------|-----------|-----------|
| 65 ⁰ C(pre) | 1.50 | 1.49 | 1.50 | 1.50 | 1.54 | 1.59 | 1.65 |
| 65 ⁰ C(post) | 1.50 | 1.49 | 1.50 | 1.49 | 1.53 | 1.56 | 1.61 |
| 60 ⁰ C (pre) | 1.48 | 1.48 | 1.48 | 1.47 | 1.54 | 1.55 | 1.60 |
| 60 ⁰ C (post) | 1.48 | 1.48 | 1.48 | 1.48 | 1.56 | 1.56 | 1.58 |

Critical angle for etching at different etching temperature for different types of PADC detectors of pre and post-gamma exposed samples are listed in Table 5.4.11 to Table 5.4.13. Again it is observed that for all the detectors, etching at lower temperature of 60⁰C is more effective and the critical angle is decreased to a significant extent. For PADC-Persshore detector, a decrease of around 10% at 65⁰C and a decrease of around 20% is observed at an etching temperature of 60⁰C. However there is no significant difference in critical angles for pre gamma or post gamma conditions. Similarly for PADC-Trastrack detector also, an average decrease of around 8%

value in critical angle takes place for both pre and post gamma exposed samples. It is very interesting to observe that in this particular case, there is no significant difference in critical angles, whether the samples are etched at 65°C or at 60°C.

But the story is different for PADC-Homalite detector. There is a drastic change in the values when the detectors are etched at different temperature. Even the mode of gamma exposure like pre or post exposure, has a significant effect on the critical angle value. For example, at an etching temperature of 65°C, a decrease of around 10% in critical angle is observed at the highest dose of 10⁶Gy for pre-gamma exposed samples, whereas for post-gamma samples, a decrease of around 50% is observed. Again at an etching temperature of 65°C, a decrease of around 30% in critical angle is observed for pre-gamma exposed samples at the dose of 10⁶Gy, whereas a decrease of around 60% is observed for post gamma exposed detectors. This clearly indicates that post gamma exposure have more effect on PADC-Homalite detectors than pre-gamma exposed samples.

Table.5.4.11 Critical angle for PADC-Homalite detector at different etching temperature

| Temperature | No dose | 10 ¹ Gy | 10 ² Gy | 10 ³ Gy | 10 ⁴ Gy | 10 ⁵ Gy | 10 ⁶ Gy |
|--------------|---------|--------------------|--------------------|--------------------|--------------------|--------------------|--------------------|
| 65°C(pre) | 41.80 | 42.80 | 42.80 | 42.80 | 42.10 | 39.26 | 37.04 |
| 65 °C(post) | 41.80 | 42.15 | 41.80 | 41.40 | 41.80 | 33.74 | 19.50 |
| 60°C (pre) | 50.20 | 49.20 | 49.20 | 48.20 | 48.20 | 47.30 | 36.03 |
| 60 °C (post) | 50.20 | 48.26 | 47.33 | 46.88 | 45.17 | 42.86 | 20.76 |

Table.5.4.12 Critical angle for PADC-Pershore detector at different etching temperature

| Temperature | No dose | 10 ¹ Gy | 10 ² Gy | 10 ³ Gy | 10 ⁴ Gy | 10 ⁵ Gy | 10 ⁶ Gy |
|--------------------------|---------|--------------------|--------------------|--------------------|--------------------|--------------------|--------------------|
| 65 ⁰ C(pre) | 39.56 | 39.20 | 39.86 | 39.56 | 39.26 | 36.78 | 35.00 |
| 65 ⁰ C(post) | 39.56 | 39.56 | 39.86 | 38.97 | 36.78 | 36.27 | 34.84 |
| 60 ⁰ C (pre) | 44.76 | 44.76 | 44.76 | 45.17 | 43.23 | 37.30 | 36.03 |
| 60 ⁰ C (post) | 44.76 | 44.76 | 44.76 | 44.76 | 44.76 | 38.97 | 35.78 |

Table.5.4.13 Critical angle for PADC-Trastrack detector at different etching temperature

| Temperature | No dose | 10 ¹ Gy | 10 ² Gy | 10 ³ Gy | 10 ⁴ Gy | 10 ⁵ Gy | 10 ⁶ Gy |
|--------------------------|---------|--------------------|--------------------|--------------------|--------------------|--------------------|--------------------|
| 65 ⁰ C(pre) | 41.80 | 42.15 | 41.80 | 41.80 | 40.49 | 38.97 | 37.30 |
| 65 ⁰ C(post) | 41.80 | 42.15 | 41.80 | 42.15 | 40.81 | 39.86 | 39.86 |
| 60 ⁰ C (pre) | 42.50 | 42.50 | 42.50 | 42.86 | 40.49 | 40.17 | 38.68 |
| 60 ⁰ C (post) | 42.50 | 42.50 | 42.50 | 42.50 | 39.86 | 39.86 | 39.26 |

Etching efficiency (%) of these detectors is shown in Table 5.4.14 to Table 5.4.16. From these results, it can be observed that with increasing gamma dose, the efficiency increases. This increase is significant at a dose higher than 10³ Gy and is more pronounced for PADC-Homalite detectors. It is to be noticed that for PADC-Pershore and PADC-Trastrack detectors, there is tendency that the etching efficiency values (%) become almost equal at the dose of 10⁶ Gy. This trend is common for both pre and post exposed samples at both etching temperatures. This observation indicates that there is a likelihood that at the dose of 10⁶Gy, probably the etching

Table.5.4.14 Etching efficiency(%) of PADC-Homalite detector at different etching temperature

| Temperature | No dose | 10 ¹ Gy | 10 ² Gy | 10 ³ Gy | 10 ⁴ Gy | 10 ⁵ Gy | 10 ⁶ Gy |
|--------------------------|---------|--------------------|--------------------|--------------------|--------------------|--------------------|--------------------|
| 65 ⁰ C(pre) | 33.33 | 31.97 | 31.97 | 31.97 | 32.88 | 36.70 | 39.75 |
| 65 ⁰ C(post) | 33.33 | 32.88 | 33.33 | 33.77 | 33.33 | 46.80 | 66.55 |
| 60 ⁰ C (pre) | 24.81 | 24.24 | 24.24 | 25.37 | 25.37 | 26.47 | 41.17 |
| 60 ⁰ C (post) | 24.81 | 25.37 | 26.47 | 27.00 | 29.07 | 31.97 | 64.53 |

Table.5.4.15 Etching efficiency(%) of PADC-Pershore detector at different etching temperature

| Temperature | No dose | 10 ¹ Gy | 10 ² Gy | 10 ³ Gy | 10 ⁴ Gy | 10 ⁵ Gy | 10 ⁶ Gy |
|--------------------------|---------|--------------------|--------------------|--------------------|--------------------|--------------------|--------------------|
| 65 ⁰ C(pre) | 36.30 | 36.70 | 35.89 | 36.30 | 36.70 | 40.11 | 42.52 |
| 65 ⁰ C(post) | 36.30 | 36.30 | 35.89 | 37.10 | 40.11 | 40.82 | 42.85 |
| 60 ⁰ C (pre) | 29.57 | 29.57 | 29.57 | 29.07 | 31.50 | 39.39 | 41.17 |
| 60 ⁰ C (post) | 29.57 | 29.57 | 29.57 | 29.57 | 29.57 | 37.10 | 41.52 |

Table.5.4.16 Etching efficiency(%) of PADC-Trastrack detector at different etching temperature

| Temperature | No dose | 10 ¹ Gy | 10 ² Gy | 10 ³ Gy | 10 ⁴ Gy | 10 ⁵ Gy | 10 ⁶ Gy |
|--------------------------|---------|--------------------|--------------------|--------------------|--------------------|--------------------|--------------------|
| 65 ⁰ C(pre) | 33.33 | 32.88 | 33.33 | 33.33 | 35.06 | 37.10 | 39.39 |
| 65 ⁰ C(post) | 33.33 | 32.88 | 33.33 | 32.88 | 34.64 | 35.89 | 35.89 |
| 60 ⁰ C (pre) | 32.43 | 32.43 | 32.43 | 31.97 | 35.06 | 35.48 | 37.50 |
| 60 ⁰ C (post) | 32.43 | 32.43 | 32.43 | 32.43 | 35.89 | 35.89 | 36.70 |

temperature and mode of gamma exposure lose their significance. Similarly for PADC-Homalite detector, etching temperature loses its significance at the highest dose but mode of gamma exposure is very significant. Post-gamma

exposed detectors have more etching efficiency than the pre-gamma exposed ones.

Figure 5.4.3 is a representative diagram of the etching efficiency of PADC-Homalite detector, etched at different etching temperatures [23]

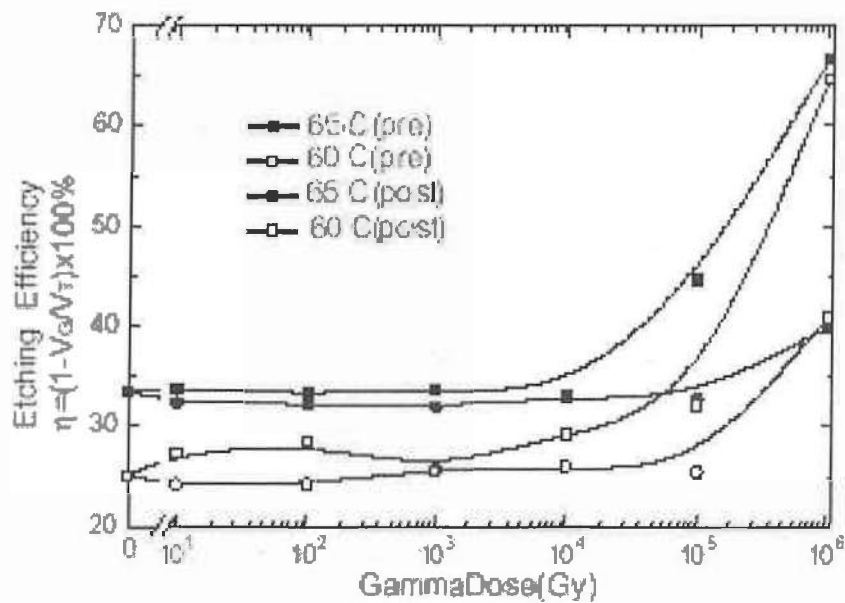


Fig.5.4.3 .Plot of gamma dose vs. etching efficiency for PADC (Homalite) detector etched at 60°C and 65°C.

CONCLUSIONS

On the basis of the present study, it is concluded that:

- Due to gamma exposure both the bulk and etch-rates of PADC-Homalite, PADC-Pershire and PADC-Trastrack increase. The increase is visible above the dose of 10^3 Gy.
- The post-gamma mode of exposure of the detectors has more effect than the pre-gamma mode of exposure.
- Among the three PADC detectors, a PADC-Homalite detector seems to be more sensitive to gamma exposure.
- Change in etch-rate ratio (S) for PADC-Pershire and PADC-Trastrack detectors are not very significant for pre and post gamma exposure, whereas for PADC-Homalite detector, the post-gamma exposure have more etch-rate ratio than pre-gamma exposed samples
- For all the detectors, Critical angle is decreased to a significant extent due to gamma exposure and etching at a lower temperature of 60°C is more effective. This decrease in critical angle is very significant for PADC-Homalite detector.
- Etching efficiency values (%) becomes almost equal at the dose of 10^6 Gy for Pershire and Trastrak detectors etched at different temperature in case of both pre and post exposed samples and for both etching temperatures. These observations indicate that there is likelihood that at the dose of 10^6 Gy, probably the etching temperature and mode of gamma exposure lose their significance.
- For PADC-Homalite detector, etching efficiency of these detectors loses its significance on the etching temperature at the highest dose. But mode of gamma exposure is very significant. Post-gamma exposed detectors have more etching efficiency than the pre-gamma exposed detectors.

REFERENCES

1. Production of single-pore membranes for the measurement of red blood cell deformability. H. G. Raggenkamp, H. Kiesewetter, R. Spohr, U. Daur and L. C. Busch. *Biomedizinische Technik*. 26, 167-169, 1981.
2. Production and use of nuclear tracks: Imprinting structure on solids. B. E. Fischer and R. Spohr. *Rev. Mod. Phys.* 55, 907-948, 1983.
3. Fission track dating of Bed I, Olduvai Gorge. R. L. Fleischer, P. B. Price, R. M. Walker and L.S.B. Leakley. *Science*. 148, 72-74, 1965.
4. Fission track ages and track annealing behaviour of some micas..R. L. Fleischer, P. B. Price, E. M. Symes and D.S. Miller. *Science* 143, 349-351, 1964.
5. Characteristics of fission tracks in Zircon: Applications to Geochronology and cosmology. S. Krishnaswami, D.Lal, N. Prabu and D. Mac Dougall. *Earth Planet. Science. Letters*. 22, 51-59, 1973.
6. Ternary fission produced in Au, Bi, Th and U with Ar Ions. V. P. Perelygin, N. H. Shadieva, S. P. Tretyakova, A.H. Boos and R. Brandt *Nuclear. Physics. A*. 127, 577-585, 1969.
7. Gamma ray dosimetric studies on CR-39 detectors. A. Joseph and K. M. Varier. *Indian Journal of Pure and Applied Physics*. 33, 406-409, 1995.
8. Effect of Gamma rays on etching of heavy ion tracks in Polyimide. Y. Komaki, N. Ishikawa and T. Sakurai. *Radiation Measurements*. 24, 193-196, 1995.
9. Effect of high gamma doses on the etching behaviour of different types of PADC detectors, D. Sinha, R. Mishra, S.P. Tripathy, K.K. Dwivedi *Radiation Measurements*. 33, 139-143, 2001.
10. The etching and structural studies of gamma irradiated induced effects in CR-39 plastic track recorder. S. Singh and S. Prasher. *Nuclear Instruments and Methods in Physics Research B*. 222, 4, 518-524, 2004.
11. Fast neutron irradiation effects on CN-85 solid state nuclear track detector. S.A. Nouh and T.M. Hegazy. *Radiation Measurements*. 41, 1, Pages 17-22, 2006.
12. Gamma-irradiation effects on track etching characteristics of polyester nuclear track detector Chhavi Agarwal, P. C. Kalsi, A. Ramaswami. *Radiation Effects and Defects in Solids*. 161, No. 2, 131 – 133, 2006.

13. Gamma-ray-induced modifications in microscopic glass slide used as a track detector Surinder Singh and Amanpreet Kaur Sandhu. *Radiation Effects and Defects in Solids*. 161, 4, 235 – 239, 2006.
14. Proceedings of the 22nd International Conference on Nuclear Tracks in Solids, *Radiation Measurements*. 40, 2-6, 125-794, 2005.
15. Dielectric plastic as high exposure gamma-ray detectors. A.L. Frank and E. V. Benton. *Radiation Effects*. 2, 269-272, 1970.
16. The effects of high gamma doses on the response of plastic track detectors. H.A.Khan, M.A. Asharf, S. Yameen, M.R. Haroom, Hussain., *Nucl. Instrum.Methods*. 127, 105 –108, 1975.
17. Studies of structural changes produced by high doses of gamma rays in some plastic track detectors. R.A. Akber, K. Nadeem, C.A. Majid. *Nucl.Instrum.Methods* 173, 217–221, 1980.
18. The Effect of gamma dose on the alpha response of CR-39. T. Portwood and D. L Henshaw. *Nuclear. Tracks*. 12, 105-108, 1986.
19. Effect of gamma irradiation on bulk etch rate of CR-39. S.L. Sharma, T. Pal, V.V. Rao, W. Enge. *Nucl. Tracks Radiat. Meas.* 18, 385 –389. 1991.
20. Effects of gamma irradiation on the bulk and track etching properties of Cellulose Nitrate (Daicel 6000) and CR-39 plastics. R. Shweikani, S. A. Durrani. and T. Tsuruta. *Nucl. Tracks Radial. Meas.* 22, 153-156, 1993.
21. Effect of high gamma dose on the CR-39 properties. F.Abu-Jarad, A.M. Hala, M. Farhat and M. Islam. *Radiation Measurements*. 28, 111-114, 1997.
22. Modifications of radiation detection response of PADC track detectors by Photons. D. Sinha and K.K. Dwivedi. *Radiation Physics and Chemistry*. 53, 99-105, 1998.
23. Gamma Effect on Track properties of PADC Detector. D. Sinha, T. Swu, S.P.Tripathy, R. Mishra, K.K. Dwivedi. *Radiation Measurements*. 36, 229–231, 2003.

Chapter - 6

CHAPTER-6**6.1. BACKGROUND**

Numerous studies have clearly demonstrated that the interaction of heavy ionizing radiation with polymers leads to irreversible modifications of the structure and chemical composition. Energetic heavy ions create cylindrical tracks with complex damage structures such as radical formation, main chain scission, intermolecular cross-linking, creation of triple bonds and unsaturated bonds and loss of volatile fragments. These complex damage structures lead to polymer modifications. Though lots of work have been done on ion beam modifications of polymer properties like optical properties, chemical and structural properties, surface properties, thermal properties, electrical properties etc., but very little attention has so far been given to areas such as crystallinity studies and its effect on related polymer properties like glass transition temperature, melting temperature, heat of enthalpy, refractive index, hardness, surface modifications, etc. In general, it is assumed that ion irradiation of polymers does not only lead to the destruction of short-range order (i.e. the polymers' chemical arrangement) but also to the destruction of its long-range order, especially what concerns the polymeric crystallinity. In fact, this observation has been made by some experimentators with several polymers, after heavy ion irradiation. Some experimentators even use the degree of residual polymeric crystallinity of originally (semi)crystalline polymers after ion irradiation as a measure of the state of polymer destruction, and swift heavy ion irradiation effective ion track radii are deduced from this parameter. Figure.1. shows the change in crystallinity due to irradiation). It has been observed that in the vast majority of all examined cases, the polymer's original degree of

crystallinity decreases with increasing fluence, first slowly and after a certain critical fluence (onset of track overlapping) quite rapidly. This decrease in overall crystallinity is accompanied by a linear increase in size of the remaining crystalline zones which is explained by a growth of larger domains at the expense of smaller ones. Again there has been accumulated meanwhile some evidence that an opposite effect also exists, namely a “*secondary radiation induced crystallization*” (SRIC), which is interpreted as the transient radiation-induced emergence of a new crystalline phase. This SRIC effect appears not to be correlated sharply with the deposited energy density, as has been observed after very low energy density deposition (e.g. after γ irradiation) after medium dose proton or fast neutron irradiation.

In contrast to swift heavy ion induced SRIC, in our recent studies on gamma irradiated polycarbonate, we found that the crystallinity steadily increases with increasing radiation dose, with no indication neither for saturation nor for a decrease in crystallinity, even at the highest observed doses.

However, a lot of un-attempted queries still persist in this field. The relation between change in crystallinity with and its effect on related polymer properties is not known. Studies have so far, not been performed to understand whether irradiation effect on change in polymer crystallinity is a permanent or transient and what happens when the polymer is subsequently annealed, and whether SRIC effect is related to energy of ion, etc. So a detail examination is required to lead to some more interesting insights.

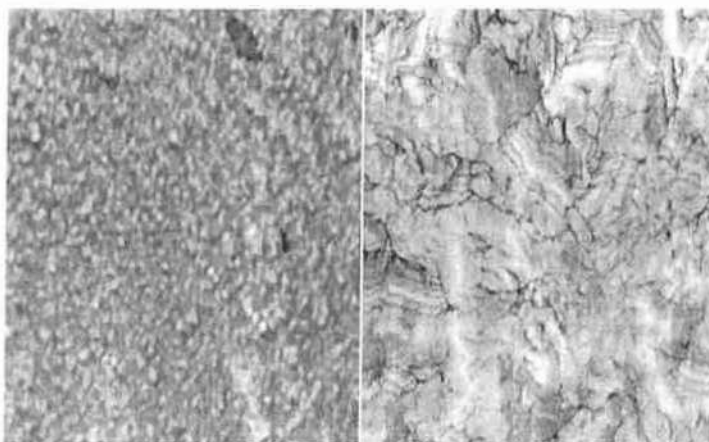


Fig.6.1. LFM micrographs (i.e. friction images) of (a) pristine PP, and (b) polypropylene foils irradiated with 3 GeV ^{238}U ions at a fluence of 10^{11} cm^{-2} . The transition from small structure less grains towards large laminar units can clearly be recognized. Image size: $1.5 \mu\text{m} \times 1.5 \mu\text{m}$ each (this figure is copied from the book "Fundamentals of Ion-Irradiated Polymers" by D. Fink, Springer, 2004.

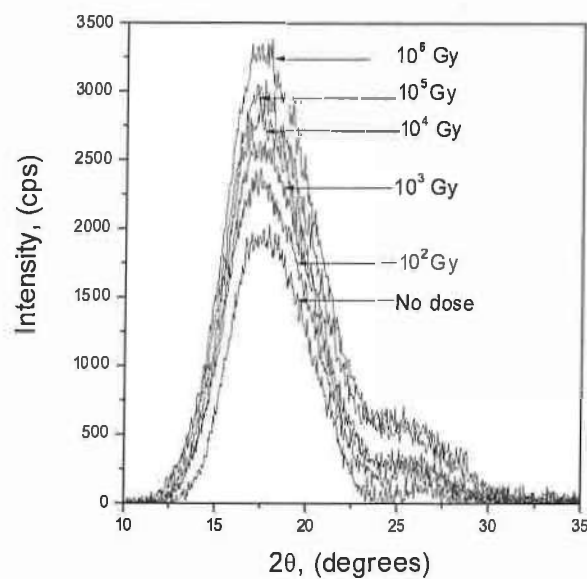


Fig.6.2... Gamma dose dependent change in XRD graph of Polycarbonate polymer. The increase in peak intensity signifies that crystallinity increases with increasing dose.

6.2. FUTURE WORK PLAN:

The work on radiation induced modifications of the polymer crystallinity and its effect on other related polymeric properties is expected to be quite significant in order to understand the details about polymer crystallinity and its effect on physical properties. The work may be restricted to ionizing irradiations, i.e. to radiation that promotes the target electrons from their valence bands to their conduction bands and/or beyond. However, it would be pertinent to remember that different types of irradiation (Gamma, electrons, light ions, heavy ions) differ from each other by the energy density deposited in the target materials during their electronic energy transfer.

Note: ions further transfer part of their energy to the target in the form of nuclear collisions, but this effect is minimized when using swift heavy ions passing through thin target foils, and therefore need not be considered here.

Since polymer irradiation affects a multitude of parameters, nearly all of which all are interconnected with each other in a delicate way, in general, their characterization requires more than just one technique, as each experimental method is sensitive to different parametric dependencies of the same property. So in the future a study on low-energy ion irradiation effect on different types of polymers may be undertaken. Different techniques like XRD, SEM, AFM, DSC, Hardness measurements, etc. may be performed to understand the change in the polymer matrix due to irradiation. All these studies are directly related to polymer crystallinity. This study is expected to understand the mechanism of change in polymer crystallinity and its effect on other polymer properties.

6.2.1. REVIEW OF LITERATURE IN THE PROPOSED AREA

The effect of irradiation on polymer's crystallinity has been studied by several authors. The studies have been done by using different techniques. Different authors have made several interesting observations and some of these significant results have been mentioned below. The **LFM** (lateral force microscope, i.e. AFM in friction image mode) image of swift heavy ion irradiated PP [1] revealed clearly that the originally grainy microstructure (with ca. 20 nm grain size) has been coarsened considerably by ion irradiation leading to formation of lamellar structures of typically 150 to 600 nm size and projected interlamellar distance of 20 to 40 nm (i.e. as seen by the LFM from the top view, Figure 1). As these structures exceed ion track diameters by far one might conclude that the ion tracks act as nuclei for polymeric crystallization which is promoted by intense electronic excitation of the target by the ions. XRD studies revealed that any polymer's original degree of crystallinity decreases with increasing fluence, first slowly and after a certain critical fluence quite rapidly [2]. This decrease in overall crystallinity is accompanied by a linear increase in size of the remaining crystalline zones which is revealed by a growth of larger domains at the expense of smaller ones [2]. Whereas Ref. [3] reports that the XRD peak positions do not shift - i.e. that the lattice parameters do not change significantly, in Ref. [4] a shift has been reported, which is explained as increasing strain resulting from density differences between the pristine and the irradiated zones. On the other hand, new reflexes build up upon irradiation, and some older existing ones increase in intensity up to a certain fluence, after which the intensity of these reflexes decreases again. These reflexes become broader with increasing fluence, indicating a decrease in crystal size. DSC results on ion-irradiated PET [5] indicate a change in crystallinity

[9, 10], and also after experiments where high power densities (typically 0.3 to 1 Watt/cm²) were deposited and where the electronic energy transfer per ion path length was as high as some 10 keV/nm. This effect has been observed preferentially in PET, and PVDF, and also occasionally in PP and PVA [11, 12].

6.2.2. OBJECTIVES OF THE FUTURE COURSE OF WORK

Since the modifications of polymer by irradiation depends on the types of radiation, its energy, fluence and lastly on types of material irradiated. So the objectives of any future work would be to study the effect of low energy ions of different energies on several polymers. Then the modifications on crystallinity could be analysed and their effect on other properties may be investigated. All these studies will definitely help to understand in better way about the low energy ion interaction with polymers.

REFERENCES

1. Fundamentals of Ion-Irradiated Polymers” by D. Fink, *Springer, 2004*.
2. Chemical modifications in polyethylene terephthalate films induced by 35 MeV/amu Ar ions. C. Liu, Z. Zhou, Y. Jin, Y. Sun, M. Hou, Z. Wang, X. Chen, C. Zhang, J. Liu, B. Li, Y. Wang. *Nuclear Instruments and Methods in Physics Research B. 166/167, 641-645, 2000*.
3. Swift heavy ion induced amorphisation and chemical modification in polycarbonate. Youmei Sun, Zhiyong Zhu, Zhiguang Wang, Yunfan Jin, Jie Liu, Mingdong Hou, Qinxiang Zhang. *Nuclear Instruments and Methods in Physics Research B. 209, 188-193, 2003*.
4. Ion irradiation induced surface modification studies of polymers using SPM A. Tripathi, Amit Kumar, F. Singh, D. Kabiraj, D.K. Avasthi and J.C. Pivin. *Nuclear Instruments and Methods in Physics Research B. Vol. 236, Issues 2, 186-194, 2005*.
5. Study of the ion beam induced amorphisation, bond breaking and optical gap change processes in PET. R.M. Papaleo, M.A. de Araujo, R.P. Livi. *Nucl Instr Meth B. 65, 442-446, 1992*.
6. Gamma induced modifications of Polycarbonate polymer D.Sinha, K.L.Sahoo, U.B.Sinha, T.Swu, A. Chemseddine, D.Fink. *Radiation Effects and Defects in Solids, Vol.159, No.10, 587-595, 2004*.
7. Radiation-induced transformation of polypropylene morphology and visco-elastic behaviour. M. Mateev, S. Karageorgiev, *Radiation Effects and Defects in Solids 152, 109-138, 2000*.
8. Proton induced modification in Polyethylene Terephthalate. S.P. Tripathy, R. Mishra, K.K. Dwivedi, S. Ghosh, D. Fink. *Rad EffDefSol. 158, 583-591, 2003*.
9. Radiation-induced crystallinity changes in pressure crystallized ultra high molecular weight polyethylene. S.K. Bhateja. *Jr. Macromol. Sci. Phys. B. 22, 159-168, 1983*.
10. Study of electrical and optical frequency response of neutron irradiated polyvinyl acetate thick films. A.K. Srivastava, H.S. Virk. *Rad PhysChem 59, 31-37, 2000*.
11. Proceedings of the 14th International Conference on Ion Beam Modification of Materials. *Nuclear Instruments and Methods in Physics Research B. Volume 242, Issues 1-2, 2006*.

12. Effect of γ -radiation on the structure and morphology of polyvinyl alcohol films. N.V. Bhat, M.M. Nate, M.B. Kurup, V.A. Bambole and S. Sabharwal. *Nuclear Instruments and Methods in Physics Research B. Vol. 237, Issues 3-4, 585-592, 2005.*

CURRICULUM VITAE

NAME TOKASWU

DATE OF BIRTH 14TH JULY 1971

EDUCATIONAL QUALIFICATION:

| Examination Passed | Board/University | Year | Result |
|--------------------|---------------------|------|----------------------|
| B.Sc. (Chemistry) | N.E.H. University | 1992 | 2 nd Div. |
| M.Sc. (Chemistry) | Nagaland University | 2000 | 1 st Div. |

List of Publications

1. Gamma Effect on Track properties of PADC Detector. D.Sinha, **T.Swu**, S.P.Tripathy, R. Mishra, K.K. Dwivedi.
Radiation Measurements. Vol.36, 229-231, 2003.
2. Spectroscopic and Thermal studies of Gamma-irradiated Polypropylene films. D. Sinha, **T. Swu**, S.P. Tripathy, R. Mishra, K.K. Dwivedi and D. Fink.
Radiation Effects and Defects in Solids. 158 (No. 7), 531-537, 2003.
3. Gamma-Photon induced modification of Polyvinylchloride (PVC) film. D. Sinha, **T. Swu**, S.P. Tripathy, R. Mishra, K.K. Dwivedi and D. Fink.
Radiation Effects and Defects in Solids. Vol. 158, No.8, 593-598, 2003.
4. Gamma induced modifications of Polycarbonate polymer. D.Sinha, K.L.Sahoo, U.B.Sinha, **T.Swu**, A. Chemseddine and D.Fink.
Radiation Effects and Defects in Solids. 159 (No.10), 587-595, 2004.